Lahar Initiation and Sediment Yield in the Pasig-Potrero River Basin, Mount Pinatubo, Philippines

By

Norman Manuel Tuñgol

A thesis
submitted in partial fulfillment
of the requirements for the degree
of

Doctor of Philosophy in Engineering Geology

2002

There is no end… only a deadline.

For My Beloved Wife, Malou,

and My Four Angels: Athena, Alyssa, Ava and Alexie

Acknowledgments

The opportunity to study at the University of Canterbury was made possible through the initiative of Prof. Jim Cole, who enjoined me to apply at Canterbury during his visit to the Philippines in 1995. New Zealand's Ministry of Foreign Affairs and Trade, through its Official Development Assistance Postgraduate Scholarship (NZODA-PGS) program, provided financial support not only for my studies but for my family's stay in New Zealand as well. Personal thanks to the University's resident ODA administrator, Dr. John Pickering, and International Student Adviser, Eunice McKessar, who looked after my and my family's welfare during our stay in New Zealand.

My study leave from the Philippine Institute of Volcanology and Seismology (PHIVOLCS) was granted by its Director, Dr. Raymundo S. Punongbayan, who has always encouraged his staff to pursue graduate studies in line with his vision of developing PHIVOLCS into a world-class volcanological and seismological research center. We hope to be able to sustain this vision.

PHIVOLCS also provided logistical support for my research. Colleagues from the institute, particularly from the Geology and Geophysics Research and Development Division shared their technical expertise as well as their friendship. I am especially thankful to Peejay, Mabel and Myla for cheerfully accompanying me in my fieldwork; the staff of the Pinatubo Volcano Observatory (PVO) – Jimmy, Mona, Joel and Jun – for technical support; and the drivers – Teody, Lito and Edwin – for taking me around my field area. I owe personal gratitude to my dear friend and *kumare*, Peejay Delos Reyes, who shared both the hardships and joys of my research. I wish her all the best in her Masteral studies at Canterbury.

My thesis greatly benefited from scientific discussions with my supervisors, Dr. Jim McKean and Prof. Cole; visiting scientist Dr. Josh Roering; and Lincoln University staff Prof. Tim Davies and Dr. Katy Hodgson. Dr. Chris Newhall, a friend and colleague from the USGS, and one of those who encouraged me to go to graduate school, has unselfishly shared his field notes and his many insights about Pinatubo. Chris' relentless effort to foster international collaboration among scientists has helped in opening the world to me and my fellow researchers at PHIVOLCS.

Being far away from home was made pleasant in the company of Filipinos in Christchurch, be they tourists, New Zealand permanent residents or Kiwi citizens. My family and I specially cherish the camaraderie that we have developed with members and friends of the Filipino Students Association at Canterbury and Lincoln Universities.

I always derive inspiration from my family: my dearest wife, Malou, who sacrificed her career to be with me; my beautiful daughters, Ayen, Aly, Ava and Alexie, who are my pride and joy; and my parents and siblings, who have always believed in me.

I hope this is all worth it.

Abstract

A systemic basin-wide consideration of the complex interaction of many hydro-geomorphic and volcanic processes involved in lahar initiation emphasizes the role of rill erosion, both on tephra-covered hillslopes and on the valley-filling pyroclastic-flow deposits. Rill erosion is found to be as important as erosion in the main river channel in terms of sediment contribution. In addition, erosion is fed by mass-wasting processes that are profoundly affected by secondary explosions. The observed decrease in lahar activity is inferred to be related to the depletion of the pyroclastic deposits, which in turn has affected the frequency of secondary explosions, and allowed the development of relatively stable river channels that are in synchrony with their tributary rills and gullies. The decrease in secondary explosion activity has also allowed hillslope recovery that has resulted in reduced rill erosion.

Rainfall-normalized sediment yield and the lahar-triggering rainfall threshold in the Pasig-Potrero River are analyzed using near-complete data from rain gauges and acoustic flow monitors (AFM), with AFM data as proxy for lahar hydrographs. Data for coincident lahars and rainstorms show the river's hydrologic response to two major watershed disturbances: the emplacement of 300 million m^3 of pumiceous pyroclastic debris during the June 1991 eruption, and the capture of the upper Sacobia catchment in October 1993. Sediment yield peaked immediately after each major watershed disturbance, followed by a non-linear decrease through time. The systematic decline is inferred to be related to the depletion of the source sediments and the development of the drainage network, particularly the decrease in drainage density and increase in channel width. These parameters influenced the volume of pumiceous sediments in contact with runoff. The rainfall threshold at which lahars are generated was found to remain at about the same low level until 1995, after which it increased progressively until 1997. No major lahar has been observed or detected by the AFM since then. The triggering rainfall is postulated to be a function of the erodibility and infiltration capacity of the surface, which together control the amount of runoff and entrainable sediments. These factors in turn are largely controlled by the areal distribution of pumiceous 1991 pyroclastic deposits, including both flow and fall deposits. Secondary

explosions have played a key role in this regard by intermittently blanketing large areas with tephra, therefore momentarily negating the effects of vegetation during the rainy season. Thus, the triggering rainfall increased only when erosion has reached the pre-eruption surface and secondary explosions have decreased substantially. The trends in laharic sediment yield and lahar-triggering rainfall together demonstrate the progressively increasing rainfall requirement for lahar generation through time. Cautious extrapolation of the data suggests that to trigger and sustain a modest lahar (<10 million m^3) now requires a rainstorm with a return period exceeding 100 years.

Lahars have also been initiated by the sudden failure of temporary lakes that have been formed by the blockage of tributaries by lahar or pyroclastic-flow deposits. Many such pyroclastic-flow or lahar dams have been observed to repeatedly form and breach, often resulting in catastrophic lahars. A few, however, have survived for many years and may pose lahar hazards in the future. Four conceivable mechanisms for the failure of pyroclastic dams are considered: (1) erosion of the dam by flows along the lahar channel; (2) gravitational collapse and/or piping; (3) lake overtopping; and (4) secondary explosions. Analyses show that the blockages are naturally susceptible to overtopping failure through breach erosion. However, material lost to bed erosion along the breach-channel may be initially compensated for by sediments delivered onto the dam by lahars or local runoff. Once sediment supply to the dam is cut off, *e.g.*, due to the depletion of source sediments, by revegetation, or by stream beheading, the dam is predicted to fail by breach erosion. It can thus be expected that, barring engineering intervention, all pyroclastic-flow and lahar dams around Mount Pinatubo will eventually fail, as suggested by their absence before the 1991 eruptions.

Table of Contents

List of Figures

List of Tables

Common Abbreviations

AFM	Acoustic flow monitor
ARRG	Ash-resistant rain gauge
ASTM	American Society for Testing and Materials
CAB	Clark Air Base
DPWH	Department of Public Works and Highways
GIS	Geographic Information System
NHRC	National Hydraulic Research Center
JICA	Japan International Cooperation Agency
PHIVOLCS	Philippine Institute of Volcanology and Seismology
PVO	Pinatubo Volcano Observatory
RG	Rain gauge
UNESCO	United Nations Educational, Scientific, and Cultural Organization
UP	University of the Philippines
USACE	United States Army Corps of Engineers
USGS	United States Geological Survey

Chapter 1

INTRODUCTION

CHAPTER 1

Introduction

1.1. Overview

The 1991 eruption of Mount Pinatubo is considered one of the largest explosive eruptions in the 20th century, second only to the 1912 eruption of Novarupta in Alaska in terms of volume of eruptive products. Although the number of casualties was minimized by timely warnings, the socioeconomic impacts of the eruption were devastating, affecting 2 million people and resulting in PHP 10.5 B (US$ 420 M) worth of losses in 1991. The volcanic disaster continued with the occurrence of lahars, which flowed down the major rivers draining Mount Pinatubo every rainy season following the eruption. Since 1991, more than 2.3 km^3 of volcanic debris have been delivered by lahars to the lowlands around the volcano, permanently dislocating more than 200,000 people, and causing billions of pesos worth of damage.

A decade after the eruption, lahar hazards have apparently diminished significantly. Since the last major lahar in August 1997, flows have been relatively modest in both volume and sediment concentration. Yet, recognizing the need to remain vigilant, and for lack of conclusive proof that the hazards have in fact become tolerable, scientists have been reluctant to lower alert levels. As the central Luzon region slowly recovers from the disaster, various sectors have exerted much pressure on scientists to change their gloomy forecasts. Scientists are now faced with an increasing demand to evaluate lahar hazards more accurately, with the perspective of striking a balance between disaster mitigation and economic growth.

1.2. Significance of research

Immediately after the eruption, lahar hazards mapping was necessarily based on worst-case forecasts, considering that the nature and magnitude of the hazards were unprecedented in Philippine history. With the apparent reduction in the hazards in the past few years, however, forecasts now need to be more accurate in both (1) determining the probability of occurrence of the hazard at different magnitudes, and (2) delineating the areas at risk from the hazard. This research aims to contribute to understanding the first aspect.

The lahars of Pinatubo are unique in their combination of volcanic and hydrologic setting: a large-scale pumiceous eruption in a tropical region. Tropical lahars, which are almost invariably rain generated, behave differently from those that are triggered by such geologic phenomena as snow melting during an eruption, or the sudden release of crater-lake water. Previous studies on tropical rain-lahars have dealt with different volcanic material (not pumiceous), and significantly smaller volumes of eruptive products. Studies specific to Pinatubo were made during the first two to three years of the lahar crisis, and did not have a long-term perspective of the hazard. None have systematically addressed the initiation and triggering mechanisms of Pinatubo lahars. One particular triggering mechanism – failure of temporary blockages – although partly documented, has not been studied in detail. Lahar hazards from the remaining blockages have not been assessed at all.

1.3. Objectives and scope

Pinatubo lahars have been triggered by two main mechanisms: (1) rapid erosion of the 1991 pyroclastic deposits during intense rainstorms, and (2) the sudden breaching of temporary river blockages. This study deals with these two discrete hydro-geologic triggers. The upper reaches of the Pasig-Potrero River on the east side of the volcano (Figure 1.1) is chosen as the study area since it typifies these processes, having generated some of the worst lahar disasters from both intense rainfall and dam-breaching episodes.

Furthermore, among all river basins around Pinatubo, lahar risks in the Pasig-Potrero have been the greatest owing to the large urban communities lying on its alluvial fan, which is composed of lahar deposits from previous eruption episodes of Mount Pinatubo. Lahars along the Pasig-Potrero have caused the most number of lahar-related fatalities and inundated the most number of heavily populated villages. They have also repeatedly damaged major infrastructure vital to the economy of Central Luzon.

Figure 1.1. Vicinity map of Pinatubo volcano showing the alignment of major rivers before the 1991 eruption. This study is focused on the upper Pasig-Potrero River catchment, indicated by the red box.

Using the Pasig-Potrero River as a type locality for Pinatubo lahars, this study aims to:

1) Describe the various factors and processes that contribute to the initiation of lahars;

2) Determine temporal variations in the rainfall threshold at which lahars are triggered;

3) Analyze laharic sediment yield in relation to rainfall; and

4) Analyze lahar hazards posed by temporary dams.

These objectives are further discussed in chapters that seek to address specific aspects of the study.

1.4. Previous works

Lahars as hazardous phenomena have long been the subject of geological research. Perhaps the most comprehensive studies of volcano-hydrologic processes in any one volcano were the pioneering series of studies made by Segerstrom (1950, 1960, 1966) in Parícutin Volcano (Mexico), and the paper by Waldron (1967) on the debris flows of Irazú Volcano (Costa Rica). After the dreadful disaster at Nevado del Ruiz in 1985 (Barberi *et al.*, 1990; Pierson *et al.*, 1990; Voight, 1996), scientists have exerted much effort toward understanding lahars and predicting their hazards. In regard to their initiation, many studies have focused on specific geologic triggers. Snowmelt lahars, such as those at Nevado del Ruiz, for example, have been scrutinized by such authors as Major and Newhall (1989), Pierson *et al.* (1990), Pierson and Janda (1994), Pierson (1995, 1999a), and Manville *et al.* (2000). Lahars from the sudden breakout of crater-lake water have been investigated by McGimsey *et al.* (1994), Kusakabe (1996), Waythomas *et al.* (1996), Manville *et al*, (1999), Pierson (1999b), and Mastin and Witter (2000). Rain-triggered lahars have been studied by Rodolfo and Arguden (1989, 1991), Hodgson and Manville (1999), and Lavigne *et al.* (2000). Other studies have

been concerned with general trends in sediment yield (*e.g.*, Shimokawa and Jitousono, 1987; Mizuyama and Kobashi, 1996; Major *et al.*, 2000), or with particular scientific problems of tephra erosion (*e.g.*, Collins *et al.*, 1983; Collins and Dunne, 1986; Leavesley *et al.*, 1989; D.F. Meyer and Martinson, 1989).

At Pinatubo, most of the studies on lahars have been done by the Philippine Institute of Volcanology and Seismology (PHIVOLCS). These may be found in agency reports, although some of them have been published in independent scientific journals. A summary of the early lahars of Pinatubo may be found in the PHIVOLCS report to UNESCO (PHIVOLCS, 1994). Many engineering studies on lahars have also been made in the overall effort of disaster mitigation. These include the works by the United States Army Corps of Engineers (USACE, 1994) and Japan International Cooperation Agency (JICA, 1996) in their capacity as consultants of the Department of Public Works and Highways (DPWH) for Pinatubo rehabilitation projects. Hydraulic simulation of lahars along the Pasig-Potrero River has also been done by the University of the Philippines' National Hydraulic Research Center (NHRC, 1998).

Some graduate students' theses have also dealt with various aspects of Pinatubo lahars. Daag (1994) quantified erosion in the Sacobia pyroclastic flow field by overlaying aerial photograph interpretation on digital elevation models using Geographic Information System (GIS). Umbal (1994) studied the evolution of the lahar-dammed Mapanuepe Lake on the southwest side of the volcano. Shields (1998) did a geotechnical evaluation of the Pasig-Potrero Megadike, and Hayes (1999) investigated low-flow sediment transport in the Pasig-Potrero.

In "Fire and Mud" (Newhall and Punongbayan, 1996a), the most authoritative scientific volume on Pinatubo to date, a whole section is devoted to the discussion of lahars. The reader is referred in particular to the papers by Arboleda and Martinez; Janda *et al.*, Major *et al.*, Martinez *et al.*, Pierson *et al.*, Rodolfo *et al.*, K.M. Scott *et al.*, Tuñgol and Regalado, and Umbal and Rodolfo. Most of these studies at Pinatubo, however, were written after only two years of observations, and therefore lack a long-term perspective. None of them attempted to discuss all the processes involved in lahar generation, but

rather have invariably focused on specific aspects of the lahar phenomenon, such as its triggers, flow behavior, deposits or the hazards it poses.

1.5. General approach and thesis organization

The main body of this thesis consists of individual papers that address specific questions about lahar initiation. Chapter 2 discusses the 1991 eruption and ensuing lahars of Pinatubo. This is intended to orient the reader with the lahars of Pinatubo, specifically in the Pasig-Potrero River basin, and provide the context for the succeeding chapters.

In Chapter 3, the various factors and processes involved in lahar initiation are considered from a hydrological and engineering geological perspective. Lahar initiation may be regarded as a problem involving erosion and mass failure of the 1991 pyroclastic deposits. Erosion and mass-wasting processes are evaluated by considering hydrologic conditions in the river basin as well as the physical properties of the deposits.

The rainfall threshold of lahar initiation is analyzed in Chapter 4 using calibrated data from acoustic flow monitors (AFM) as surrogate lahar hydrographs, together with rainfall measurements from telemetered rain gauges. If properly calibrated, AFM and rain gauge data provide an almost continuous record of lahars and rainfall in a river channel, which is invaluable in studying sediment yield and erosion processes. The direct relationship of lahar volume to rainfall amount is also analyzed using the same instrument data.

Chapter 5 analyzes the formation and failure of temporary blockages. The potential modes of failure of these natural dams are analyzed by evaluation of observations of past dam-breaching events, and by applying fundamental geotechnical methods of stability analysis. The problem of why some blockages fail and others have so far survived is addressed in this chapter.

Chapter 6 summarizes the findings in the study and provides possible directions for further research.

Chapter 2

ERUPTIONS AND LAHARS OF PINATUBO VOLCANO

CHAPTER 2

Eruptions and Lahars of Pinatubo Volcano

2.1. Mount Pinatubo

2.1.1. Geology and physiography

Mount Pinatubo is a dacitic volcano straddling the provinces of Tarlac, Pampanga and Zambales, in the island of Luzon, Philippines, at geographic coordinates 120°21' E, 15°08' N (Figure 1.1). It is one of several late Tertiary to Quaternary volcanic centers along the north-trending Luzon arc, which is associated with eastward subduction of the South China Sea oceanic plate along the Manila Trench (Figure 2.1). The volcano is nestled, together with other volcanic vents of similar age, along the axis of the Zambales Mountain Range, with a pre-1991 peak of 1745 m above sea level. Its pumiceous deposits radiate from the summit and fill topographic lows over Tertiary rock units. The Eocene-age Zambales Ophiolite Complex underlies most of the western half of the range, while Pliocene-Miocene volcaniclastic deposits dominate the eastern half. The geology of Mount Pinatubo is further discussed by Delfin (1984), Delfin *et al.* (1996) and Newhall *et al.* (1996). References on the geology of the Zambales Mountain Range include Hawkins and Evans (1983), J.A. Wolfe and Self (1983), Malihan (1987), Defant *et al.* (1989), Rossman *et al.* (1989), and Yumul (1994).

Before the 1991 eruption, five major rivers radiated from Mount Pinatubo: clockwise from north, the O'Donnell, Sacobia, Gumain, Marella and Maraunot-Balin Baquero-Bucao (Figure 1.1). Rivers on the northern and western sectors of the volcano were mostly incised in a broad pre-1991 pyroclastic fan from previous eruptions of Pinatubo. In contrast, the Sacobia and Gumain flowed through narrow V-shaped valleys incised in indurated bedrock before coming out into low-relief alluvial fans.

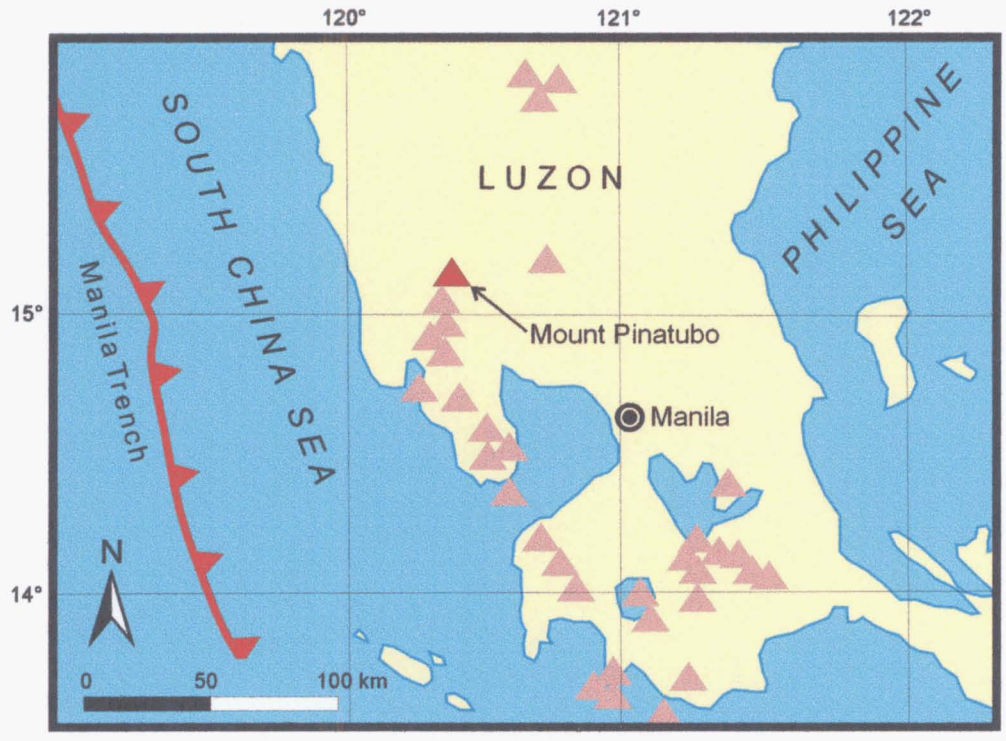

Figure 2.1. Geologic setting of Pinatubo volcano. Triangles mark Pliocene-Quaternary volcanoes. (*Modified from Newhall et al., 1996*)

2.1.2. Climate

The central Luzon region has two distinct climatic seasons: the dry season from November to April, dominated by northeasterly trade winds (locally termed *Amihan*), and the wet or rainy season from May to October, dominated by the southwest monsoon (*Habagat*). Rainfall distribution is orographically influenced by the Zambales Mountain Range, with the west side receiving more rain than the east (Figure 2.2). Of the ~20 tropical typhoons that hit the country yearly, around five pass across central Luzon, usually during the southwest monsoon season. These typhoons originate from the equatorial Pacific Ocean and move west to northwestward, commonly interacting with the southwest monsoonal flows as they approach land. Flood events in central Luzon usually coincide with the passage of such typhoons.

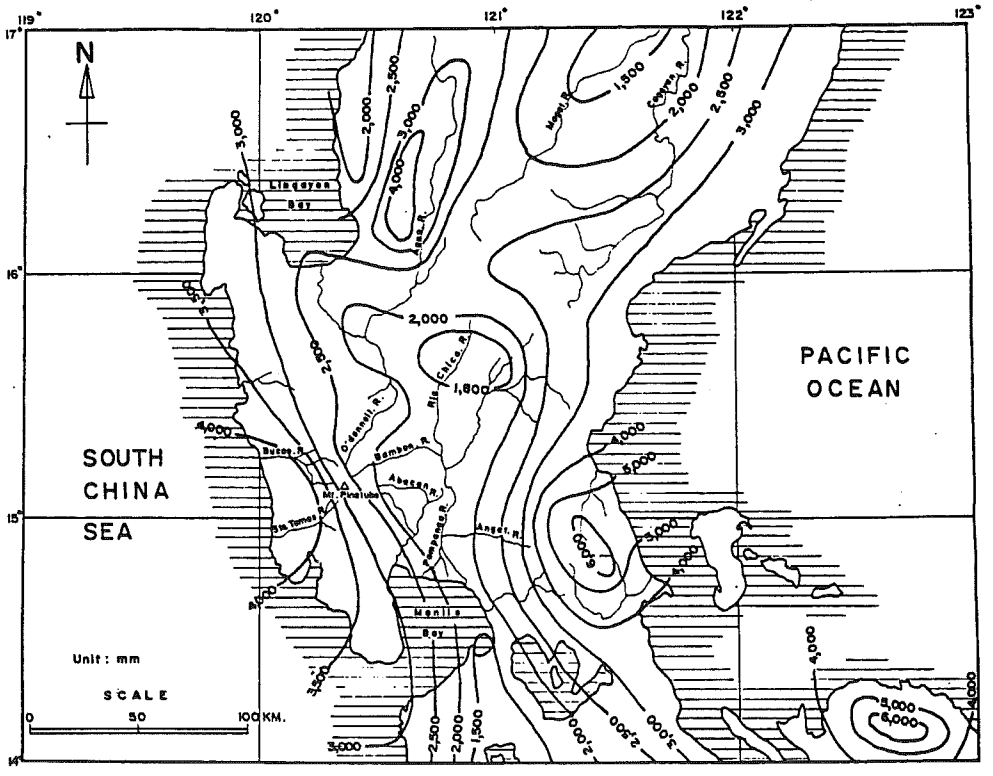

Figure 2.2. Distribution of annual rainfall in central Luzon (*Map reprinted from JICA, 1996*).

2.1.3. Eruptive history

Newhall *et al.* (1996) and Delfin *et al.* (1996) have distinguished two eruptive eras of Mount Pinatubo: an ancestral Pinatubo and a modern Pinatubo. Ancestral Mount Pinatubo, active from ~1 Ma to an unknown time before 35 ka, was an andesite-dacite stratovolcano for which no large explosive eruptions are evident. It is manifested as a partially filled 3.5 km x 4.5 km caldera, and its deposits are found as andesitic lavas that underlie much of the rugged terrain surrounding the modern edifice. Several satellite vents to the east were contemporaneous with the ancestral Pinatubo.

Modern Mount Pinatubo is a dacite-andesite dome complex and stratovolcano that is characterized by exclusively large, explosive, pumiceous eruptions at least during the last 35,000 years (Pallister *et al.*, 1993). Based mainly on radiocarbon dates, six

eruptive periods of modern Pinatubo prior to the 1991 eruption have been recognized, the last one being the Buag eruptive period about 500 years ago.

2.1.4. The 1991 eruption

The June 1991 eruption of Pinatubo volcano has caused probably the worst volcanic disaster ever in terms of social and economic impact. The eruption produced 5.5±0.5 km^3 of pumiceous pyroclastic-flow deposits (W.E. Scott *et al.*, 1996) and 3.4-4.4 km^3 of tephra-fall deposits (Paladio-Melosantos *et al.*, 1996), making this eruption one of the largest explosive eruptions in the whole world in the 20^{th} century (W.E. Scott *et al.*, 1996). Successful prediction and warning schemes kept the number of casualties directly resulting from the eruption to less than 300 (Newhall and Punongbayan, 1996; Wolfe and Hoblitt, 1996), but the socioeconomic effects of the eruption were much more devastating. The eruption directly affected more than 2 million people, with 250,000 people forced to evacuate from their homes during the height of the eruption. In 1991 alone, economic damages and production losses from the eruption amounted to about PHP 10.5 B (US$ 420 M) (Mercado *et al.*, 1996). The eruption also had profound, albeit not readily quantifiable, cultural and psychological impact to a people most of whom did not know that a volcano was in their midst (Bautista, 1996).

The geomorphic impacts of the 1991 eruption were remarkable. When the climactic eruption was over, a 2.5-km wide crater had been created, and the summit was lowered by 300 m (*Please see* Figure 2.3). The pyroclastic flows completely devastated the summit area, stripping both vegetation and topsoil in a 30-km^2 area (W.E. Scott *et al.*, 1996). Beyond this stripped zone to about 15 km downstream, the pyroclastic flows quickly dumped their loads, burying valleys with hot pumiceous deposits as thick as 200 m. The result was a monochromatic, desert-like landscape with subdued relief. Drainages that head on the volcano were buried, although they re-established themselves quickly after the eruption.

Tephra-fall and co-ignimbrite ash deposits blanketed a large area around the volcano. In the upland areas, tephra thickness exceeded 50 cm, burying or destroying vegetation.

The plinian ash that reached stratospheric heights circled the globe and temporarily affected global climate.

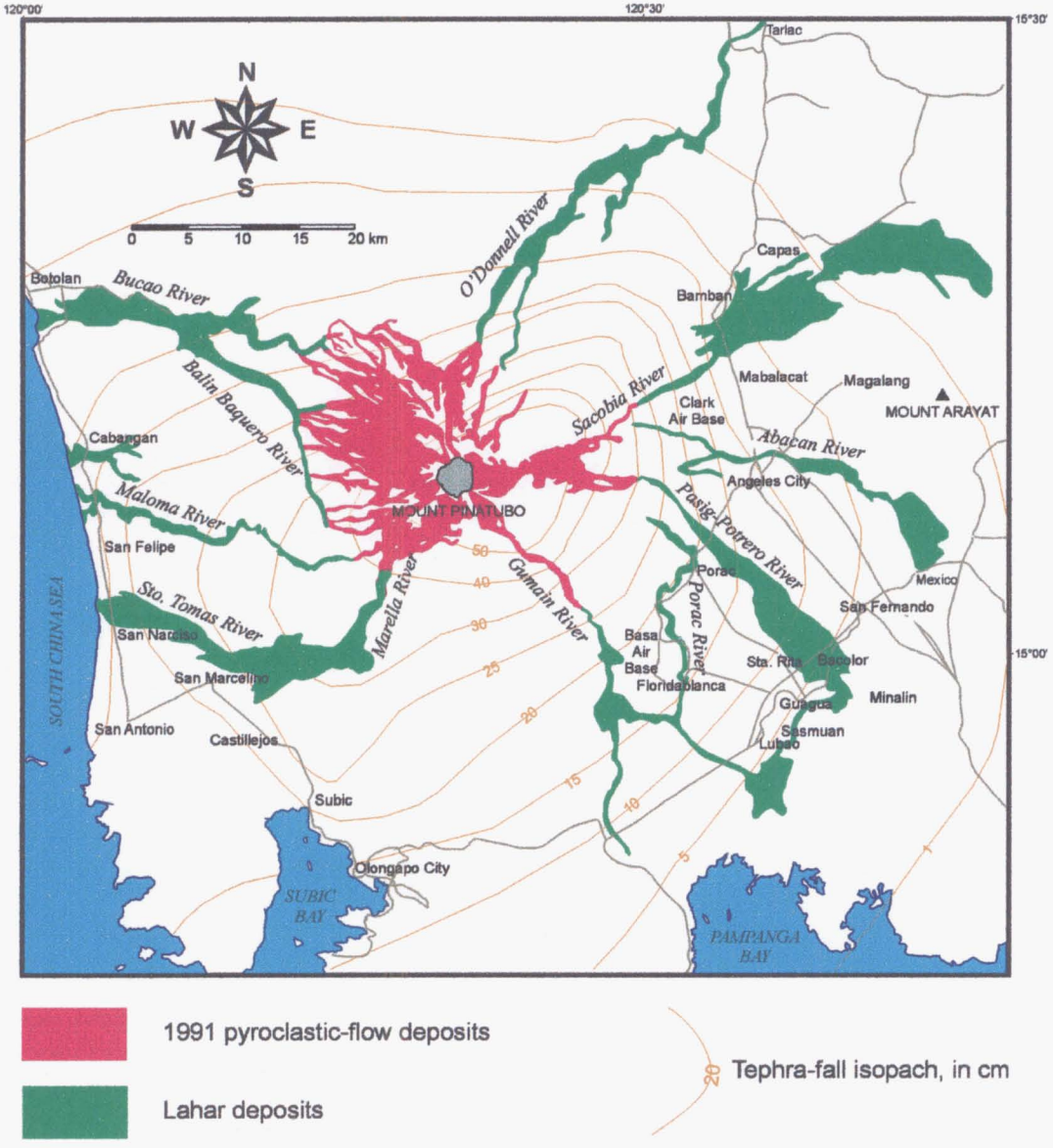

Figure 2.3. Deposits of the 1991 eruption and ensuing lahars of Mount Pinatubo (*from PHIVOLCS, unpublished map*). Lahars source their sediments mostly from the 1991 pyroclastic-flow deposits and the 1991 tephra-fall deposits.

2.2. Lahars

2.2.1. Definition

Lahar is a term of Indonesian origin, which was defined during the 1989 Geological Society of America Penrose Conference as "...a rapidly flowing mixture of rock debris and water (other than normal stream flow) from a volcano" (Smith and Fritz, 1989, p. 375). In this definition, lahar is a flow – a process or event – and its deposits are referred to accordingly as lahar deposits. The definition specifically excludes normal streamflow, although lahars may originate from bulking up of normal streamflows and may thus form a rheological continuum with them. Although non-volcanic debris flows and hyperconcentrated flows have been studied as distinct processes, the term lahar has been found indispensable as it emphasizes the unique, complex behavior of volcano-hydrologic processes while recognizing that these processes are not always directly related to eruptions.

Rheologically, lahars may be classified as debris flows or hyperconcentrated flows. Debris flows are classified by Pierson and Costa (1987) as slurry flows, which normally have significantly higher yield strengths than hyperconcentrated flows due to the dominant effects of internal friction and/or cohesion. In contrast to non-volcanic debris flows, however, debris-flow lahars typically have little clay content. Their strength is thus mainly derived from grain collisions, although a degree of cohesion may be achieved between silt-sized ash particles (Iverson, 1997; Smith and Lowe, 1991).

Hyperconcentrated flows appear to flow like liquids but have measurable, albeit low – probably less than 40 Pa – yield strengths (Pierson and Costa, 1987). They are characterized by markedly dampened turbulence, and generate deposits by grain-by-grain deposition that are intermediate in nature between those of debris flows and dilute streamflows (Smith and Lowe, 1991).

2.2.2. Pinatubo lahars

Lahars closely followed the 1991 eruption of Pinatubo, remobilizing some of the pyroclastic-flow and tephra-fall deposits to the downstream areas. In 1991 alone, more than 800 million m^3 of pyroclastic debris was brought by lahars to the lowlands. By 1996, lahar deposits had increased to more than 2.3 km^3. Aside from causing billions of pesos worth of damage, the lahars permanently displaced more than 200,000 people, necessitating massive resettlement efforts.

The lahars of Pinatubo generally form by erosion by surface water of the 1991 pyroclastic-flow deposits on the flanks of the volcano, although sediments have also come from the tephra-fall deposits on surrounding hillslopes especially during the 1991 season. Where lahars were derived from the hot pyroclastic-flow deposits, they were steaming, with measured temperatures sometimes exceeding 80°C. Lahars have also formed by the sudden failure of temporary drainage blockages that had earlier formed by rapid deposition of pyroclastic flows and lahars (Arboleda *et al.*, 1994; Umbal, 1994; Arboleda and Martinez, 1996; K.M. Scott *et al.*, 1996).

2.3. The Pasig-Potrero River

2.3.1. Pre-eruption watershed conditions

Before the 1991 eruptions, the eastern flank of Mount Pinatubo was solely drained by the Sacobia River (Figure 2.4A). The Pasig River headed on Mount Dorst, about 7 km from the Pinatubo summit, where it was separated from the upper Sacobia channel by a low dissected fan of pre-1991 pyroclastic flow deposits of modern Pinatubo. The upper Pasig River consisted of the Bucbuc Creek, which joined the Yangca Creek to form the Papatac Creek near Mount Cutuno, about 12 km from the summit. As it emerged from the hilly upland area into the alluvial plains, the Papatac Creek joined the Timbu Creek to become the Pasig River (JICA, 1978). The Pasig River becomes the Potrero River about 12 km downstream of this confluence. Prior to the 1991 eruption of Pinatubo, the total upper catchment area of the Pasig River was about 21 km^2, measured from the

headwaters of the Bucbuc down to the confluence of the Papatac and Timbu Creeks (Figure 2.4A).

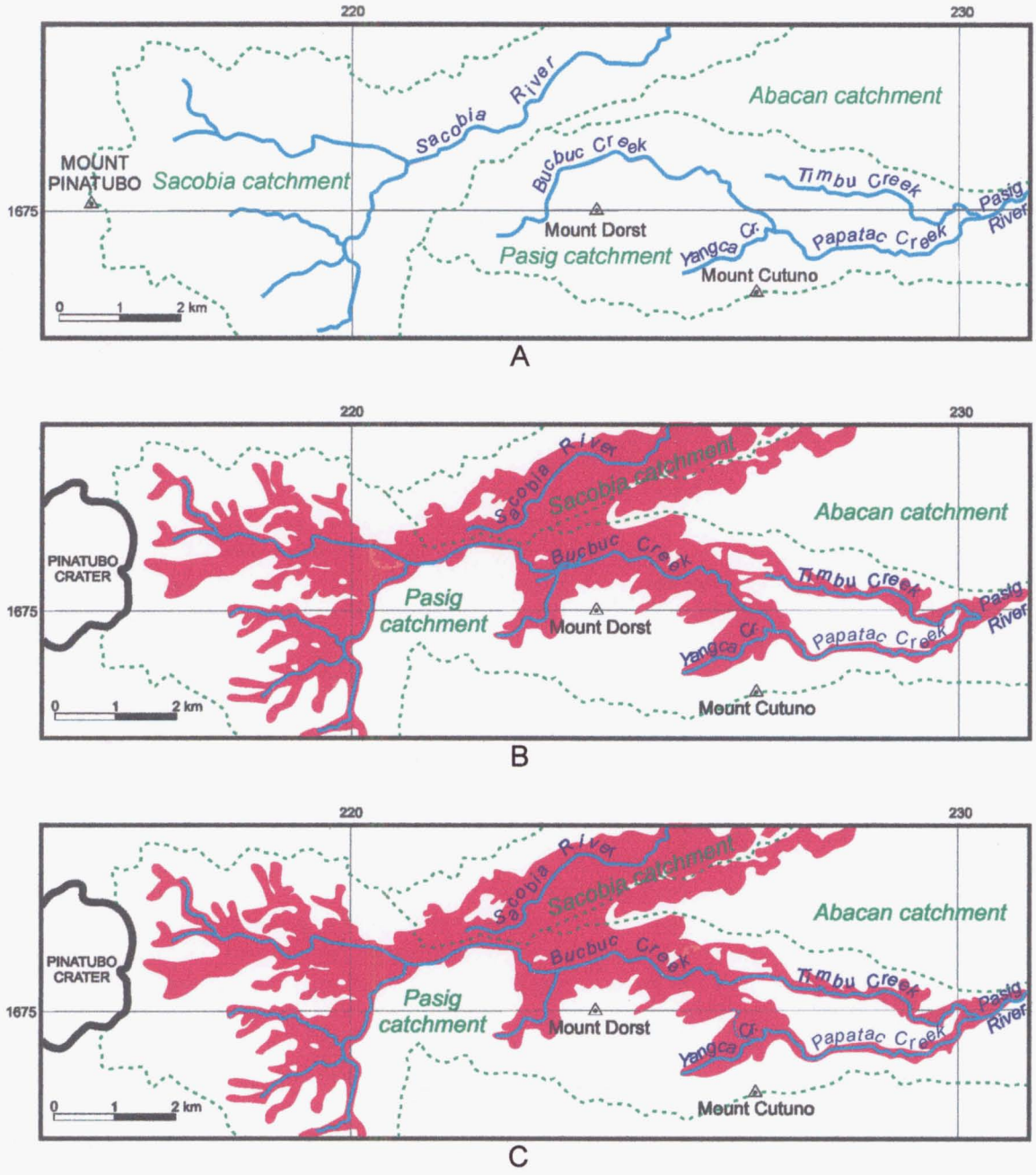

Figure 2.4. Changes in the upper catchment of the Sacobia and Pasig Rivers (*map coordinates in UTM kilometers*). Before the 1991 eruption (A), the Sacobia solely drained the eastern sector of Pinatubo. A secondary explosion (headscarp indicated by yellow symbol) led to the capture of the upper Sacobia catchment by the Pasig River in early October 1993 (B). Another secondary explosion in June 1994 resulted in the diversion of the Bucbuc Creek into the Timbu channel (C).

In their study for a sabo project, consultants from JICA (1978) have estimated various hydrological parameters for the Pasig-Potrero River; these are noted here for reference. Average annual rainfall in the Pasig River was at least 2000 mm, possibly exceeding 2500 mm in the upland area (*See also* Figure 2.2). As shown in Figure 2.5, probable maximum rainfall with a 100-year return period was estimated at 470 mm, 1050 mm and 2700 mm for 24 hours, 3 days and one month duration, respectively. The worst flooding in central Luzon in recent history occurred in July 1972. Maximum rainfall recorded during that event is given in Table 2.1.

Figure 2.5. Probable maximum rainstorms and their return period in Porac (Data from JICA, 1978).

Table 2.1. Maximum rainfall recorded during the central Luzon flood in July 1972, the worst in recent history.

	Date (1972)	Amount (mm)	Estimated return period (years)	Recording station
24 hours	19 July	292	11	Clark Air Base
3 days	18-20 July	734	25	Clark Air Base
Storm duration	16-21 July	970	65	Sta. Cruz, Porac
One month	01-31 July	2274	56	Sta. Cruz, Porac

At a stream gauging station a short distance downstream of the Papatac-Timbu confluence, the runoff coefficient (volumetric ratio of annual stream runoff to annual rainfall) for the Pasig River was estimated to be 0.34 m^3 of runoff per m^3 of rainfall on average. This was noted to be smaller than the nearby Porac River, perhaps due to more underground flow in the Pasig (JICA, 1978).

Sediment production in the Pasig River catchment was relatively high. Using unspecified field survey methods, JICA (1978) estimated that, on average, 3.3 x 10^5 m^3 (1.6 x 10^4 m^3/km^2) of sediment was being produced from hill erosion every year from 1966 to 1976. An additional 1.5 x 10^5 m^3 (7.1 x 10^3 m^3/km^2) per year was derived from channel erosion in the alluvial fan. Within an order of magnitude, the total annual sediment production of 2.3 x 10^4 m^3/km^2 is comparable to the sediment yield from the 1980 debris-avalanche deposit at Mt. St. Helens twenty years after its emplacement. Sediment yield from this deposit was estimated at 10^4 Mg/km^2, which was 100 times above typical background rates (Major *et al.*, 2000). From the total sediment produced in the Pasig-Potrero River from 1966 to 1976, it was estimated that about 80% or 4.4 x 10^6 m^3 (2.1 x 10^5 m^3/km^2) – including both hillslope and channel erosion – was produced during the flood-disaster year of 1972.

2.3.2. Post-eruption lahars and watershed changes

Impacts of the 1991 eruption

Dramatic changes in watershed hydrology of the Pasig-Potrero occurred as a direct consequence of the plinian eruption of Mount Pinatubo in June 1991 (Major *et al.*, 1996). The most significant impact of the eruption was the emplacement of about 0.9 km^3 of valley-filling pyroclastic-flow deposits that straddled the contiguous catchments of the Sacobia, Pasig and Abacan (Figure 2.4B). These deposits were as thick as 200 m, thus obliterating pre-existing drainage channels. The pyroclastic flows that entered the Pasig catchment went down both the Bucbuc-Papatac and Timbu channels, which quickly responded by extending their head channels by a few kilometers. By the end of the 1991 rainy season, the upper catchment area of the Pasig had increased slightly to 24 km^2 (Daag, 1994). Of the total volume of pyroclastic-flow deposits in the Sacobia-Pasig-Abacan catchment, 0.3 km^3 were emplaced within the new boundaries of the Pasig catchment.

Lahars from 1991 to 1993

Lahars along the Pasig-Potrero River apparently commenced during the pre-climactic phase of the 1991 eruption, as evidenced by hyperconcentrated-flow deposits between the pre-1991 soil and the 15 June plinian fall deposit (C.G. Newhall, written comm.). The first large lahar in the Pasig, however, occurred on 15 June. The 1991 lahars initially proceeded to the downstream end of the Potrero channel, inundating large urban communities of Bacolor and Guagua (Figure 2.6). With the raised base level, the locus of deposition progressively migrated upstream, and by the end of 1993, the apex of the lahar fan had moved upstream of the Porac-Angeles Road. Annual lahar deposition in the Pasig-Potrero was almost constant from 1991 to 1993, with a total of 145 million m^3 emplaced during the three-year period.

Two lahar events in the Pasig-Potrero in 1991 and 1992 were generated by the breaching of temporary blockages, both of which formed at the confluence of the Bucbuc River and Yangca Creek. The first one occurred on 07 September 1991 during

relatively light rainfall; the other occurred on 29 August 1992 during heavy rainfall. Lake-breakouts are discussed further in Chapter 5.

The 1993 Sacobia-Pasig stream piracy

On 05-06 October 1993, at the height of Typhoon *Kadiang*, a large secondary pyroclastic flow occurred in the upper reaches of the Sacobia River, completely filling up the Sacobia channel with debris and partially flowing down the Pasig channel (Punongbayan *et al.*, 1994). The filled channel of the Sacobia thus became topographically higher than the Pasig River channel. Succeeding flows from Pinatubo were thus shunted toward the Pasig. By 1:30 a.m. of 06 October, flows from the former upper Sacobia tributaries had been completely captured by the Pasig River (Figure 2.4B). The Pasig channel immediately responded to the capture by channel incision near the capture point, further increasing the elevation difference between the Sacobia and the Pasig.

The October 1993 stream piracy increased the Pasig's watershed to 45 km^2, and allowed the river to assimilate the pyroclastic-flow deposits that were hitherto in the upper Sacobia. Before the capture, about 0.15 km^3 of pyroclastic-flow deposits remained in the Pasig catchment. With the extended catchment, the volume became 0.3 km^3 – practically back to the original post-eruption pyroclastic-flow deposit volume in the Pasig.

Upstream migration of the depositional area

Because of the 1993 stream piracy, lahar activity in the Pasig was considerably increased during the 1994 rainy season, while lahars in the Sacobia River had practically ceased. Perhaps due to invigorated erosion rates in the newly extended Bucbuc channel, numerous "secondary explosions" (*Please see Section 3.6*) also occurred in the now Pasig pyroclastic-flow field. Meanwhile, the headward migration of the apex of the lahar depositional zone continued. By August 1994, the bulk of the deposits of lahars and secondary pyroclastic flows had been emplaced in the Bucbuc-Papatac and Timbu channels, with the deposits in the alluvial fan nearing the level of the highest pre-eruption terraces.

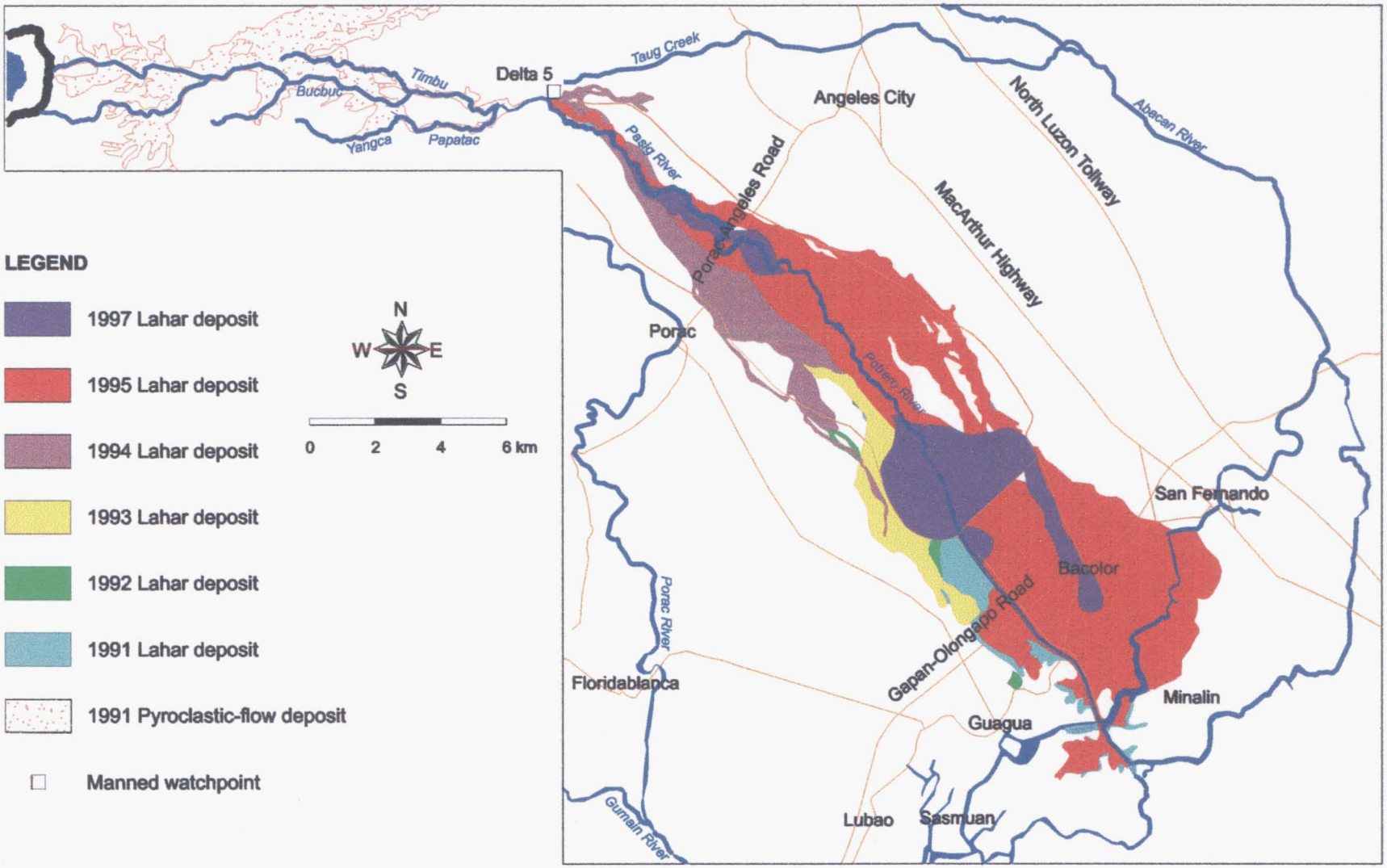

Figure.2.6. Lahar deposits in the Pasig-Potrero River basin (*from PHIVOLCS, unpublished maps*).

Stream piracy of July 1994

Fresh deposits of a relatively large secondary pyroclastic flow (*See Section 3.6*), were seen in a video taken by PHIVOLCS on 24 June 1994. The secondary pyroclastic flow apparently occurred along the Bucbuc where its divide with the Timbu Creek was narrowest (Figure 2.4C). The deposits from this event mostly went into the Bucbuc-Papatac channel and up into the Yangca Creek, with some deposits spilling onto the Timbu. Judging from the observed renewed rate of aggradation along the Timbu, it appears that flows from the upper Bucbuc Creek started to enter the Timbu soon after the June 1994 secondary pyroclastic flow (C.G. Newhall, written comm.). In contrast, lahar aggradation in the Papatac slowed down in July, and had virtually ceased by 10 August (Figure 2.7). This indicates that the diversion of the Bucbuc Creek into the Timbu had been completed by 10 August 1994. While this capture did not have any effect on catchment size or pyroclastic source volume, it must have altered the overall longitudinal profile of the Pasig River, thus changing erosion rates along the river.


B
10 August 1994


C
30 August 1994

Figure 2.6. Bed-level changes in the Papatac Creek channel, from 14 July to16 September 1994, in area near the Papatac-Timbu confluence, 2-3 km downstream of the Cutuno blockage. Aggradation in the Papatac is noted between 14 July (A) and 10 August (B), as indicated by the level of submergence of two reference hills (marked by arrows) in the Papatac channel. No significant deposition is noted after 10 August (B, C and D), suggesting that the Bucbuc Creek had been completely diverted into the Timbu, thus effectively beheading the Papatac, by 10 August. (*Photos A, B and C courtesy of C.G. Newhall; photo D courtesy of PHIVOLCS*)

The 22-23 September 1994 lake-breakout lahars

The most destructive lahar event in the Pasig-Potrero in 1994 was generated by another lake-breakout on 22-23 September, which resulted in at least 24 fatalities. Just like in 1991 and 1992, the lake was formed by a blockage at the Bucbuc-Yangca confluence. Whereas early 1994 lahars deposited their sediments upstream of the alluvial fan, the lake-breakout lahars incised through the pyroclastic debris along the Papatac gorge, lowering the channel bed by 50 m. They also incised a large canyon down the proximal and medial parts of the alluvial fan, cutting through former sugarcane fields. The lahars

reached the downstream end of the fan, again inundating the Bacolor area. The September 1994 lake-breakout is discussed in more detail in Chapter 5.

01 October 1995 Typhoon Mameng lahars

The first few lahars of 1995 used the incised channel created by the September 1994 lake-breakout to convey sediments to the medial and distal reaches of the Pasig-Potrero alluvial fan. Virtually all of the deposits from these events were emplaced downstream of the Porac-Angeles Road (JICA, 1996c).

During the passage of Typhoon *Mameng* from 30 September to 01 October, 340 mm of rain falling within 18 hours (*See Section 4.4*) brought perhaps the most devastating lahar event in the Pasig-Potrero River. The lahars swamped the town proper of Bacolor anew and inundated previously unaffected areas, killing a large, though unknown, number of people. The *Mameng* lahar was the first event that remobilized pre-eruption deposits on a grand scale. It created a meandering channel within the low-gradient Pasig-Potrero alluvial fan, through both post- and pre-eruption materials. Its deposits contained abundant clasts of large dense channel-lag boulders and otherwise fragile brown soil ripped out by debris-flow lahars from channel banks and bed. The mechanics of river meandering and remobilization processes during *Mameng* are poorly understood, but these may have been the natural response of the low-gradient alluvial-fan channel to the high discharge rates and sediment load of the flow, which in turn was related to the intensity and duration of the rainstorm that generated it. This subject is beyond the scope of this study.

20 August 1997 Typhoon Ibiang lahars

After the 1995 season, and with previous lahar-containment structures completely buried or destroyed by lahars, government engineers built the last of a series of levees, called the Megadike, which enclosed a 5-km wide area extending from the head of the alluvial fan down to the Gapan-Olongapo Road (Figure 2.6). The Megadike included a "transverse dike", which was designed to trap lahar sediments and slow down flows before reaching the Gapan-Olongapo Road, a major transportation route in south-central Luzon.

The last major lahar event in the Pasig-Potrero occurred on 20 August 1997 during the passage of Typhoon *Ibiang*, which dropped 585 mm of rainfall in 26 hours (*See Section 4.4*). The flows from this event incised the Pasig River channel in the proximal reaches of the alluvial fan, lowering the bed by as much as 18 m (Arante *et al.*, 1997). The lahar deposits were confined in the meandering channel before fanning out just upstream of the transverse dike. The *Ibiang* lahars deposited about 20 million m^3 of sediments that were rich in coarse, dense lithics (PHIVOLCS, unpublished data). After *Ibiang*, flows along the Pasig have been relatively small in terms of both volume and sediment concentration.

Chapter 3

LAHAR INITIATION PROCESSES

CHAPTER 3

Lahar Initiation Processes

3.1. Introduction to Chapter 3

3.1.1. Overview and objectives

The lahar initiation process encompasses a wide range of mechanisms, and involves an even wider range of physical factors. It includes discrete geologic triggers such as melting of snow, intense rainfall or sudden failure of dams, as well as such hydro-geomorphic processes as erosion and mass wasting. While lahars may be formed during periods of volcanic quiescence, they are generated largely in response to massive watershed disturbances caused by eruptions. The study of lahar initiation requires consideration of erosion and mass wasting processes that are complicated by intermittent volcanic eruptions, derived either from the vent or from the newly emplaced hot deposits.

In this chapter, erosion and mass wasting processes pertinent to the generation of tropical rain-lahars are reviewed and evaluated using principles of soil mechanics, hydrology and geomorphology. This involves critical review of relevant publications and some analyses of empirical observations. Complications arising from volcanic activity are discussed qualitatively. The discussions are inevitably broad; each of the lahar initiation mechanisms discussed here may comprise a whole dissertation on its own right. Nevertheless, they are useful in gaining a systemic appreciation of basin-wide processes involved in lahar initiation. Considering the unique setting of Pinatubo – a large-scale pumiceous eruption in a tropical region – such a study is valuable in order to fully understand the dynamic physical context of tropical lahars. This chapter seeks to help fill this knowledge gap.

3.1.2. Conceptual framework of evaluation

Lahar generation is basically a sediment production and transport problem, albeit complicated by volcanic processes. That is, lahars observed in river channels are the result of large amounts of sediments being rapidly entrained by rainfall and runoff from different parts of a catchment, then concentrated and delivered by flows to the channels. Erosion and mass wasting processes are thus fundamental to lahar generation. In this study, lahar initiation is regarded as a product of these two degradational processes that occur in greatly increased rates following a major tephra-producing volcanic eruption.

3.1.3. Organization

The ultimate cause of Pinatubo lahars – the hydro-geomorphic disturbance caused by the 1991 eruption – is first discussed in Section 3.2. Then, the discussions follow the path of water and sediments as they interact to form lahars, from the atmosphere to the main river channels (*See* Figure 3.1). Rainsplash and hillslope processes are discussed in Section 3.3; erosion of the valley-fill pyroclastic deposits in Section 3.4; and main-channel processes in Section 3.5. Secondary hydroeruptions, pyroclastic flows and slides, which are unique volcano-hydrologic phenomena that have great impacts on lahar occurrence, are discussed separately in Section 3.6. Observed changes in the lahar-generating factors and processes through time, and the resulting changes in sediment yield, are described in Section 3.7. Section 3.8 summarizes the discussions, and provides recommendations for future research.

3.2. Origin of Pinatubo lahars

3.2.1. Some definitions

In this chapter, *sediment source area*, or simply *source area*, refers to the upper catchment of a river where lahars derive most of their sediments. This area is where the 1991 pyroclastic-flow deposits were emplaced, and includes both the valleys filled with

the deposits and the adjacent hillslopes. The source area varies from river to river, but is generally within 15 km from the volcano summit.

Rills, *gullies* and *(main) river channels* are used with reference to the relative size and origin of drainage channels. Rills formed after the eruptions essentially as "storm drains", are ephemeral, and provide the first channels to catch overland flow. These include the subparallel rills that formed on the tephra-covered hillslopes, as well as the dendritic network that formed on the 1991 pyroclastic-flow deposit. Post-eruption rills are typically V-shaped, with steep valley walls. Gullies are comparatively larger, but still ephemeral, channels. They may evolve from rill enlargement and integration, or may be inherited from the pre-eruption hillside topography. Gullies that develop from rill enlargement in pyroclastic deposits may be distinguished by their wider beds, although for most discussion purposes, they are regarded to be the same as rills. Gullies inherited from pre-eruption topography are considered on their own right. The main river channels comprise the perennial, first- and second-order streams. These are mostly the main trunks of pre-eruption rivers, which reestablished dynamic channels shortly after the 1991 eruption.

3.2.2. Pre-eruption sedimentation

Prior to the 1991 eruption of Pinatubo, most of the hillslopes around the volcano were covered with tropical trees, shrubs and grasses, and rivers did not manifest any laharic activity. However, even after almost 500 years since the previous eruption, sedimentation rates in some rivers around the volcano remained relatively high. Field surveys conducted by consultants of Japan International Cooperation Agency (JICA) for a flood-control project in the Pasig-Potrero River showed sediment production in the upland catchment to be around 1.6×10^4 m^3/km^2 per year (JICA, 1978). This is comparable to erosion rates in the Toutle River basin within twenty years after the 1980 eruptions of Mount St. Helens (Collins and Dunne, 1986; Major *et al.*, 2000). During the 1972 floods – the largest recorded in the central Luzon region – they estimated that upland sediment production was 1.2×10^5 m^3/km^2, with another 8.5×10^4 m^3/km^2 produced by scouring of the riverbed farther downstream. The JICA consultants

attributed this high rate of erosion mainly to "collapse on the hillsides caused by riverbank erosion" and "surface erosion on the collapse slope" (JICA, 1978, p. 13).

While sediment production rates were relatively high, no report of debris flow occurrence has ever been recorded around Mount Pinatubo prior to the 1991 eruption. The uppermost pre-1991 stratigraphic units in the alluvial fans mainly consist of sequences of normal streamflow deposits (Figure 3.1), suggesting that lahars have ceased to occur an unknown time after the preceding eruption.

Figure 3.1. Uppermost stratigraphic sequence of the pre-1991 Pasig-Potrero alluvial fan; photo taken near the apex of the fan at Delta 5. This >15-m sequence consists of stratified, loose, sandy layers characteristic of normal streamflow deposits. Debris-flow units are conspicuously absent in this sequence.

3.2.3. Hydro-geomorphic impacts of the 1991 eruption

The most significant hydro-geomorphic impacts of the 1991 eruption are:

1) The devastation of the summit area of the volcano, including the removal of its summit dome and the stripping of soil and vegetation in a 3-km radius;

2) The deposition of 5.5 km^3 of hot pyroclastic-flow deposits, which filled up valleys to as much as 200 m; and

3) The mantling of the surroundings with a tephra layer that changed the infiltration capacity of the surface.

From a systemic perspective, a river affected by pyroclastic flows will adjust to both head valley devastation and the emplacement of a large amount of loose debris on its upper reaches by adjusting its longitudinal profile, that is by rapid erosion in the upper reaches and deposition of the remobilized material in the lower reaches (Figure 3.2). As seen at Pinatubo, most of the erosion and deposition is done by lahars. The river's longitudinal profile initially changes rapidly as it copes with all the simultaneous erosional and depositional processes in the entire catchment, until a relatively stable profile is attained.

Devastation of the summit area

The 1991 eruption produced a 2.5-km wide caldera, and reduced the summit elevation by 300 m. This in itself reduced the catchment areas of rivers that headed on the volcano, although the reduction in size is probably insignificant compared to the other effects of the eruption. Perhaps of greater effect is the devastation of a 30-km^2 area around the summit by energetic pyroclastic flows. Although the 1991 pyroclastic flows were considered relatively sluggish by world standards, their energy was sufficient to completely strip the area within a 3-km radius of all vegetation, topsoil and colluvium. Only minor deposits were emplaced in this zone of total devastation (W.E. Scott *et al.*, 1996). The stripped material added to the volume of the pyroclastic-flow deposits. In addition, the stripping of the surface layer must have decreased infiltration and enhanced runoff.

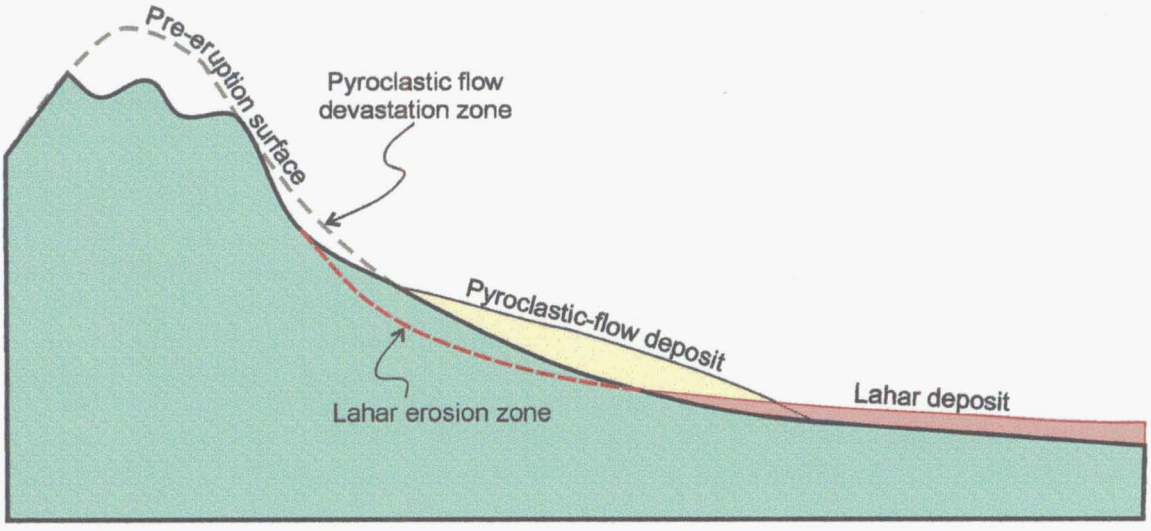

Figure 3.2. Schematic diagram showing changes in the longitudinal profile of a river affected by a large volcanic eruption.

Pyroclastic-flow deposits

Beyond the devastated zone, the pyroclastic flows were much less erosive; rather, they filled valleys with deposits as thick as 200 m, drowned low hills, and, in instances, obliterated major drainage divides. In total, the 1991 pyroclastic flows of Pinatubo emplaced about 5.5 km^3 of loose, hot deposits (pyroclastic-flow deposits) over a 400-km^2 area in all sectors of the volcano.

W.E. Scott *et al.* (1996) identified three facies of the 1991 pyroclastic-flow deposit: (1) massive pumiceous facies, (2) stratified pumiceous facies, and (3) lithic-rich facies. The massive pumiceous facies constitute the bulk of the pyroclastic-flow deposit, occurring mainly as thick valley fills. The stratified pumiceous deposits typically occur as <5-m thick veneers in areas within 2-5 km from the summit. Both massive and stratified pumiceous deposits are dominantly sand-sized, generally poorly sorted, with less than 18% fines (silt and clay). The lithic-rich facies include lag breccias and late-stage caldera-collapse deposits confined to head valleys just beyond the devastated zone. These deposits typically contain decimeter-sized angular to subangular clasts of dense lava dome fragments in a coarse sand-sized pumiceous matrix. Compared to other pumiceous pyroclastic-flow deposits elsewhere in the world, the 1991 Pinatubo

pyroclastic-flow deposit was somewhat better sorted and contained less fine material, which perhaps account for the flow's lower mobility (W.E. Scott *et al.*, 1996). Pertinent properties of the various facies of the 1991 pyroclastic-flow deposits of Pinatubo are listed in Table 3.1.

Table 3.1. Properties of the 1991 Pinatubo pyroclastic-flow deposit (*condensed from W.E. Scott et al., 1996 and Torres et al., 1996*)

	Massive pumiceous facies	Stratified pumiceous facies	Lithic-rich facies
Distribution	Valley-fill	Veneer over upland area	Confined to head valleys
Thickness	10 - 200 m	<5 m	5 – 10 m (?)
Sedimentary structure	Massive	Stratified	Massive
Median grain size	0.1 - 1 mm	0.3 – 1 mm	~1 mm
Sorting	Poor (1.7-3.1 ϕ)	Moderate to poor (1.3-2.5 ϕ)	Poor (2.9-3.5 ϕ)
Composition	Pumiceous	Pumiceous	Dense lithics
Density	10 – 15 kN/m^3	10 - 15 kN/m^3	17 – 21 kN/m^3 (?)
Temperature of emplacement	>450°C	>450°C (?)	Unknown

Owing to its volume and thickness, the valley-filling massive facies of the 1991 pyroclastic-flow deposits probably have the greatest impact on the hydrology of affected river basins. The low bulk density (1000 to 1500 kg/m^3) of the pumiceous deposits makes them very susceptible to erosion. Their high emplacement temperature – >450°C (Bina *et al.*, 1999) – permitted en masse remobilization of deposits by secondary hydroeruptions and secondary pyroclastic flows even years after their deposition. Furthermore, by filling river valleys, the deposits drastically altered longitudinal profiles of river channels (Figure 3.2), raised the groundwater table and reduced the infiltration capacity of the surface.

Tephra-fall deposits

Four distinct layers of the 1991 Pinatubo tephra-fall deposits, representing various phases of explosive eruptions from 12 June to mid-August, were identified by Paladio-Melosantos *et al.* (1996). These are shown in Figure 3.3. The tephra-fall sequence consists of three units of generally sand- to granule-sized ash and lapilli (Layers A, B and C) that are overlain by a laminated silt- to fine sand-sized ash layer (Layer D). From a hydrological perspective, Layers A, B and C may be grouped as the lower coarse tephra unit, while Layer D may be considered as the upper fine tephra unit (Pierson *et al.*, 1996). In total, the 1991 tephra-fall deposits had a volume of around 4 km^3, including the ash that fell in the South China Sea, and attained a cumulative thickness of at least 0.5 m in the source area.

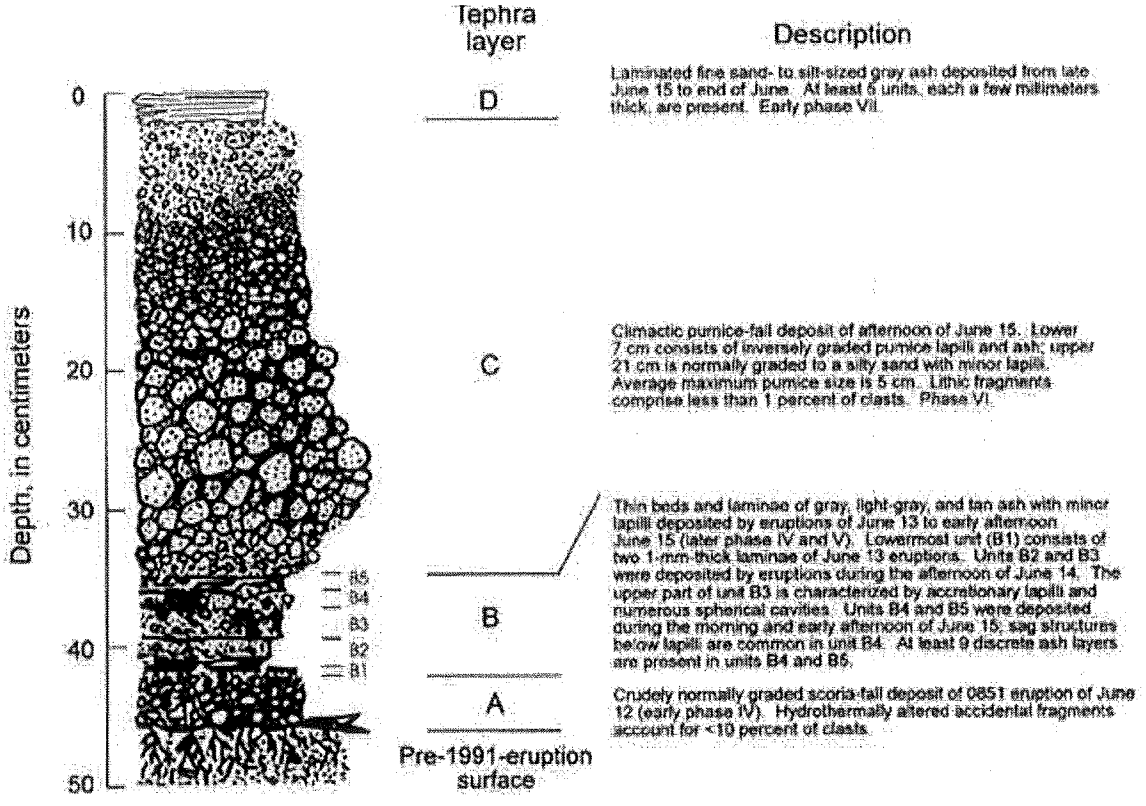

Figure 3.3. Stratigraphy of the 1991 tephra-fall deposits of Pinatubo volcano (from Paladio-Melosantos *et al.*, 1996).

Tephra-fall deposits have been known to alter hillslope hydrology by burying or destroying vegetation, and by forming an impermeable crust that reduces infiltration and increases runoff. Pinatubo is no exception. While conceding that the valley-filling pyroclastic-flow deposit had the greatest impact on watershed hydrology, Major *et al.* (1996) emphasized the effects of airfall tephra in such disturbance, citing evidence of greatly increased runoff even before the emplacement of the bulk of the pyroclastic-flow deposits on 15 June 1991.

The formation of an impermeable crust on newly deposited tephra is a well-documented, yet generally poorly understood, phenomenon around volcanoes. Segerstrom (1950) described such a crust on the surface of the ash at Parícutin Volcano, and considered it a result of mechanical compaction and sorting of the surficial ash by raindrop impact. Waldron (1967), on the other hand, proposed a chemical origin for a similar crust at Irazú Volcano to explain its persistence in the uppermost layer – that is, the absence of buried crusts – despite the continuous deposition of new ash. He ascribed this to some halogen brought to the surface by capillary action where it was precipitated by evaporation in the upper few millimeters of the ash. He further postulates that "when the crust is buried by fresh ash, the precipitated salts are redissolved and again carried upward by capillary action* * *" (Waldron, 1967), p. 18), thus keeping the crust at the top of the ash deposit.

Although tephra crusts at Pinatubo have not been the subject of particular research, they have indeed been directly observed (*e.g.*, Pierson *et al.*, 1996, p. 928). During fieldwork in 1999, rigid crusts were found capping some narrow inter-rill ridges in pyroclastic-flow deposits. The crust may have been formed in part by the fine ash from the post-climactic eruptions (Layer D) and from numerous secondary explosions. J.E. Bailey (University of Hawaii, oral comm.) had photographs of undissected surfaces of the 1991 pyroclastic-flow deposits, which he noted were capped by Tephra Layer D. Mechanical compaction of this layer by rainfall impact and sheetwash is believed to have promoted the development of the impermeable tephra crust.

3.2.4. Overview of the lahar-initiation process at Pinatubo

To model lahar initiation processes at Pinatubo, an initial condition where valleys are filled with pyroclastic-flow deposits and the surrounding hillslopes are blanketed by tephra is assumed. The surface of the valley-filled deposits is relatively smooth, although surface irregularities exist. In the hillslopes, vegetation is either buried by or coated with tephra. Rainfall mixes with the tephra coating as well as with airborne ash from secondary explosions to produce muddy rain, which turn to muddy overland runoff that has greater erosive power than clean runoff. Erosion by rilling proceeds rapidly on both hillslope and valley-fill surfaces, with rills preferentially formed on microtopographic lows in the valley-fill deposits. Because of the high initial sediment concentration of the runoff (from muddy rainfall) and the high erodibility of the loose tephra surface, rill-erosion rates are high, and lahars start to form in the rills. Simultaneously, rapid headward erosion starts at the downstream reaches of the pyroclastic-flow deposits where river channels are not fully buried. The rapid channel erosion promotes bank collapses in the pyroclastic-flow deposits, which further feed the flows with sediment. The rills and river channels quickly form an integrated system, which at Pinatubo had formed within two months after the climactic phase of the eruption (Rodolfo *et al.*, 1996). The bulking up process continues for as long as enough rain falls on the affected river catchment.

Figure 3.4 illustrates the different erosional processes in an upland catchment that contribute to the initiation of lahars. The processes are further discussed in the following sections.

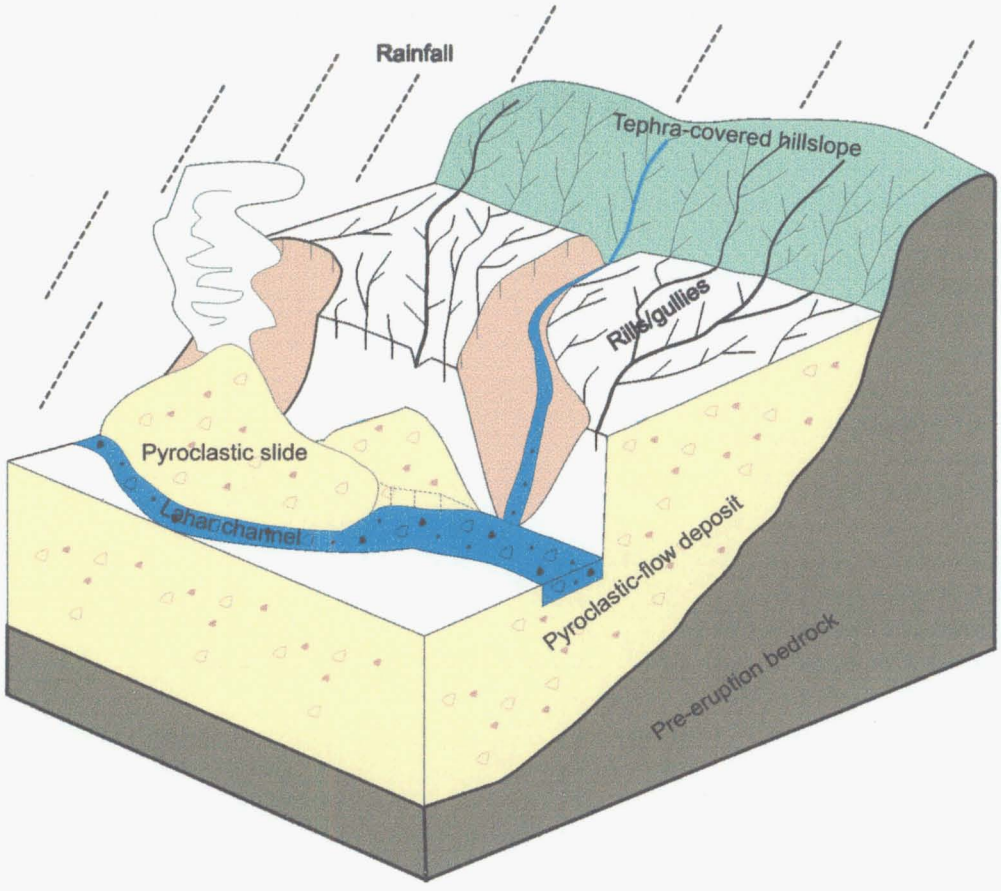

Figure 3.4. Schematic illustration of the path of water in a volcanically disturbed watershed, from rainsplash on tephra-covered hillslopes to channelized flows in a river incised in loose valley-fill pyroclastic deposits. Sediment entrainment starts as soon as muddy rain falls on the tephra-covered landscape. Muddy runoff quickly bulks up with sediments as it forms an intricate system of rills, where its sediment concentration begins to reach laharic levels. Lahars bulk up even more as they get concentrated in larger channels where they are further fed by bank collapses, the failure rates of which are enhanced by the high temperature of the material.

3.3. Erosion processes on tephra-covered hillslopes

Hillslope processes are generally classified into *inter-rill* and *rill* erosion based on the dominant sediment entrainment mechanism (Bryan, 2000). Sediment entrainment in inter-rill areas is dominated by rainsplash and overland flow, whereas channelized runoff is the main agent of rill erosion.

3.3.1. Rainsplash and inter-rill erosion

In the overall lahar sediment budget, the volume of sediments contributed by rainsplash erosion is probably negligible. However, rainsplash may have played a significant role in terms of initiating runoff erosion. The impact energy exerted by raindrops on the ground surface is given by the kinetic energy equation, $KE = \frac{1}{2}mv^2$. The impact velocity, v, is mainly influenced by wind and canopy disturbance. The splash process is also affected by soil water conditions, with saturated soil more vulnerable to entrainment due to reduced soil shear strength. However, ponding of water on the surface may suppress splash entrainment if the water is deep enough. Kinnell (1990) found a marked decrease in soil detachment at pond depths greater than three times the median raindrop diameter. Rainsplash is considered to have little effect on deep surface flow, but can strongly influence shallow flow hydraulics (Bryan, 2000).

In erupting volcanoes, rainsplash energy is further affected by ash. Airborne ash, and that which coats trees and grasses – whether vent-derived or deposit-derived) – readily mixes with rainwater to produce "muddy" rain. Such muddy rain was often experienced around Pinatubo until 1992, and was certainly common in the pyroclastic-flow deposit fields around the volcano until 1994. If rainfall was light in relation to the amount of airborne ash, accretionary lapilli deposits might form by quiet settling. Secondary ash eruptions, however, often occurred during intense rainfall, thus muddy rain usually splashed on the ground with significant impact, as lahar observers have personally experienced during field monitoring activities. The actual effect of ash on raindrop kinetic energy was not measured during the course of this particular study. As an illustration, a modest 10% increase in raindrop volume due to adhering ash (density $\approx$ 1500 kg/m^3) increases the raindrop mass – and therefore the kinetic energy – by 15%.

The increased splash energy on a surface covered by loose tephra promotes inter-rill erosion. Sustained by rain, the sediment-laden inter-rill overland flow is quickly channeled into incipient rills, which develop rapidly into an intricate sediment delivery system.

3.3.2. Rill and gully development

Even with enhanced rainsplash, inter-rill erosion on hillslopes around Pinatubo is minor compared to rill erosion resulting from the channelization of overland flow. For overland flow on a planar slope, Horton (1945) defines a critical length or "belt of no erosion" – the inter-rill area – by the physically based equation:

$$x_c = \frac{65}{q_s n}\left(\frac{R_i}{f(S)}\right)^{5/3} \qquad \text{Equation 3-1}$$

where x_c is the critical length, measured in ft from the top of the slope

R_i is initial erosion resistance of soil, in lb/ft^2

q_s is runoff intensity, in inches per hr

n is Manning's surface-roughness factor; and

$f(S) = \frac{\sin\alpha}{\tan^{0.3}\alpha}$ is a function of slope, α

Unfortunately, none of the parameters in Equation 3-1 has been measured in the field, particularly during the early stages of tephra deposition. A qualitative evaluation of the significance of the equation may nevertheless be considered. More than the other parameters, the critical length is sensitive to the erosion resistance of the surface, which may vary by one or two orders of magnitude, and the runoff intensity. The tephra cover, especially the ephemeral ash produced by intermittent secondary explosions, reduces R_i, by burying vegetation and providing a loose sediment cover. Reid (1989) has found that a barren soil may have an erosion resistance that is an order of magnitude lower than an equivalent but vegetated soil. Immediately after its deposition, the loose tephra blanket provides an immediate source of sediment that is easily entrained by rain and inter-rill runoff to increase runoff intensity, q_s, as discussed in Section 3.3.1. Very soon after, rainfall impact and sheetwash combine to mechanically compact the tephra to form a crust that inhibits infiltration. With reduced R_i and increased q_s, Equation 3-1 predicts a narrow inter-rill area in tephra-covered catchments. This is supported by observations of extensive hillslope rills that extend close to watershed lines.

The erosive power of runoff at Pinatubo is greatly enhanced by the flow's high initial sediment content (*See Section 3.3.1*). Unconfined centimeter-scale debris flows have been observed at other volcanoes such as Parícutin, Mexico (Segerstrom, 1950) and Ruapehu, New Zealand (Manville *et al.*, 2000), attesting to the high sediment concentration of rain-derived overland flow on tephra-covered surfaces. Given enough rainfall to sustain it, overland flow quickly collects in surface depressions to transform into sediment-rich rill flow. This has been observed in tephra-covered unvegetated ground, such as unpaved roads, which were rapidly incised to form deep rills. Such rate of erosion was not evident at Pinatubo before the 1991 eruption.

3.3.3. Sediment contribution of hillslope processes

The most often stated effect of tephra cover is the reduction in infiltration and increase in runoff (*e.g.*, Segerstrom, 1950; Waldron, 1967; Collins and Dunne, 1986). Interestingly, in his ongoing PhD research, A.S. Daag (International Institute for Aerospace Survey and Earth Sciences / PHIVOLCS, written comm.) found that infiltration on Pinatubo deposits is chiefly a factor of rainfall intensity, with the different types of deposits showing very similar infiltration capacity. However, he was not able to compare infiltration rates between post-1991 and pre-1991 surfaces, and his measurements were made long after the deposition of the various deposits.

Aside from reducing infiltration, the tephra itself is a rich source of sediment, considering that its loose emplacement and low density makes it very erodible. Thus, a substantial change in runoff activity was noted around Pinatubo even before the climactic phase of the 1991 eruption – that is, before the emplacement of the valley-filling pyroclastic-flow deposits (Major *et al.*, 1996). Debris-flow and hyperconcentrated-flow lahars were recorded immediately after the 15 June climax (Major *et al.*, 1996; Pierson *et al.*, 1996; Rodolfo *et al.*, 1996; K.M. Scott *et al.*, 1996; Umbal and Rodolfo, 1996), even before river channels were fully established.

In catchments where little or no pyroclastic-flow deposits were emplaced, such as the Tanguay (west of Pinatubo), Bangat (northeast), Porac-Gumain (southeast) and Maloma

(southwest), lahars were derived chiefly from the tephra-fall deposits (Janda *et al.*, 1996; Punongbayan *et al.*, 1994). The tephra-fall deposits in these catchments were practically depleted by the end of 1991. Aerial surveys before the 1992 rainy season also revealed relatively tephra-free hillslopes, with recovered vegetation. These indicate that erosion of hillslope tephra was sufficient to form lahars by themselves. Assuming that all the tephra-fall deposits on hillslopes not covered by the 1991 pyroclastic-flow deposit were eroded during the 1991 season, the volume contribution of hillslope erosion with respect to the total lahar-deposit volume may be estimated. As detailed in Table 3.2, the tephra cover on hillslopes may account for a maximum of 20% of the total lahar volume during the 1991 season.

Table 3.2. Sediment contribution of tephra-fall deposits on hillslopes.

	Total upland area (km^2)[†]	Area covered by pf (km^2)[†]	Area of hillslopes not covered by pf (km^2)	Average thickness of tephra (m)[††]	Volume of hillslope tephra (10^6 m^3)	Volume of 1991 lahar deposits (10^6 m^3)[†]	Ratio of hillslope tephra to 1991 lahar deposits
O'Donnell-Bangat	89	10	79	0.3	24	80	0.30
Sacobia-Pasig	69	22	47	0.5	24	250	0.09
Gumain	41	2	39	0.5	20	60	0.32
Marella-Sto. Tomas	79	22	57	0.5	28	185	0.15
Balin Baquero-Bucao	262	65	197	0.3	59	250	0.24
Total / average	540	121	419	0.4	155	825	0.19

[†] From (Janda *et al.*, 1996); pf = pyroclastic-flow deposit
[††] Approximated from unpublished isopach map by PHIVOLCS

3.4. Rill erosion on valley-fill pyroclastic deposits

Rainsplash and rill erosion proceeded very rapidly on the surface of the 1991 pyroclastic-flow deposit due to the total absence of vegetation. The irregularly undulating surface of the deposits promoted quick transformation of overland sheetflow to rill flow, and the high sediment load of the initial flows promoted bed incision on the very erodible, low-density pumiceous surface. Almost immediately after the climactic eruptions, main river channels began to re-establish themselves on the valley-fill deposits by rapid headward erosion (Rodolfo *et al.*, 1996; K.M. Scott *et al.*, 1996). As the rills integrated with the main river channels (See also Section 3.5), the local base level for the rills changed, thus further accelerating rill erosion. Headcuts in the Sacobia River valley were estimated by K.M. Scott *et al.* (1996) to be greater than 10 meters in height, while Rodolfo *et al.* (1996) observed deep, narrow tributaries, about 15 to 70 m wide and less than 20 m deep, feeding the Bucao and Santo Tomas Rivers. By the end of the 1991 rainy season, an intricate system of rills had developed on the fresh pyroclastic-flow deposit all around Pinatubo, providing an efficient sediment delivery system that promoted the formation of lahars.

3.4.1. Controls on rill erosion

The rate of rill incision on the pumiceous pyroclastic-flow deposits is controlled by (1) intensity and duration of rainfall, (2) longitudinal profile of the rill, (3) erodibility of the material in which the rill is incised, and (4) contributing area to each rill, which is a function of rill density. The longitudinal profile of the rill is controlled by local base level, which is provided by the fluctuating larger channel to which the rill connects. The erodibility of the material may be appreciated by considering the shear stress necessary to erode it. For a laminar flow, bed erosion starts when the critical shear stress of the bed material is exceeded by the basal shear stress exerted by the flow. The critical boundary shear stress for such a flow is:

$$\tau_c = \gamma h_c \sin\alpha$$ Equation 3-2

where τ_c is the critical boundary shear stress

γ is the unit weight of the eroding liquid

h_c is the critical flow depth at which bedload transport starts

α is the slope of the flow surface

Montgomery *et al.* (1999) found that for low-flow conditions in the Pasig-Potrero, the critical flow depth is ½ the diameter of the grain. Thus, on an undissected pyroclastic-flow deposit, with a surface slope of 3 degrees and a median grain size of 1 mm, the critical boundary shear stress is 0.26 Pa, which is an order of magnitude lower than that measured by Reid (1989) for unvegetated cohesionless soils.

3.4.2. Sediment contribution of rills

During rainstorms, flows in rills and gullies were invariably sediment-laden. This was observed in the field during monitoring activities, and supported by common observations of small, lobate debris-flow deposits at the mouth of rills (*e.g.*, Rodolfo *et al.*, 1996). Similar small-scale debris-flow deposits have been documented in other volcanoes (*e.g.*, Segerstrom, 1950; Manville *et al.*, 2000).

Daag (1994) measured drainage density on the pyroclastic-flow deposit in the Sacobia-Pasig catchment by overlaying aerial photographs using Geographic Information System (GIS) techniques, and came up with a figure of 0.013 to 0.032 (average = 0.023) m/m^2 after the 1991 season. This figure is comparable to pre-eruption drainage density on "highly dissected" pumiceous pyroclastic-flow deposits (Daag, 1994). Thus, it appears that an efficient drainage network had been established less than 5 months after the emplacement of the deposits. The volume of sediments contributed by rill erosion may roughly be approximated using the drainage density and an estimate of average cross-sectional area of the rills. As shown in Table 3.3, rill erosion may have contributed about 30% of the total lahar volume in 1991.

Table 3.3. Sediment contribution of rills and gullies on the pyroclastic-flow deposit.

	Area covered by 1991 pyroclastic-flow deposit (km^2)	Total rill length (km)*	Volume of rills (10^6 m^3)**	Volume of 1991 lahar deposits (10^6 m^3)	Ratio of rill volume to lahar deposit volume
O'Donnell-Bangat	10	200	20	80	0.25
Sacobia-Pasig	22	440	44	250	0.18
Gumain	2	40	4	60	0.07
Marella-Sto. Tomas	22	440	44	185	0.24
Balin Baquero-Bucao	65	1300	130	250	0.52
Total	121	2420	242	825	0.29

* Computed from average drainage density (~0.02 m/m^2) of the surface of the pyroclastic-flow deposits by the end of the 1991 rainy season (Daag, 1994)

** As a rough approximation, rill cross-sectional area was assumed to be 100 m^2 based on observations of headcutting rills in the Sacobia (K.M. Scott *et al.*, 1996) and the estimates of rill dimensions in the Marella in 1991 by (Rodolfo *et al.*, 1996).

3.5. Processes in main river channels

As rills and gullies were forming on hillslopes and on the surface of the pyroclastic-flow deposits, main river channels were rapidly extending headward. Within two months after the climactic eruptions, the rills had integrated with the main channels (Rodolfo *et al.*, 1996; K.M. Scott *et al.*, 1996), forming a complex sediment transport system in which rills and river channels dynamically influenced each others' processes. The main channel provided a rapidly fluctuating base level for its rill-tributaries, while the rills provided large quantities of sediments that had profound influence on the aggradation or degradation of the main channel. This feedback loop makes it virtually impossible to predict channel response, except perhaps by viewing it in a system-wide and long-term context.

During rainstorms, flows entering main river channels were invariably laden with sediments. Small-scale debris-flow deposits were commonly found as lobes at the mouth of rills, temporarily stored along the main channels until they were eroded by subsequent flows.

3.5.1. Bed erosion

At Pinatubo, pumiceous channel-beds have been observed to be extremely mobile, even at low flow conditions and on relatively low-gradient channels (<5%), chiefly owing to the low density of the material and the low bed roughness (Montgomery *et al.*, 1999). Lahars are far more erosive than normal streamflow because of their density, and have been observed to incise channel-beds to depths as much as a few tens of meters during a single storm event. During the passage of Typhoon *Ibiang* in August 1997, for example, lahars lowered the channel-bed at Delta 5 by 18 m (Arante *et al.*, 1997). In some occasions, they have even carved new valleys out of cohesive pre-eruption deposits. Further evidence to the scouring power of lahars is the prevalence of large (few meters in diameter), subrounded boulders in lahar deposits, presumably channel-lag deposits entrained by the flows, such as those found in the deposits of the 1995 *Mameng* lahars.

Whether channel-bed erosion can actually transform normal streamflow into lahar is uncertain. Tognacca and Bezzola (1997) studied debris flow initiation by channel-bed failure using laboratory experiments, and found that debris flows can indeed be initiated by bed failure depending on slope, bed-material properties, and surface and groundwater discharge. However, their experiments were performed on ≥18° flumes – much steeper than the <3-degree gradients of most lahar channels at Pinatubo. No debris flow of significant size has been observed in channels with little source sediments even when the channels themselves had beds made of pumiceous, sandy material.

Observations of rapid channel-bed degradation at Pinatubo were during lahar events, when flows in the main channel were already sediment-laden to begin with, with most of the sediments delivered by tributary rills. The shear stress on the channel bed is

directly proportional to the product of flow density and flow depth (Equation 3-2). During lahar events, flow densities can increase by as much as 100%, and flow depths increase several times in proportion to the volume added by the entrained sediments.

3.5.2. Bank failures

Even before the 1991 eruption, riverbanks on old lahar and pyroclastic deposits were tall and steep. JICA (1978) noted substantial bank failures in the upper Pasig-Potrero that contributed much of the sediments delivered by the river to the lowlands. During post-eruption observations, lateral erosion and bank collapse were found to be effective mechanisms of generating and sustaining lahars. Large blocks of bank material as much as five meters across have been seen being rafted by lahars. Active lahars, especially in hyperconcentrated-flow form, were highly effective in undercutting riverbanks. During low-flow conditions, bank-collapse material would be temporarily stored in the channel until the next lahar eroded it.

While banks made of Pinatubo pyroclastic-flow deposits often fail, they do sustain tall, near-vertical slopes for extended periods, especially when they are not exposed to undercutting by flows, indicating that the deposits possess a degree of strength. During fieldwork in 1999, slope heights and angles were measured on banks along the Papatac Creek. The banks were made mostly of secondary pyroclastic-flow deposit, which are considered to be of similar strength to primary pyroclastic-flow deposits. The slope data are shown in Figure 3.5. The soil cohesion necessary to maintain each of these slopes may be calculated using the equation for critical height of dry slopes (Lohnes and Handy, 1968, p 249):

$$H = \frac{4c \sin i \cos \phi}{\gamma[1 - \cos(i - \phi)]} \qquad \text{Equation 3-3}$$

where i is the slope angle. Substituting typical values of internal friction angle, $\phi = 48°$ (JICA, 1996) and unit weight, $\gamma = 13$ kN/m^3 (W.E. Scott *et al.*, 1996), the apparent cohesion of Pinatubo pyroclastic-flow deposits may be calculated. The steepest slopes plotted in Figure 3.5 require a cohesion, c, of 13 kPa, which may be considered the

minimum amount necessary to sustain them. Using this set of parameters (ϕ, γ, c), a critical height for every slope angle may be determined, as shown in Figure 3.5. For comparison, in laboratory tests of borehole samples of unclassified Pinatubo deposits, JICA (1996) measured average values of $\phi = 48°$, $\gamma = 18.5$ kN/m^3 and $c = 18.5$ kPa. A critical height curve derived from these values plots identically to that shown in Figure 3.5. The critical height for Pinatubo pyroclastic-flow deposits is lower than that found in other loosely consolidated pumiceous deposits in Japan (Figure 3.5; Matsukura, 1987).

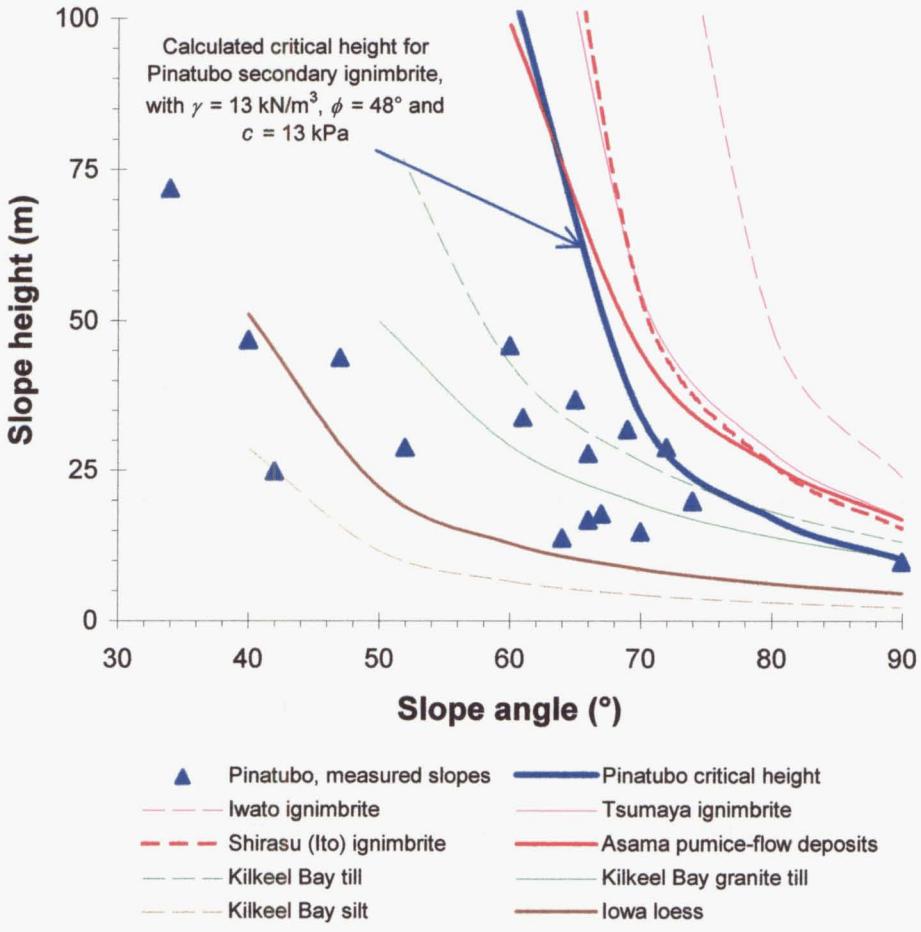

Figure 3.5. Critical height of slopes made of Pinatubo secondary pyroclastic-flow deposit compared to other unconsolidated deposits, as compiled by *Matsukura (1987)*.

Source of cohesion

The slope data indicate that the Pinatubo pyroclastic-flow deposit possesses a degree of cohesion, yet the deposits typically contain <3% clay-sized particles (Figure 3.6; Pierson *et al.*, 1996; W.E. Scott *et al.*, 1996). According to Mitchell (1993), granular soils may develop true cohesion from cementation, stating that even 5% cement is sufficient to give them cohesive strength. While cementation cannot be totally discounted – and would require more careful laboratory work – no cementation was observed in scanning electron microscopy of a limited sample of secondary pyroclastic-flow deposit grains. Alternatively, the inferred cohesion of the deposits may be "apparent cohesion" from capillary stresses (negative pore water pressure), or mechanical forces due to particle geometry and packing (Mitchell, 1993). Vesicles in adjoining pumice grains may provide negative pore pressure, while the extremely angular glass shards and mineral fragments may give the pyroclastic-flow deposits some mechanical strength. The problem of apparent cohesion in coarsely granular pyroclastic-flow deposits needs further scientific research.

3.5.3. Temporary blockages

The blockage of tributaries by pyroclastic flows or lahars is a common phenomenon in volcanoes (*e.g.*, Segerstrom, 1950; Kuenzi *et al.*, 1979; Youd *et al.*, 1981; W. Meyer *et al.*, 1985; W. Meyer *et al.*, 1986; Smith, 1991; Umbal, 1994; Arboleda and Martinez, 1996). Some of them survive for decades (*e.g.*, Kuenzi *et al.*, 1979); most, however, fail catastrophically after a relatively short time. At Pinatubo, the sudden breaching of many temporary pyroclastic dams has resulted in large lahars. The mechanisms of failure of such dams are discussed in more detail in Chapter 5.

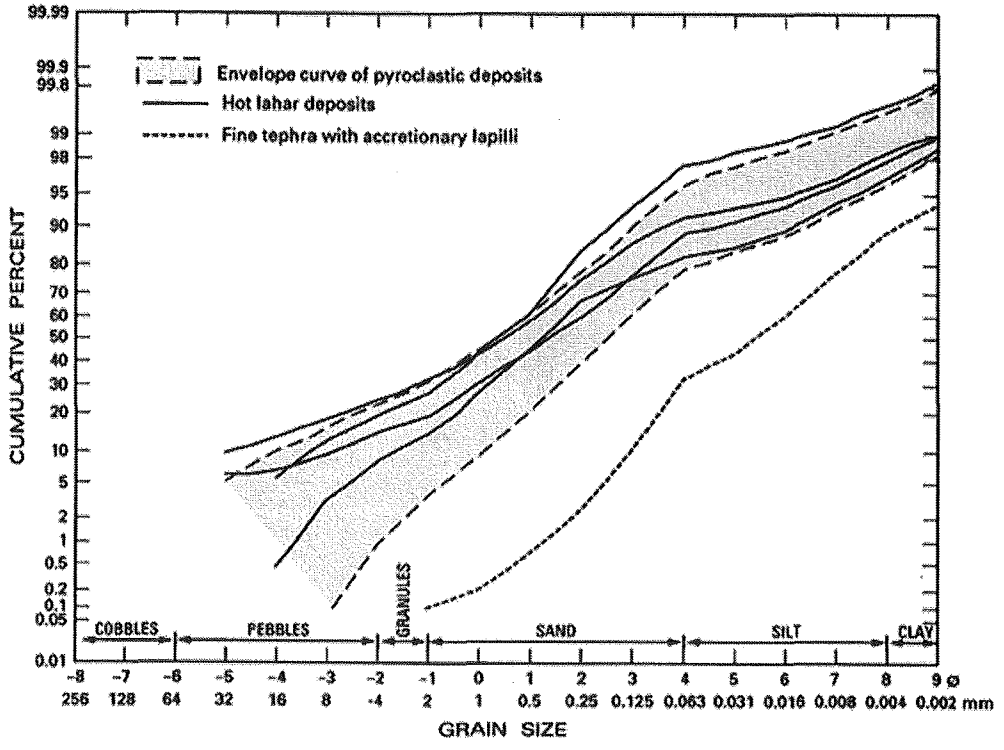

Figure 3.6. Grain-size distribution of Pinatubo deposits (*from Pierson et al., 1996, and W.E. Scott et al., 1996*)

3.6. Secondary explosions

3.6.1. General

Secondary explosion is a term loosely used by PHIVOLCS to refer to tephra-steam eruptions derived from the hot pyroclastic-flow deposits. As used, the term includes both *secondary hydroeruptions* (Moyer and Swanson, 1987), which result from the direct interaction of surface water or groundwater with the hot deposits, and *secondary pyroclastic flows* (Torres *et al.*, 1996), which result mainly from gravitational collapse of steep banks. Secondary hydroeruptions have been found to span a range of ejection rates, with "explosion" representing the energetic end of the spectrum (Moyer and Swanson, 1987). Secondary pyroclastic flows, also called deposit-derived pyroclastic flows (Self and Torres, 2001), are essentially hot landslides with relatively high mobility due to gas and steam pressure. Less mobile gravitational failures in hot

deposits are here referred to as *secondary pyroclastic slides*, following landslide terminology used by Cruden and Varnes (1996). While recognizing the term's inaccuracy, secondary explosion is retained here in the original usage by PHIVOLCS to accommodate observations of secondary tephra columns whose genesis could not be confirmed.

Secondary pyroclastic-avalanche scarps are distinguished from secondary hydroeruption craters by their typically arcuate shapes (compared to the circular craters of hydroeruptions), and their occurrence along the edges of river banks. Furthermore, deposits of pyroclastic avalanches are usually found only in the direction of collapse (toward and along the channel), while secondary hydroeruption tephra is typically scattered in all directions, depending on wind direction at the time of their occurrence (Moyer and Swanson, 1987).

3.6.2. Observations at Pinatubo

After the 1991 eruption until 1994, numerous secondary explosions occurred on almost a daily basis during the rainy season. This can be seen in Figure 3.7, although the number of observations reported is probably underestimated for the period 1992-1994, when thick ash clouds from large secondary explosions often obscured ash columns from smaller explosions. Most of the secondary explosions originated from gravitational collapse of channel banks made of hot pyroclastic deposits, although some were indeed the result of true secondary hydroeruptions. Numerous secondary hydroeruption craters were found right after the 1991 eruption, commonly aligned along buried river valley thalwegs. As river channels developed, hydroeruptions became rarer, perhaps replaced by secondary pyroclastic slides, which took advantage of gravity to release built-up steam pressure.

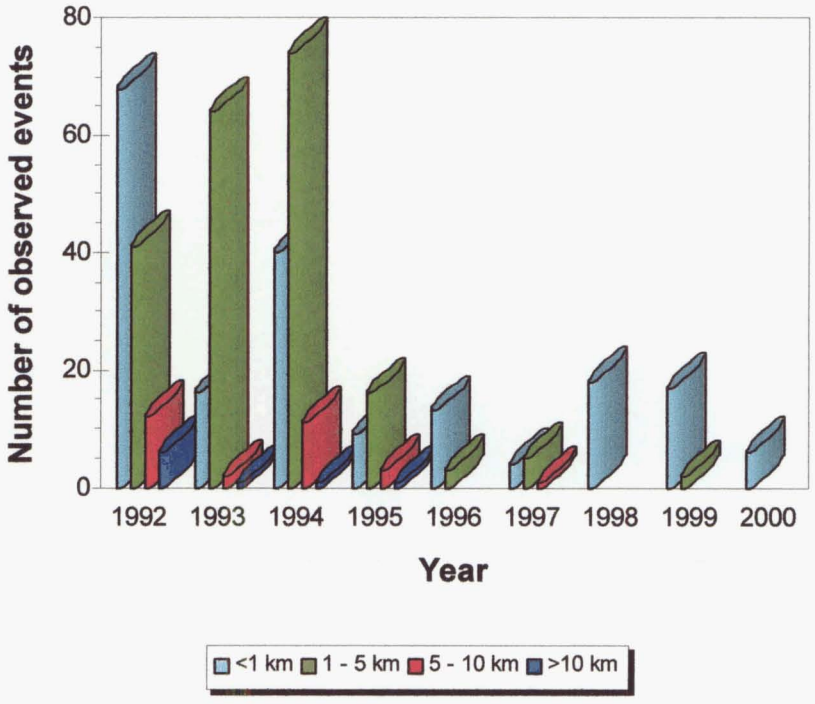

Figure 3.7. Number of recorded secondary explosions, with different column heights, in the Sacobia-Pasig pyroclastic-flow deposit field (*from PHIVOLCS, unpublished data*).

Secondary pyroclastic slides commonly occurred when channel banks made of hot pyroclastic-flow deposit were undercut by streamflow. The slides usually transform into mini pyroclastic flows, with small elutriation clouds. In addition, large blocks of hot channel-bank material sometimes exploded upon contact with the water in the channel, producing small ash columns. Larger collapses generated secondary pyroclastic flows that travel a few kilometers (Torres *et al.*, 1996). Such flows have been found to have profound effects on erosion rates and lahar generation, and in some cases, have triggered large-scale stream piracy (*See Section 2.3*).

Sometimes, dry blocks of pyroclastic-flow deposits that are several meters across were rafted by debris-flow lahars. Such rafted blocks have been observed to fall over a 3-m high nickpoint, exploding and hurling tephra 30 m into the air.

3.6.3. Mechanisms of formation

The exact mechanism of formation of secondary explosions remains enigmatic. Any effort to model their internal dynamics must take into account several constraints:

1) The hot body is a valley-fill deposit of coarse, granular material that is several tens of meters thick, with interior temperatures greater than 450°C;

2) Freshly-exposed sections are dry, indicating that water has not permeated the deposit;

3) The uppermost parts are invariably wetted by precipitation; this wet surface layer thickens with time; and

4) Some perennial streams flow on top of the deposits, indicating a saturated zone below the surface but above the dry interior of the deposit.

Figure 3.8 illustrates the possible path of surface and groundwater through a hot pyroclastic-flow deposit. In this model, heat in the interior of the pyroclastic-flow deposit vaporizes groundwater inflow, while meteoric water partly infiltrates the deposit. A zone of condensation and water-saturation decimeters to meters below the surface forms a confining layer that promotes steam pressure buildup. This zone thickens through time, as indicated by thermal probes done by PHIVOLCS and the Geological Survey of Japan from 1995 to 1999 (Bornas *et al.*, 2000). Secondary hydroeruptions occur when steam pressure overcomes overburden pressure. Secondary pyroclastic flows are formed when gravitational collapse suddenly removes considerable confining pressure. The steam release may accelerate retrogressive development of the collapse, which may sustain the mobility of the secondary pyroclastic flow.

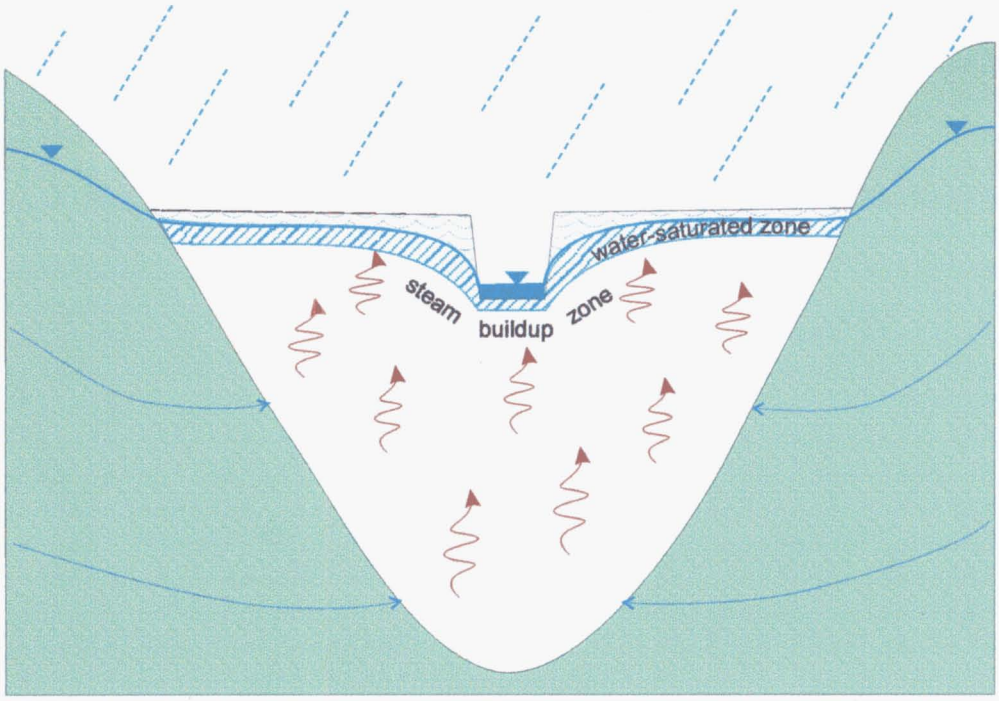

Figure 3.8. Schematic diagram showing flow of surface water and groundwater through the hot valley-fill pyroclastic-flow deposit. The water-saturated zone is usually a thin layer above which the material is only partially saturated. Below the saturated layer is the dry interior of the pyroclastic-flow deposit. Secondary explosions occur when steam pressure exceeds overburden pressure, as when gravitational collapse suddenly removes a large chunk of the overburden.

3.6.4. Effects on erosion rates

Both secondary hydroeruptions and secondary pyroclastic slides and flows affect erosion rates by:

1) Re-filling lahar channels with loose, hot deposits that are easily entrained by succeeding flows;

2) Blanketing the surrounding areas with ash from elutriation clouds, which may form crusts that affect infiltration rates;

3) Creating steep headscarps that may lead to further mass failures;

4) Changing the longitudinal profile of the river channel;

5) Damming tributaries, which may fail catastrophically; and

6) Effecting stream piracy.

Most other erosion and mass-wasting processes can be modeled using common hydraulic and mechanical analyses. The complicated effects of secondary explosions, on these processes, however, require further research.

3.7. Watershed recovery

Lahar activity at Pinatubo has progressively declined since the 1991 eruption, although geomorphic changes resulting from stream piracy have complicated the trend. No major lahar has been recorded after the August 1997 Typhoon *Ibiang* event. Major *et al.* (2000) have observed a similar declining trend in lahar activity at Mount St. Helens. The decrease in activity is considered a product of temporal changes in the inter-related processes described in the preceding sections, although these are ultimately controlled by the depletion of the pyroclastic-flow deposits. The depletion of the pyroclastic-flow deposits has resulted in less frequent secondary explosions, which influenced erosion rates dramatically. It has also allowed river channels to lie directly on more resistant pre-eruption surfaces, with the pyroclastic-flow deposits found high up on the valley walls. At Pinatubo, the pre-eruption surface began to be unearthed in significant scale in 1995. The frequency and magnitude of secondary explosions also decreased dramatically that year (*See* Figure 3.7). Judging from the volume of lahars, the volume of pyroclastic-flow deposits in the upper Pasig catchment is estimated to have been reduced from 300 to <200 million m^3 after the 1994 season, then down to <100 million m^3 by the end of 1995 (PHIVOLCS, unpublished data).

Part of the hillslope recovery may be attributed to the regrowth of vegetation, although Collins and Dunne (1986) attributed the decline in post-eruption inter-rill and rill erosion rates at Mount St. Helens to the incision of runoff through the tephra and to the

development of a stable rill network, rather than to vegetation recovery. Perhaps owing to the tropical climate, vegetation around Pinatubo actually recovered rapidly, as evidenced by the green hills during the dry seasons starting 1992. However, the recovery was intermittently negated by ash from secondary explosions, which served to momentarily revert the landscape close to the initial condition where tephra covered much of the surface. The explosions often occurred during the rainy season when lahars were also occurring. Beginning 1995, secondary explosion activity decreased, thus promoting unhampered vegetation recovery.

With the recovery of vegetation and the depletion of the pyroclastic-flow deposits, the development of the entire drainage network was hastened. The main river channel attained a more stable profile that changed in synchrony with its tributary gullies. This was largely achieved in the Pasig-Potrero River by the end of 1995, when almost the entire length of the upper Pasig became incised through pre-eruption deposits (Figure 3.9) and secondary explosions became limited in both frequency and vigor. Only minor lahars were observed in 1996, and the only major lahar after that – the August 1997 Typhoon *Ibiang* event – was generated by an unusually heavy rainstorm.

Observed changes in all the processes and factors involved in lahar initiation indicate the significantly reduced probability of lahars. By 1998, for example, the activity in the Pasig-Potrero has been largely reduced to muddy streamflow, perhaps transitional to hyperconcentrated flows. Both magnitude and frequency of lahars have been reduced considerably. This may be attributed to the gradual recovery of the entire river basin, which now features large channels incised through pre-eruption deposits, a considerably reduced cache of pyroclastic-flow deposits with partly vegetated surfaces, and healthily vegetated hillslopes (Figure 3.10).

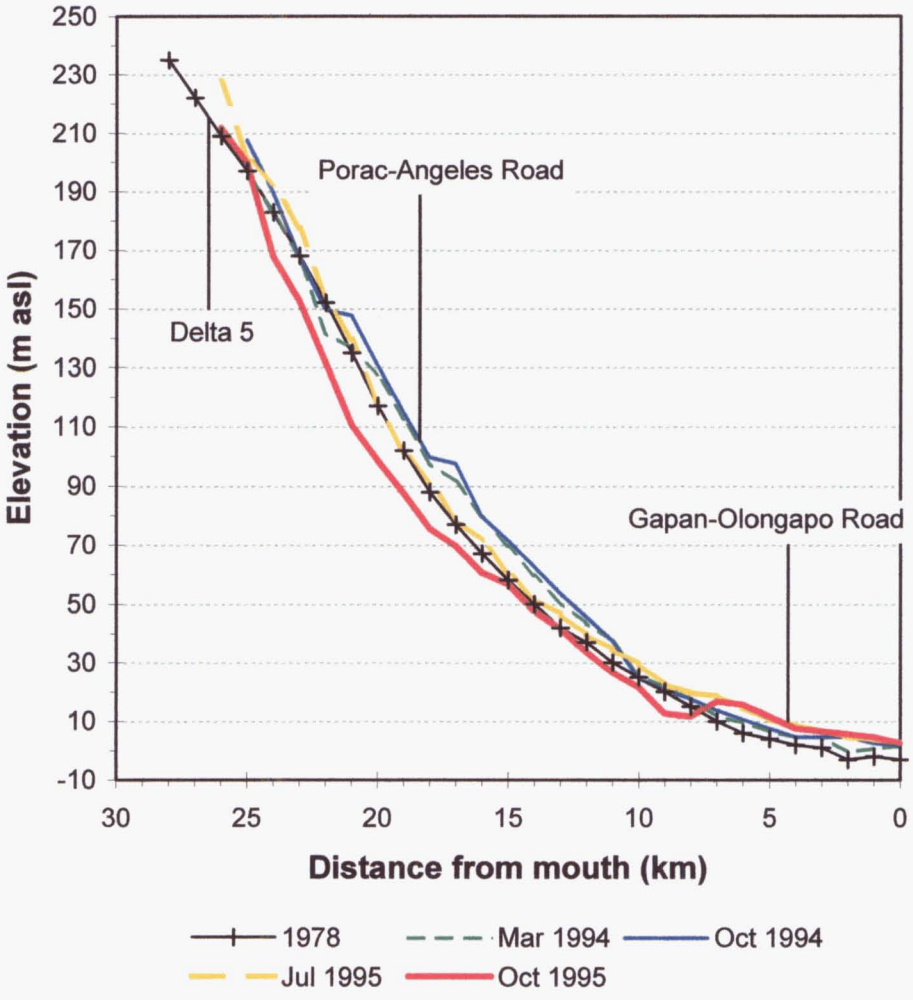

Figure 3.9. Changes in the longitudinal profile of the Pasig-Potrero riverbed (*from* JICA, 1996c). Note the massive remobilization and channel incision after the October 1995 Typhoon *Mameng* lahars.

Figure 3.10. 1999 photo of the upper Pasig (formerly Sacobia) catchment showing depleted, partly vegetated pyroclastic-flow deposits, large channels incised in pre-eruption deposits, and thickly vegetated hillslopes. View is upstream; Pinatubo is in the center background partly hidden by clouds.

3.8. Recommendations for future work

The various processes involved in lahar initiation are only broadly covered here. Specific topics that may be explored further include:

1) The mechanics of erosion on tephra-covered hillslopes – this may include the formation and effects of tephra crusts, and the development of rills;

2) The dynamic interaction between river channels and their tributary rills in a rapidly fluctuating system;

3) The source of cohesion of granular pyroclastic deposits; and

4) The mechanics of secondary explosions and their effects on erosion.

A better understanding of these processes, especially those that occur in the source area, requires direct observation. Some of them require observation immediately after an eruption. At Pinatubo, some information may have been lost to time, as the watersheds have evolved considerably after 1991. For other volcanoes, direct observation may not always be possible during or immediately after an eruption due to the hazards involved, but the loss of field data may be minimized by carefully preparing a program of study beforehand, and implementing it as soon as safety conditions improve.

Chapter 4

LAHAR-TRIGGERING RAINFALL

CHAPTER 4

Lahar-Triggering Rainfall

4.1. Introduction to Chapter 4

4.1.1. Background

Occurring in a tropical climatic setting, all the lahars of Mount Pinatubo are ultimately generated by rainfall. While some lahars have been linked to the sudden breaching of temporarily dammed lakes (See Chapter 5), most of them have been triggered directly by rainfall that is usually brought about by monsoonal storms or by tropical typhoons.

The relationship between Pinatubo lahars and rainfall has been established in many studies, notably Arboleda and Martinez (1996) Pierson et al. (1996) and Tuñgol and Regalado (1996) for the Sacobia-Pasig River; and Rodolfo et al. (1996), Umbal (1994) and Umbal and Rodolfo (1996) for the Marella-Sto. Tomas River. In these studies, lahar frequency and magnitude have been positively correlated with rainfall amount. The rainfall threshold at which lahars are generated, usually expressed in terms of the intensity and duration, has also been determined. The studies, nevertheless, have so far been limited to events immediately following the 1991 eruptions of Pinatubo, at best up to the 1993 season. This chapter is intended to use the benefit of a longer record of observation to give a more detailed long-term perspective on lahar-rainfall relationships on the east side of Mount Pinatubo.

4.1.2. Objectives and methodology

In this chapter, data from lahar monitoring instruments are used in conjunction with field observations to analyze the relationship of lahar-runoff and rainfall in the Pasig-Potrero watershed in order to understand better the hydrologic response of the basin to the extreme disturbance caused by the 1991 eruptions. The data covers the period from 1992 to 2000. However, only the 1992-1997 data are of particular significance

inasmuch as lahars have ceased occurring after 1997. In addition, the instruments suffered many outages in 1998 to 2000 for various reasons. In analyzing the data, the following procedures were adopted:

1) Acoustic flow monitor (AFM) data were calibrated in terms of field estimates of lahar volumes;

2) The AFM data were used to back-calculate the volume of individual lahar events in the Pasig-Potrero River;

3) The calculated lahar-runoff was correlated with coincident rainstorms recorded by rain gauges installed in the upper Pasig catchment to obtain rainfall-normalized sediment yield;

4) The rainfall threshold at which lahars have been generated was analyzed; and

5) The results of the statistical analyses were interpreted to make inferences on geomorphic and hydrologic phenomena in the Pasig-Potrero catchment.

4.1.3. Organization

To aid in understanding the physical context of the subsequent analyses and discussions, the reader is referred to Section 2.3 for a discussion of the physiography and post-eruption evolution of the Pasig-Potrero River basin. This chapter focuses on the statistical analyses of AFM and rainfall data. The characteristics of the instrument data used in the analyses are described in Section 4.2. Section 4.3 deals with the calibration of the Pasig-Potrero AFM and the calculation of lahar volumes from the AFM data. Section 4.4 presents the correlation of lahar-runoff with coincident rainstorms and the derivation of rainfall-normalized sediment yield, while the rainfall threshold at which lahars have been generated are discussed in Section 4.5. In Section 4.6, the results of the statistical analyses are used to make inferences on the geomorphic and hydrologic evolution of the Pasig-Potrero River basin.

4.2. Collection and treatment of instrument data

4.2.1. Lahar-monitoring instruments

A network of remotely operated rain gauges and acoustic flow monitors (AFM) form the instrument core of the PHIVOLCS lahar monitoring and warning system that became fully operational before the 1992 rainy season (Figure 4.1). Rain gauges in specific lahar-affected watersheds provide an early, though not infallible, warning system premised on the assumption that most lahars are triggered by rain. The AFM offers a more direct method of detecting the occurrence of lahars by providing continuous pseudohydrographs of streamflows at the instrument site (LaHusen, 1996; Marcial *et al.*, 1996; Tuñgol and Regalado, 1996). The rain gauges and AFM sensors are strategically located around Mount Pinatubo and are linked by radiotelemetry to computers at the Pinatubo Volcano Observatory (PVO) in Clark Air Base. Pertinent features of the rain gauges and AFM as used in Pinatubo are described in detail by Marcial *et al.* (1996) and Tuñgol and Regalado (1996), and summarized in the following sections.

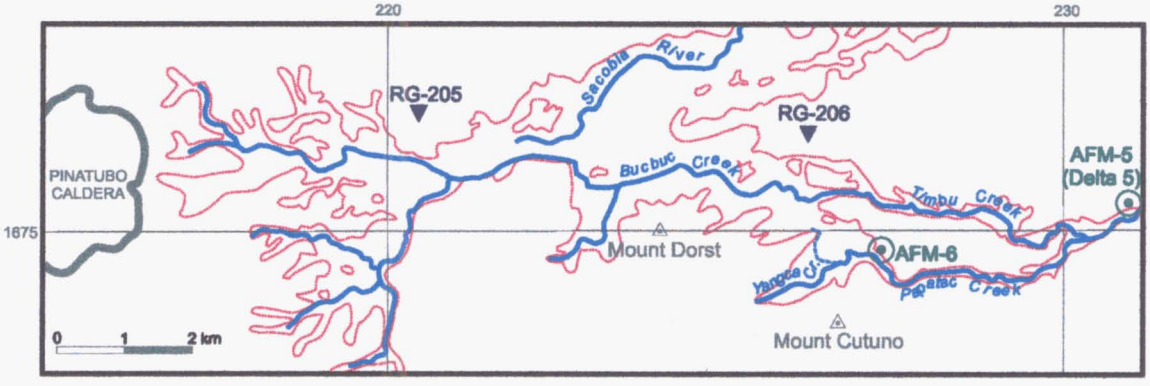

Figure 4.1. Location map of lahar monitoring instruments in the upper Pasig catchment. RG = rain gauge, AFM = acoustic flow monitor. AFM-5 site is located in a manned lahar watchpoint called Delta 5.

Rain gauge

Designed specifically for the purpose of monitoring lahars at Mount Pinatubo, ash-resistant rain gauges (ARRG) were installed by a joint team of PHIVOLCS and the U.S. Geological Survey (USGS) in the upper reaches of major river basins around the volcano soon after the 1991 eruptions (Marcial *et al.*, 1996). The ARRG consists of a magnetic-switch tipping-bucket recorder with a microprocessor-controlled digital counter. To counter the effects of ashfall, the ARRG is fitted with a vertical PVC pipe to collect ash and rainwater, with a spillover outlet that leads to the ash-protected tipping bucket (Figure 4.2). Field calibration of the rain gauges used in the Sacobia-Pasig has shown that each bucket-tip corresponded to 1 mm of rainfall. Data from the rain gauge are radiotelemetered to PVO-CAB every 30 minutes during light or no rain, or every 10 tips during heavy rain.

Acoustic flow monitor

The AFM has proven to be a convenient, reasonably effective instrument in remotely monitoring lahar activity. When properly calibrated, AFM data can be used as surrogate for a continuous hydrograph of a monitored river channel.

Designed by Hadley and LaHusen (1995), the AFM uses rugged digital exploration geophones buried at least 1 m deep at a pre-selected site along the valley wall of a lahar-channel, to measure the vertical ground velocity (in 10^{-6} cm/s) of acoustic waves generated by flows in the river channel. The AFM detects acoustic waves within the 10-300 Hz range, with the signal recorded in three frequency bands: the full band (10-300 Hz), the low band (10-100 Hz) and the high band (100-300 Hz). Lahars, having significantly higher sediment concentration than normal streamflows, are characteristically accompanied by a low rumbling noise, the acoustic energy of which has been found to be concentrated in the low-frequency (10-100 Hz) range (LaHusen, 1996; Marcial *et al.*, 1996; Tuñgol and Regalado, 1996). The AFM amplitude has been found by Tuñgol and Regalado (1996) to correlate linearly with lahar discharge (Figure 4.3).

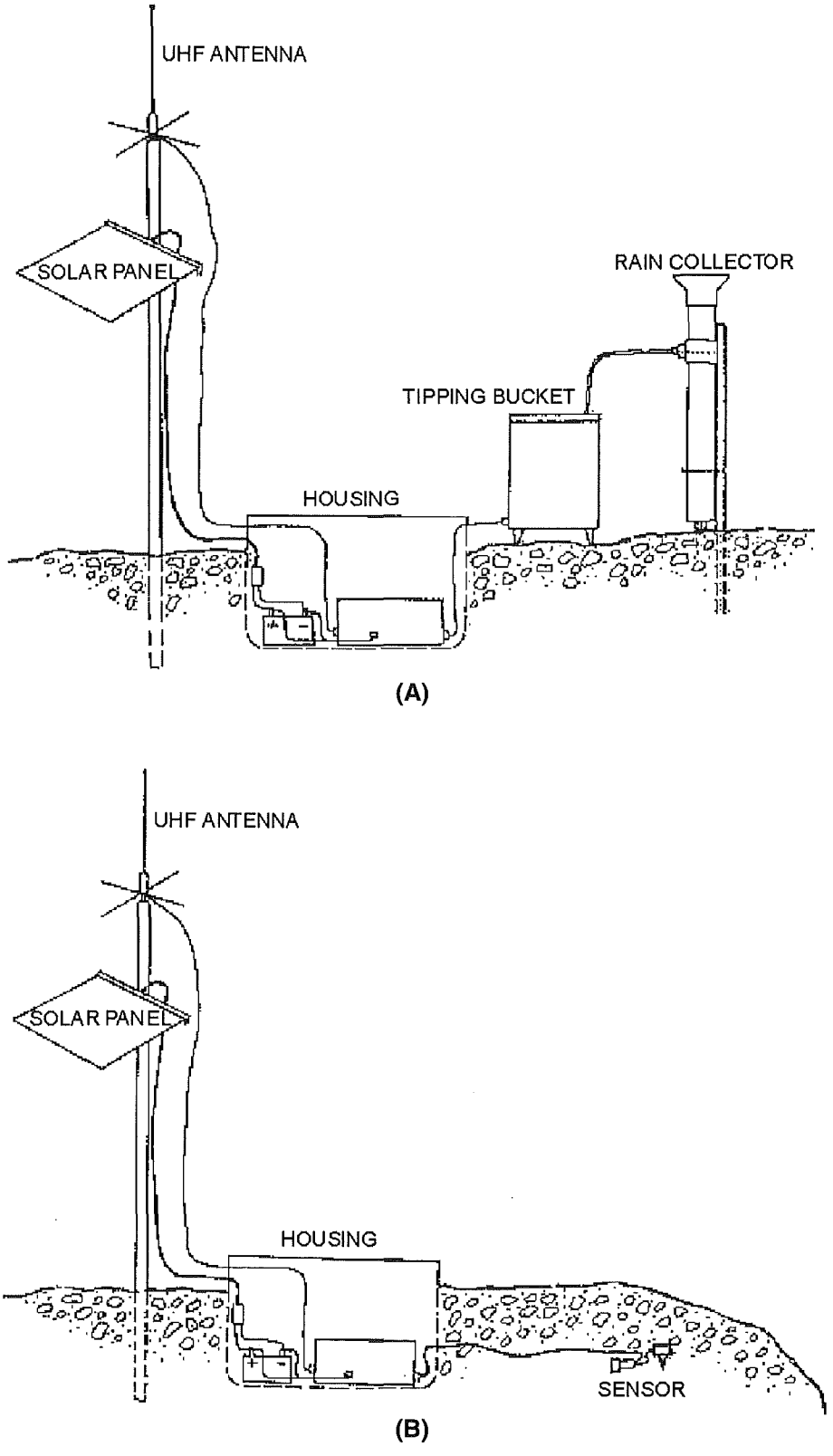

Figure 4.2. Setup of the ash-resistant rain gauge (A) and acoustic flow monitor (B) (*from Marcial et al., 1996*).

Like the rain gauge, the AFM normally sends signals by radio to PVO-CAB every 30 minutes. When a pre-set amplitude and duration threshold is exceeded, however, an alert is triggered, and data is transmitted at 1-min intervals. AFM settings are empirically determined at each site. A plot of AFM amplitude against time, as can be viewed in real-time at PVO-CAB, resembles a stream hydrograph, with AFM amplitude as a substitute for discharge (LaHusen, 1996; Marcial *et al.*, 1996; Tuñgol and Regalado, 1996). Continuous AFM recording virtually ensures detection of all lahars of significant magnitude passing the sensor.

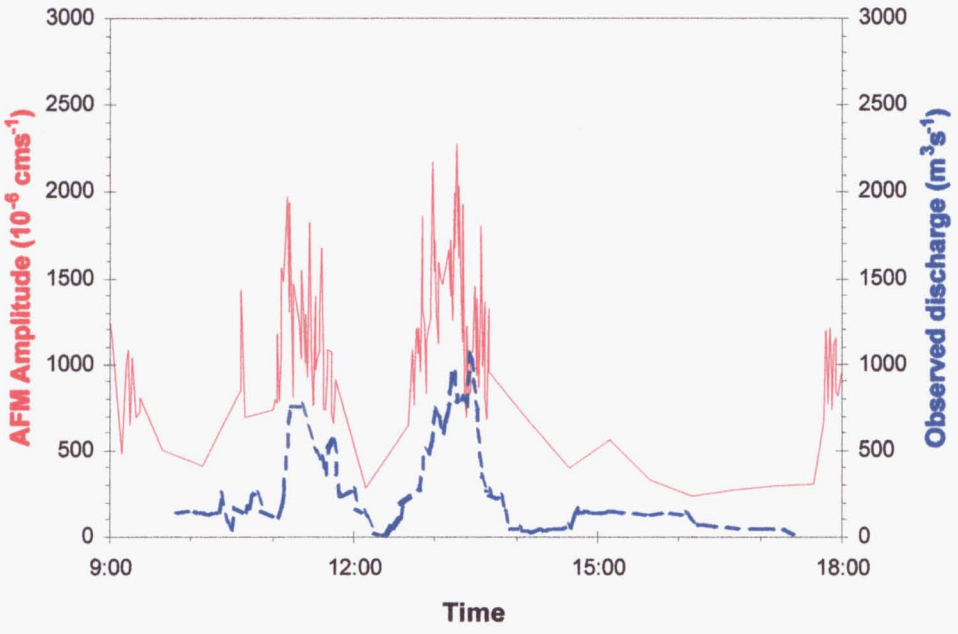

Figure 4.3. Example of an acoustic flow monitor signal (solid red line) showing its good correspondence with observed lahar discharge (dashed blue line). Data shown is for the 29 August 1992 lahars in the Sacobia River (*from Tuñgol and Regalado, 1996*).

Data format

Data from the ARRG and AFM are received in real time by a computer at PVO, and are saved as delimited text files, with a filenaming system based on the Julian calendar (*e.g.*, `day001.raw` corresponds to the record for 01 January of the current year). In each file, the data comes in three columns: time, sensor code and reading or value.

1) The first column is time recorded in 24-hour format.

2) The second column, the sensor code, contains a 3-digit identifier unique for each rain gauge or AFM. The rain gauges are identified by a 3-digit code in 20x format (*e.g.*, RG-206, also known as RG-F, is the Middle Sacobia). The AFM code starts with a 0 or 1; 0 in normal mode (no lahar detected) and 1 in "event" mode (lahar event). The middle digit in the AFM code corresponds to the sensor site; and the right-hand digit indicates the frequency band (0 for full band, 1 for low band and 2 for high band). Thus, 151 in the second column indicates a lahar event detected by AFM-5 in the low-frequency band.

3) The third column contains the instrument reading. Rain gauge readings are in terms of the cumulative number of bucket tips, which are numerically identical to cumulative rainfall in mm. AFM values are acoustic amplitudes (vertical ground velocities) in 10^{-6} cm/s.

The rain gauge and AFM data may be viewed in real time at PVO. The data may also be opened with any text editor, or parsed and manipulated using a spreadsheet program.

Lahar-monitoring instruments in the Pasig-Potrero

When the remote network was established in 1991, RG-206 (a.k.a. RG-F or Middle Sacobia) was used to denote rainfall in the Pasig watershed. In late July 1994, however, PHIVOLCS transferred RG-205 (RG-E) to the upper half of the Sacobia pyroclastic-flow field, while RG-206 was out of order. Using RG-205 to measure rainfall in the Pasig River was reasonable at that time because after the capture of the upper Sacobia

by the Pasig River in October 1993, the sediment source area of the Pasig River had extended to the former upper Sacobia catchment. At any rate, on average, little difference in rainfall has been found between rain gauge stations on the east side of Mount Pinatubo before or after the 1991 eruptions (JICA, 1978; Newhall, 1994). The difference is more pronounced for localized rainstorms, and becomes insignificant for regional storms. In consonance with PHIVOLCS practice, RG-206 was used alternately with RG-205 to represent rainfall in the Pasig-Potrero River basin, as shown in the schedule in Table 4.1.

Table 4.1. Codes and locations of lahar-monitoring instruments used in this study.

Date	Rain Gauge	AFM
1992	206 (F) Middle Sacobia	6 (Pasig)
1993	206 (F) Middle Sacobia	6 (Pasig)
1994 April to July	206 (F) Middle Sacobia	6 (Pasig)
1994 August to November	205 (E) Upper Sacobia	5 (Delta 5)
1995	205 (E) Upper Sacobia	5 (Delta 5)
1996	205 (E) Upper Sacobia	5 (Delta 5)
1997 January to April	205 (E) Upper Sacobia	5 (Delta 5)
1997 May to November	206 (F) Middle Sacobia	5 (Delta 5)

Lahars along the Pasig River were initially monitored by AFM-6 (a.k.a. Pasig-Potrero), which was located along the Papatac gorge. The location of AFM-6 was ideal as it was in a reach where flows were confined to a narrow valley, thus minimizing errors from changes in channel-to-sensor distance. In mid-1994, however, flows were diverted into the Timbu River, consequently bypassing AFM-6. Because of this, PHIVOLCS transferred another instrument, AFM-5, to the Delta 5 watchpoint, where the Papatac and Timbu converge (Figure 4.1). For purposes of correlating AFM signal with lahar measurements, the AFM-5 site has been found to be less ideal than AFM-6 since the river channel in this reach have shifted laterally, being near the apex of the alluvial fan. Nevertheless, it was found to be the best location to record flows from both the Papatac and Timbu channels.

In this study, AFM-6 is used to represent Pasig flows from 1992 to July 1994, and AFM-5 for flows from August 1994 onwards (Table 4.1). Since this study is concerned primarily with debris-flow and hyperconcentrated-flow lahars and not normal streamflow, the low-frequency (10-100 Hz) channel of the AFM is used.

4.2.2. Field data

Flow vs. deposit

Observations and measurements of active flows along the Pasig-Potrero are scarce, mainly owing to difficulties in maintaining viewpoints that are both safe and offering a good vantage of the flows. This is compounded by the fact that the Pasig-Potrero channel often shifted laterally within its wide alluvial fan. Aside from the few observations made during the early part of the 1992 rainy season, the only few observations of active flows were made during low-flow, non-lahar conditions (*e.g.*, (Hayes, 1999; Montgomery *et al.*, 1999; Hayes *et al.*, 2002).

To supplement the lack of active flow observations, field investigation has been generally geared towards mapping lahar deposits in the alluvial fan. From this mapping, deposit volumes were calculated after every lahar season, or in some instances, after major lahar events. Estimates of lahar deposit volumes are poorly constrained, owing to the very rapid rates of lahar activity. Deposits of one event were quickly overlain, or eroded, by the next, making delineation of extent and thickness difficult. Nevertheless, yearly sediment accumulation in the alluvial fan of the Pasig-Potrero River has been reported by PHIVOLCS from 1991 to 1997 (Punongbayan *et al.*, 1994; Arboleda *et al.*, 1995; Umbal, 1997). In addition, JICA (1996c) has mapped lahar deposits in the Pasig-Potrero after each major lahar event in 1995. The error in the volume estimates is considered to be around ±20% (Pierson *et al.*, 1996).

Remobilization of deposits

One notable limitation of field estimates is that lahar deposit mapping of the Pasig-Potrero has been invariably limited to the alluvial fan downstream of Delta 5, largely

because most of the deposits are emplaced there, partly because of the inaccessibility of the upper reaches of the river. This is acceptable for 1991-1993 when deposition was actually limited to the fan area, the upper reaches essentially acting as non-depositional transport or erosional zones. However, after the 1993 capture of the Sacobia, extensive deposition has occurred along the upper reaches of the Pasig, including the Bucbuc, Papatac and Timbu channels. In 1994 especially, many lahars, as well as secondary pyroclastic flows and landslides, occurred in the upper Pasig, the bulk of which barely reached the apex of the alluvial fan at Delta 5. For example, from June to July 1994, around 100 million m^3 of sediments were delivered to the Pasig-Yangca confluence, thus building up the Cutuno blockage (*See Chapter 5*). Very rapid aggradation was also witnessed along the Timbu channel in July-August 1994 (PHIVOLCS video footages; C.G. Newhall, written communication). Aggradation in the upper reaches of the Pasig has likewise been noted in the following years, especially during small lahars.

Much of the sediments initially emplaced in the upper reaches of the Pasig were later remobilized by large-magnitude lahars to eventually be deposited in the alluvial fan. Thus, the mapped lahar deposits may in effect represent the sediment moved, through a series of processes, from the pyroclastic-flow source area to the alluvial fan. Massive remobilization occurred during two notable lahar events: the September 1994 lake-breakout and the October 1995 Typhoon *Mameng* events. The volume of the deposits represents only the ultimate product, not necessarily the complete series of flows that delivered them. Use of the AFM is a better way to estimate the volume of actual flows, considering they directly measure flow signals. The AFM data also provides a near continuous recording of flows for as long as the flows pass the sensor site.

4.3. Calibrating AFM data to flow volumes

Aside from the effects of site-specific instrument settings, the strength of the AFM signal is a function of many factors, *e.g.*, distance of the sensor to the channel, sediment concentration, flow rheology, channel roughness, *etc.* (Newhall, 1994). Given a site at a fixed distance to the channel, however, past AFM calibration work has shown that the

AFM signal reflects flow volume very well (Marcial *et al.*, 1996; Tuñgol and Regalado, 1996). This is probably because sediment concentration of lahars generally varies with discharge or volume, and the difference in flow density between hyperconcentrated-flow and debris-flow lahars is probably not enough to significantly affect the acoustic signal. Other factors such as flow turbulence, clast size and density, and the occurrence of bank collapse may also conceivably affect AFM signal but these are also partly dependent on volume/discharge.

4.3.1. Method of calibration

Neglecting the effect of sediment concentration and other parameters, there are two ways by which AFM data may be calibrated to denote volumetric flow of lahars along a channel: (1) by comparing AFM amplitude to instantaneous discharge, and (2) by comparing the "acoustic flux" of each distinct lahar event to the total volume of the event (Tuñgol and Regalado, 1996).

AFM amplitude vs. discharge

Theoretically, AFM amplitude could be directly calibrated with stream discharge. This is feasible if the observation point is relatively close to the AFM geophone, and it was successfully done by Hayes (1999) for low-flow, non-lahar conditions in the Pasig River in 1997. However, during a lahar event when the AFM is recording every minute, too much random noise picked up by the geophone makes it virtually impossible to make a one-to-one correspondence between instrument reading and discharge. Further ambiguity arises from the fact that the sensor may record signals from several hundred meters away. That is, what an observer sees may not necessarily be what the AFM detects. This problem may be addressed by averaging AFM readings over, for example, 5-minute intervals to correspond more closely with discharge measurement intervals, but again, this could work only if the observation point is right by the AFM sensor.

Other difficulties in calibrating AFM data to discharge lie in the inherent uncertainty involved in estimating the discharge of sediment-rich flows in the field. Lahar channels have very mobile beds; in the absence of flow depth indicators such as rolling boulders,

the rate at which the channel bed is scoured or aggraded during a lahar event is hard to estimate in the field. In addition, velocity measurements of lahars are usually limited to surface velocities, and cross-sectional velocity profiles of lahars are generally unknown.

Lastly, relating AFM amplitude to stream discharge requires vigilant visual monitoring of active flows. This has proved difficult to do in practice because of safety and logistical limitations. Discharge measurements were done only for a very limited number of large-magnitude lahars in the Pasig-Potrero River, and these were done down in the alluvial fan, far from the AFM sensor.

Acoustic flux vs. flow volume

Another way to calibrate the AFM is by comparing individual lahar events, as identified by distinct onset, swell and ebb in the AFM plot as well as in the observed stream hydrograph. By integrating AFM readings over the duration of an identified lahar event, the event's acoustic flux can be calculated and compared to the volume of the entire flow measured in the field (Tuñgol and Regalado, 1996). Procedurally, the acoustic flux is calculated by multiplying instantaneous AFM readings with the time until the next reading, then adding the products, starting from the time that the signal exceeds a pre-selected threshold AFM amplitude until it reverts to background level. Similarly, lahar volume may be calculated from the summed products of discharge and interval measurements made in the field. The acoustic flux may then be backcalculated to convert AFM amplitudes to discharge. Using the acoustic flux for AFM calibration addresses the problem of time lag and random instrument noise more effectively.

In the absence of direct observations of active lahars, the volume of lahar deposits may serve as an alternative with which acoustic flux may be calibrated. For debris-flow lahars, deposits are roughly equivalent to the flows that deposited them since most of the water is interstitial, and debris-flow deposits "freeze" as they are emplaced. For hyperconcentrated flows, however, deposit volume is invariably less than flow volume, considering that typical sediment concentration of hyperconcentrated-flow lahars at Pinatubo range from 20 to 40%. Considering that majority of lahar deposits are from debris flows, the deposit volume is estimated to be at least 70% of the flow volume.

Combining the inherent error in using deposit volume in lieu of flow volume (-30%) with the error in estimating deposit volume (±20%) yields a net error margin of about 36%. For comparison, Tuñgol and Regalado (1996) used observed flow discharges and volumes to calibrate the AFM in the Sacobia River in 1992, and found that the mapped deposit volume was around 70% of the total AFM-derived flow volume for the year.

In this study, the acoustic flux is used to calibrate the AFM to lahar volume, either for individual lahar events or for several events. Except for one instance, all field estimates of lahar volumes are from deposits. Low-flow AFM readings are excluded, considering that in normal practice, the volume contribution of low-flow events is insignificant and is not generally included in lahar deposit mapping. To identify lahar events in the AFM records, an amplitude threshold of 200 units (in 10^{-6} cm/s) with a minimum duration of one hour is used. This set of criteria is different from that used by Tuñgol and Regalado (1996), who used 100 AFM units without any cutoff duration. Their study, however, was based on direct measurements of both low- and high-discharge flows, while only high-discharge flows are considered here to filter out small flows that may or may not be lahars. The lahar-event threshold in the AFM in the Pasig-Potrero has been electronically set in the instruments at 500 amplitude units, but this was found to be too high, as some observed major lahar events had AFM amplitudes lower than this. The threshold amplitude and duration used in this study were arrived at after careful consideration – including many trial-and-error tests – of the AFM data vis-à-vis the field observations.

4.3.2. Results of AFM calibration

AFM calibration factors

Volume estimates from observed lahar events or deposits are compared to corresponding AFM-detected flow events or group of events, as shown in Table 4.2. From this table, calibration factors for AFM-5 and AFM-6 were derived. Table 4.2A shows that AFM-6 data correlates well with observed lahar volumes for 1992 and 1993 ($R^2 = 0.93$), with a calibration factor of 2200 (m^3 lahar per amp-hr AFM, where 1 amp = 1 x 10^{-6} cm/s). This reflects the fact that AFM-6 was essentially in a non-depositional

transport reach of the Pasig during that time so that all flows passing the instrument were conveyed directly to the alluvial fan, thus favoring one-to-one correspondence between instrument recording and deposit volume. The 1992 and 1993 lahars were also dominated by pumiceous debris-flows, hence the consistency in the signal. The variation in the calibration factor for AFM-6 is well within the error margin inherent in using the deposit volume instead of flow volume in the calibration (*Please see Section 4.3.1*).

Table 4.2. Calibration of the acoustic flow monitors in the Pasig-Potrero; amp = 10^{-6} cm/s.

(A) AFM-6

Date	Lahar Volume (10^6 m^3)	AFM Acoustic Flux (amp-hr)	Calibration Factor (m^3/amp-hr)	Remarks
29 Aug 1992	20	10119	1976	Lahar volume from visual monitoring of active flow (Arboleda and Martinez, 1996).
Whole of 1992	40	15695	2549	Deposit volume from Janda *et al.* (1996); acoustic flux total for 8 AFM-detected lahar events.
04-06 Oct. 1993	25	11079	2257	Deposit volume from JICA (1996); acoustic flux total for 3 events.
Whole of 1993	55	27172	2024	Deposit volume from Janda *et al.* (1996); acoustic flux total for 9 events.
Average factor			2201	

Calibration factor used for AFM-6 = 2200

(B) AFM-5

Date	Lahar Volume (10^6 m^3)	AFM Acoustic Flux (amp-hr)	Calibration Factor (m^3/amp-hr)	Remarks
28-31 Jul. 1995	15	12163	1233	Deposit volume from JICA (1996); acoustic flux total for 6 events. Lahar cleared/incised the channel from Delta 5 to about 5 km downstream.
15-19 Aug. 1995	14	11195	1251	Deposit volume from JICA (1996); acoustic flux total for 5 events. Lahar followed pre-existing channel; deposition confined to within the dike system downstream of the Porac-Angeles Road.
29 Aug. - 04 Sep. 1995	27	11231	2404	Deposit volume from JICA (1996); acoustic flux total for 4 events. Significant remobilization of deposits downstream of Delta 5.
30 Sep. - 01 Oct. 1995	22	11966	1839	Deposit volume from JICA (1996); acoustic flux total for 2 events. Large-scale remobilization of deposits along >15 km stretch of the channel, from the Timbu channel down to the medial parts of the alluvial fan in Bacolor.
20-21 Aug. 1997	20	8060	2481	Deposit volume from PHIVOLCS (unpublished); acoustic flux for 1 event. 18-m vertical incision at Delta 5; significant remobilization farther downstream.
Average factor			1842	

Calibration factor used for AFM-5 = 1800

Calibrating AFM-5 appears more uncertain. As seen in Table 4.2B, the lahar volume to acoustic flux ratio varies rather widely from about 1200 to more than 2400, with an R^2 value of 0.42, although the variation of about 35% from the mean is still within the error margin inherent in the calibration method (*Please see Section 4.3.1*). The relatively large variance in the ratios of lahar volume to AFM-5 acoustic flux may be related to unquantified physical changes in the depositional pattern of lahars during the observation periods used in the calibration. In particular, two distinct but related depositional scenarios could have significant effects on the correlation between AFM data and lahar deposits:

1) Until the middle of August 1995, many small lahars emplaced considerable deposits near Delta 5. All these would have been detected by AFM-5. In contrast, JICA's lahar mapping was concentrated on the main alluvial fan near and downstream of the Porac-Angeles Road, and may not have fully accounted for the deposits near Delta 5. Thus, field estimates of lahar deposit volumes, particularly for the first two events in Table 4.2B, may have been conservative compared to those detected by AFM-5, thereby lowering the AFM calibration factor.

2) Lahar remobilization was observed on a significant scale starting late August 1995, and was very pronounced during the 01 October 1995 Typhoon *Mameng* event (PHIVOLCS, unpublished reports; JICA, 1996) and the August 1997 Typhoon *Ibiang* event (Arante *et al.*, 1997). In those events when lahars bulked up with sediments downstream of Delta5, the lahar deposits in the alluvial fan would be larger than those indicated by AFM-5, thus increasing the AFM calibration factor.

Since the data used in calibrating AFM-5 (Table 4.2B) represent the above two scenarios in varying degrees, the derived average value of 1800 (±35%) m^3/amp-hr is deemed acceptable as a rough calibration factor for AFM-5.

AFM-calculated lahar volumes

Table 4.3 lists all individual lahars detected by the AFM in the Pasig-Potrero River using the criteria set in Section 4.3.1. Very few lahars escaped detection by the AFM; the instruments were rendered out of order only on rare occasions such as when heavy ashfall covered the solar panels resulting in the draining of the batteries (Marcial *et al.*, 1996). The cutoff criteria have eliminated flows with volumes that were much less than 1 x10^6 m^3, which is deemed reasonable considering that such flows hardly left mappable deposits. On an annual basis, it is believed that Table 4.3 sufficiently summarizes lahars in the Pasig-Potrero in terms of volume.

Table 4.3. All lahar events detected by AFM-5 and AFM-6 in the Pasig-Potrero River from 1992 to 1997. Lahar events are here defined at a cutoff amplitude of 200 amplitude units (amp = 10^{-6} cm/s) and minimum duration of one hour.

Date	Storm Event	Duration (hr)	Acoustic flux (amp-hr)	Calibration factor (m^3/amp-hr)	Lahar volume calculated from AFM (10^6 m^3)	Average AFM amplitude (amp)	Average discharge calculated from AFM (m^3/s)
1992							
1992 May 10	(Monsoon)	1.22	521	2200	1	429	262
1992 Jun 19	(Typhoon)	2.13	780	2200	2	365	223
1992 Jul 11	Typhoon Konsing	1.93	947	2200	2	490	299
1992 Jul 13	(Monsoon)	1.23	508	2200	1	412	252
1992 Aug 04	(Monsoon)	1.23	694	2200	2	563	344
1992 Aug 28	(Typhoon)	2.48	682	2200	2	275	168
1992 Aug 29	(Typhoon)	10.08	10119	2200	22	1004	613
1992 Aug 30	(Typhoon)	4.02	1443	2200	3	359	220
Total for 1992			**15695**		**35**		
1993							
1993 Aug 4	(Monsoon)	3.28	993	2200	2	302	185
1993 Aug 18-19	Typhoon Rubing	20.28	4494	2200	10	222	135
1993 Aug 28	(Monsoon)	1.28	391	2200	1	304	186
1993 Oct 04-05	Typhoon Kadiang	8.00	2565	2200	6	321	196
1993 Oct 05-06	Typhoon Kadiang	17.50	7771	2200	17	444	271
1993 Oct 06	Typhoon Kadiang	2.00	744	2200	2	372	227
1993 Oct 07	Typhoon Epang	4.15	3257	2200	7	785	480
1993 Oct 15	(Monsoon)	1.80	1181	2200	3	656	401
1993 Oct 31 - Nov 01	Typhoon Husing	11.50	5777	2200	13	502	307
Total for 1993			**27172**		**60**		
1994							
1994 May 30	(Monsoon)	1.52	1018	2200	2	671	410
1994 Jun 05	(Monsoon)	1.80	987	2200	2	548	335
1994 Jun 22	Typhoon Gading	5.12	3199	2200	7	625	382
1994 Jun 23	Typhoon Gading	8.33	5904	2200	13	708	433
1994 Jul10-11	Typhoon Iliang	17.50	10889	2200	24	622	380
1994 Jul 11	Typhoon Iliang	1.12	1029	2200	2	921	563
1994 Jul 11	Typhoon Iliang	2.67	712	2200	2	267	163
1994 Jul 15	(Monsoon)	5.05	3409	2200	8	675	413
1994 Jul 18-19	Typhoon Norming	28.77	18707	2200	41	650	397
1994 Jul 19	Typhoon Norming	9.23	5297	2200	12	574	351
1994 Jul 20	Typhoon Norming	2.85	1289	2200	3	452	276
1994 Jul 20-21	Typhoon Norming	13.40	4955	2200	11	370	226
1994 Jul 21-22	Typhoon Norming	24.00	11926	2200	26	497	304
1994 Jul 23	Typhoon Oyang	6.50	4647	2200	10	715	437
1994 Jul 24-25	Typhoon Oyang	27.10	35155	2200	77	1297	793
1994 Aug 03	Typhoon Paring	1.60	4155	1800	7	2597	1298
1994 Aug 06	Typhoon Ritang	1.00	426	1800	1	426	213
1994 Aug 07	Typhoon Ritang	3.23	1043	1800	2	322	161
1994 Aug 24	(Monsoon)	3.65	1440	1800	3	395	197
1994 Aug 31	(Monsoon)	3.00	2203	1800	4	734	367

1994 Aug 31	(Monsoon)	1.70	1831	1800	3	1077	538
1994 Sep 04-05	(Monsoon)	23.50	5053	1800	9	215	108
1994 Sep 13	(Monsoon)	2.00	1317	1800	2	658	329
1994 Sep 16-17	(Monsoon)	1.20	570	1800	1	475	237
1994 Sep 18	(Monsoon)	4.72	3410	1800	6	723	361
1994 Sep 19	(Monsoon)	2.52	559	1800	1	222	111
1994 Sep 21	(Monsoon)	1.50	421	1800	1	280	140
1994 Sep 21-22	(Monsoon)	3.98	3409	1800	6	856	428
1994 Sep 22	(Monsoon)	2.50	943	1800	2	377	189
1994 Sep 22	(Monsoon)	5.07	2312	1800	4	456	228
1994 Sep 22-23	Lake-breakout	5.00	2588	1800	5	518	259
1994 Sep 23	(Monsoon)	1.20	494	1800	1	412	206
1994 Sep 23	(Monsoon)	1.00	244	1800	0	244	122
1994 Sep 24	(Monsoon)	3.02	646	1800	1	214	107
1994 Sep 24	(Monsoon)	6.38	4327	1800	8	678	339
1994 Sep 25	(Monsoon)	5.08	6711	1800	12	1320	660
1994 Sep 28	(Monsoon)	3.33	2058	1800	4	617	309
1994 Sep 29	(Monsoon)	6.50	2413	1800	4	371	186
1994 Sep 30	(Monsoon)	3.00	1018	1800	2	339	170
1994 Sep 30	(Monsoon)	2.52	1269	1800	2	504	252
1994 Oct 14	(Monsoon)	2.00	633	1800	1	317	158
1994 Oct 21-22	Typhoon Katring	12.60	14404	1800	26	1143	572
1994 Oct 22	Typhoon Katring	2.53	878	1800	2	346	173
Total for 1994			**175899**		**360**		

1995							
1995 May 23	(Monsoon)	1.88	948	1800	1	503	252
1995 May 24	(Monsoon)	2.25	1044	1800	2	464	232
1995 May 25	(Monsoon)	4.22	1883	1800	3	446	223
1995 May 27	(Monsoon)	1.25	965	1800	2	772	386
1995 May 28	(Monsoon)	1.00	263	1800	0	263	131
1995 May 29	(Monsoon)	1.50	374	1800	1	249	125
1995 Jun 01-02	(Monsoon)	7.17	4951	1800	9	691	345
1995 Jun 03	(Monsoon)	6.13	2252	1800	4	367	184
1995 Jun 06	(Monsoon)	4.33	2655	1800	5	613	306
1995 Jun 07	(Monsoon)	4.65	2054	1800	4	442	221
1995 Jun 08	(Monsoon)	1.50	854	1800	2	569	285
1995 Jul 03	(Monsoon)	1.78	450	1800	1	252	126
1995 Jul 07	(Monsoon)	4.65	4750	1800	9	1021	511
1995 Jul 09	(Monsoon)	2.18	1476	1800	3	676	338
1995 Jul 09	(Monsoon)	2.23	1557	1800	3	697	349
1995 Jul 10	(Monsoon)	2.85	1605	1800	3	563	282
1995 Jul 10	(Monsoon)	3.62	2850	1800	5	788	394
1995 Jul 11	(Monsoon)	4.85	2823	1800	5	582	291
1995 Jul 18	(Monsoon)	4.18	2796	1800	5	668	334
1995 Jul 19	(Monsoon)	3.00	1935	1800	3	645	322
1995 Jul 22	(Monsoon)	2.22	1178	1800	2	531	266
1995 Jul 28	Typhoon Karing	1.50	467	1800	1	311	156
1995 Jul 28	Typhoon Karing	4.03	3105	1800	6	770	385
1995 Jul 29	Typhoon Karing	1.00	400	1800	1	400	200
1995 Jul 30	Typhoon Karing	10.12	6619	1800	12	654	327
1995 Jul 30	Typhoon Karing	1.50	605	1800	1	403	202

1995 Jul 30-31	Typhoon Karing	2.00	967	1800	2	483	242
1995 Aug 03	(Monsoon)	1.72	973	1800	2	567	283
1995 Aug 08	(Monsoon)	2.57	1103	1800	2	430	215
1995 Aug 09	(Monsoon)	1.75	970	1800	2	555	277
1995 Aug 10	(Monsoon)	1.50	1709	1800	3	1139	570
1995 Aug 10	(Monsoon)	1.22	1300	1800	2	1069	534
1995 Aug 11	(Monsoon)	1.20	962	1800	2	802	401
1995 Aug 15	(Monsoon)	2.28	3440	1800	6	1507	753
1995 Aug 16-17	(Monsoon)	1.62	746	1800	1	461	231
1995 Aug 17	(Monsoon)	2.88	1571	1800	3	545	272
1995 Aug 19	(Monsoon)	1.35	2718	1800	5	2013	1007
1995 Aug 19	(Monsoon)	2.15	2720	1800	5	1265	633
1995 Aug 29	Typhoon Gening	1.18	2411	1800	4	2037	1019
1995 Aug 29-30	Typhoon Gening	4.68	3195	1800	6	682	341
1995 Aug 30	Typhoon Gening	2.33	1670	1800	3	716	358
1995 Sep 03-04	Typhoon Helming	5.00	3955	1800	7	791	396
1995 Sep 10	(Monsoon)	2.05	1265	1800	2	617	309
1995 Sep 13	(Monsoon)	2.75	1654	1800	3	601	301
1995 Sep 16	(Monsoon)	2.85	1821	1800	3	639	320
1995 Sep 17-18	(Monsoon)	4.70	3057	1800	6	650	325
1995 Sep 18	(Monsoon)	2.53	2164	1800	4	854	427
1995 Sep 30 - Oct 01	Typhoon Mameng	2.00	1042	1800	2	521	260
1995 Oct 01	Typhoon Mameng	16.78	10924	1800	20	651	325
Total for 1995			**103193**		**186**		

1996							
1996 Jul 09		1.48	700	1800	1	472	236
1996 Jul 24		2.02	935	1800	2	464	232
1996 Jul26		2.05	902	1800	2	440	220
1996 Jul 26		1.07	556	1800	1	521	261
Total for 1996			**3094**		**6**		

1997							
1997 Aug 20-21	Typhoon Ibiang	13.67	8060	1800	15	590	295
Total for 1997			**8060**		**15**		

Using annual totals, AFM-derived lahar volumes compare to mapped deposits as follows (Table 4.4):

Table 4.4. Annual lahar volumes calculated from AFM data compared to field estimates.

Year	AFM-calculated volume (10^6 m^3)	Field estimate of deposit volume (10^6 m^3)
1992	35	40
1993	60	55
1994	360	140
1995	190	90
1996	6	30 (Muddy streamflow deposits)
1997	15	20

The 1992, 1993 and 1997 figures are well within the 30-40% error margin inherent in the AFM method. The large discrepancies for the 1994, 1995 and 1996 data, however, require further explanation.

The discrepancy in the 1994 figures is interpreted to reflect the remobilization of lahar deposits. In June-July 1994, AFM-6 recorded a total of 240 million m^3 of flows (*Please see* Table 4.3). These emplaced around 100 million m^3 of deposits at the Yangca-Papatac junction, thus forming the Cutuno blockage (*Please see Chapter 5*). These deposits were not included in the estimate of deposit volume. Similar rapid aggradation just upstream of Delta 5 that was recorded by AFM-5 in August 1994 was likewise underreported in the deposit volume estimate. The remobilization of lahar deposits during and after the September 1994 Cutuno lake-breakout may have resulted in "double counting" by the AFM. The June-August lahars clearly deposited >100 million m^3 of sediments upstream of Delta 5. Much of these deposits were remobilized during and after the lake-breakout. Only the remobilized sediments were effectively recorded in the deposits, while the AFM recorded both the initial emplacement of the deposits as well as the succeeding remobilization.

In 1995, many small lahars recorded by the AFM escaped field observation, perhaps because they were mostly confined within the large Pasig River canyon incised in late 1994. The mapped deposits (PHIVOLCS, unpublished data; JICA 1996c) basically included only those lahars that avulsed from the main Pasig-Potrero channel.

The deposits mapped in 1996 were mostly of non-lahar, albeit sediment-laden, flows, which had AFM signals that were below the amplitude and duration criteria used for this study. In fact, no major lahars were observed in the field or detected by the AFM during that season. The AFM-derived lahar volume for 1996 is thus considered reasonable.

Overall, the lahar volumes derived from the AFM data are judged to be reasonable estimates of actual flows that passed the sensor site, hence these are used in the following analyses and discussions.

4.4. Rainfall-normalized sediment yield: lahar-runoff vs. rainfall

4.4.1. Definitions

A *rainstorm* is here defined as a continuous rainfall event recorded by a rain gauge, with a minimum duration of one hour and with no pause more than one hour. Lahar events are those detected by the AFM with amplitudes greater than 200 amplitude units (in 10^{-6} cm/s) and durations longer than one hour (*See* Table 4.1 *on which instruments were used*). The one-hour cutoff is used to filter out small events, which are more susceptible to the effects of localized rainfall. This is also consistent with the general observation that lahars that are obviously rain-generated ebb to background levels after an hour of lull in rainfall.

Those rainstorms that coincide in time with AFM-detected lahar events are classified as *lahar-generating rainstorms*; others are considered *non-lahar rainstorms*. AFM-detected lahar events with no coincident rainfall as defined above have been discarded in the analyses; rainfall during these events may have been under-recorded by the rain

gauges, or the flows were generated by other events such as breaching of temporary lakes or secondary pyroclastic flows or avalanches.

4.4.2. Analysis

Table 4.5 lists all coincident rainstorm and lahar events in the Pasig-Potrero River from 1992 to 1997. To account for the increase in watershed size during the 1993 stream piracy, rainfall is normalized by multiplying the amount with the prevailing watershed size; this yields the volume of rainfall in the entire catchment. The ratio of lahar-runoff to rainfall is calculated for each event; this ratio represents the rainfall-normalized laharic sediment yield.

Table 4.5. Coincident rainstorm and lahar events in the Pasig-Potrero from 1992 to 1997. Annual totals of lahar and rainfall are shown; annual lahar-rainfall ratios are obtained by dividing total lahar volume by rainfall volume. This list is a subset of Table 4.3 that excludes lahar events which do not correlate in time with discrete rainstorms as defined in Section 4.4.1.

Date	Acoustic Flow Monitor Data			Associated Rain					Ratio of lahar-runoff to rainfall
	Duration (hr)	Acoustic flux (amp-hr)	Lahar volume (10^6 m^3)	Duration (hr)	Amount (mm)	Intensity (mm/hr)	Volume 10^6 m^3)	Volumetric intensity (10^6 m^3/hr)	
1992 May 10	1.22	521	1.1	2.00	41	20.5	1.0	0.5	1.17
1992 Jul 11	1.93	947	2.1	4.67	77	16.5	1.8	0.4	1.13
1992 Jul 13	1.23	508	1.1	1.35	83	61.5	2.0	1.5	0.56
1992 Aug 4	1.23	694	1.5	2.67	28	10.5	0.7	0.3	2.27
1992 Aug 28	2.48	682	1.5	10.00	110	11.0	2.6	0.3	0.57
1992 Aug 29	10.08	10119	22.3	24.65	246	10.0	5.9	0.2	3.77
1992 Total		**13471**	**29.6**		**585**		**14.0**		**2.11**
1993 Aug 4	3.28	993	2.2	6.45	62	9.6	1.5	0.2	1.47
1993 Aug 18	20.28	4494	9.9	35.52	301	8.5	7.2	0.2	1.37
1993 Aug 28	1.28	391	0.9	6.23	105	16.8	2.5	0.4	0.34
1993 Oct 31	11.50	5777	12.7	15.50	148	9.5	6.7	0.4	1.91
1993 Total		**11655**	**25.7**		**616**		**17.9**		**1.43**

1994 Jun 22	5.12	3199	7.0	3.00	26	8.7	1.2	0.4	6.01
1994 Jun 23	8.33	5904	13.0	1.50	66	44.0	3.0	2.0	4.37
1994 Jul 15	5.05	3409	7.5	9.22	121	13.1	5.4	0.6	1.38
1994 Jul 18	28.77	18707	41.2	30.82	332	10.8	14.9	0.5	2.75
1994 Jul 19	9.23	5297	11.7	8.67	22	2.5	1.0	0.1	11.77
1994 Jul 20	13.40	4955	10.9	12.67	40	3.2	1.8	0.1	6.06
1994 Jul 21	24.00	11926	26.2	9.67	62	6.4	2.8	0.3	9.40
1994 Jul 23	6.50	4647	10.2	11.63	92	7.9	4.1	0.4	2.47
1994 Jul 24	27.10	35155	77.3	52.03	345	6.6	15.5	0.3	4.98
1994 Aug 3	1.60	4155	7.5	10.00	94	9.4	4.2	0.4	1.77
1994 Aug 6	1.00	426	0.8	2.00	21	10.5	0.9	0.5	0.81
1994 Aug 7	3.23	1043	1.9	3.50	60	17.1	2.7	0.8	0.70
1994 Aug 24	3.65	1440	2.6	5.00	106	21.2	4.8	1.0	0.54
1994 Aug 31	3.00	2203	4.0	1.00	17	17.0	0.8	0.8	5.18
1994 Aug 31	1.70	1831	3.3	3.00	65	21.7	2.9	1.0	1.13
1994 Sep 4	23.50	5053	9.1	14.00	12	0.9	0.5	0.0	16.84
1994 Sep 16	1.20	570	1.0	7.00	68	9.7	3.1	0.4	0.34
1994 Sep 21	3.98	3409	6.1	3.00	41	13.7	1.8	0.6	3.33
1994 Sep 22	5.07	2312	4.2	3.28	64	19.5	2.9	0.9	1.44
1994 Sep 22	5.00	2588	4.7	3.98	19	4.8	0.9	0.2	5.45
1994 Sep 24	6.38	4327	7.8	2.00	21	10.5	0.9	0.5	8.24
1994 Sep 25	5.08	6711	12.1	4.00	76	19.0	3.4	0.9	3.53
1994 Sep 30	3.00	1018	1.8	1.50	10	6.7	0.5	0.3	4.07
1994 Sep 30	2.52	1269	2.3	4.50	27	6.0	1.2	0.3	1.88
1994 Oct 14	2.00	633	1.1	1.50	19	12.7	0.9	0.6	1.33
1994 Oct 21	12.60	14404	25.9	13.98	231	16.5	10.4	0.7	2.49
1994 Oct 22	2.53	878	1.6	6.50	10	1.5	0.5	0.1	3.51
1994 Total		**147469**	**302.8**		**2067**		**93.0**		**3.25**

1995 May 24	2.25	1044	1.9	1.50	12	8.0	0.5	0.4	3.48
1995 May 25	4.22	1883	3.4	4.50	51	11.3	2.3	0.5	1.48
1995 May 27	1.25	965	1.7	1.00	23	23.0	1.0	1.0	1.68
1995 Jun 1	7.17	4951	8.9	2.00	55	27.5	2.5	1.2	3.60
1995 Jun 3	6.13	2252	4.1	10.00	52	5.2	2.3	0.2	1.73
1995 Jun 6	4.33	2655	4.8	3.00	24	8.0	1.1	0.4	4.43
1995 Jun 7	4.65	2054	3.7	3.50	19	5.4	0.9	0.2	4.32
1995 Jun 8	1.50	854	1.5	2.00	16	8.0	0.7	0.4	2.13
1995 Jul 3	1.78	450	0.8	3.00	31	10.3	1.4	0.5	0.58
1995 Jul 7	4.65	4750	8.5	2.35	75	31.9	3.4	1.4	2.53
1995 Jul 9	2.23	1557	2.8	3.50	29	8.3	1.3	0.4	2.15
1995 Jul 10	3.62	2850	5.1	3.70	29	7.8	1.3	0.4	3.93
1995 Jul 18	4.18	2796	5.0	3.50	90	25.7	4.1	1.2	1.24
1995 Jul 19	3.00	1935	3.5	1.50	28	18.7	1.3	0.8	2.76
1995 Jul 22	2.22	1178	2.1	4.50	17	3.8	0.8	0.2	2.77
1995 Jul 28	1.50	467	0.8	3.00	19	6.3	0.9	0.3	0.98
1995 Jul 28	4.03	3105	5.6	4.35	58	13.3	2.6	0.6	2.14
1995 Jul 29	1.00	400	0.7	6.50	35	5.4	1.6	0.2	0.46
1995 Jul 30	10.12	6619	11.9	16.00	121	7.6	5.4	0.3	2.19
1995 Jul 30	2.00	967	1.7	2.32	27	11.7	1.2	0.5	1.43
1995 Aug 3	1.72	973	1.8	2.00	30	15.0	1.4	0.7	1.30
1995 Aug 8	2.57	1103	2.0	4.10	49	12.0	2.2	0.5	0.90
1995 Aug 9	1.75	970	1.7	2.50	12	4.8	0.5	0.2	3.23
1995 Aug 15	2.28	3440	6.2	4.00	60	15.0	2.7	0.7	2.29
1995 Aug 17	2.88	1571	2.8	2.50	18	7.2	0.8	0.3	3.49

1995 Aug 19	2.15	2720	4.9	2.00	38	19.0	1.7	0.9	2.86
1995 Aug 29	4.68	3195	5.8	10.00	98	9.8	4.4	0.4	1.30
1995 Aug 30	2.33	1670	3.0	9.50	53	5.6	2.4	0.3	1.26
1995 Sep 3	5.00	3955	7.1	5.50	96	17.5	4.3	0.8	1.65
1995 Sep 10	2.05	1265	2.3	3.00	54	18.0	2.4	0.8	0.94
1995 Sep 13	2.75	1654	3.0	4.00	32	8.0	1.4	0.4	2.07
1995 Sep 16	2.85	1821	3.3	5.50	44	8.0	2.0	0.4	1.66
1995 Sep 17	4.70	3057	5.5	9.00	67	7.4	3.0	0.3	1.83
1995 Sep 18	2.53	2164	3.9	5.00	40	8.0	1.8	0.4	2.16
1995 Sep 30	2.00	1042	1.9	6.50	35	5.4	1.6	0.2	1.19
1995 Oct 1	16.78	10924	19.7	18.00	340	18.9	15.3	0.9	1.29
1995 Total		**85256**	**153.4**		**1877**		**84.5**		**1.82**
1996 Jul 9	1.48	700	1.3	1.33	28	21.0	1.3	0.9	1.00
1996 Jul 24	2.02	935	1.7	5.23	35	6.7	1.6	0.3	1.07
1996 Jul 26	2.05	902	1.6	4.67	90	19.3	4.1	0.9	0.40
1996 Jul 26	1.07	556	1.0	1.67	63	37.8	2.8	1.7	0.35
1996 Total		**3094**	**5.6**		**216**		**9.7**		**0.57**
1997 Aug 20	**13.67**	**8060**	**14.5**	**26.33**	**585**	**22.2**	**26.3**	**1.0**	**0.55**

Figure 4.4 is a plot of lahar volume against rainfall volume, which shows rough positive correlation (correlation coefficient R = 0.64). The scatter in the correlation reflects the many physical variables affecting lahar-rainfall relations in addition to the residual effects of localized rainfall. Physical factors that may affect the relationship of lahar-runoff to rainfall include flow properties such as flow turbulence, sediment concentration, and clast size and density, and hydrological variables such as antecedent rainfall and soil infiltration. The occurrence of secondary hydroeruptions, secondary pyroclastic flows and lake breakouts also have significant effects on lahar-runoff.

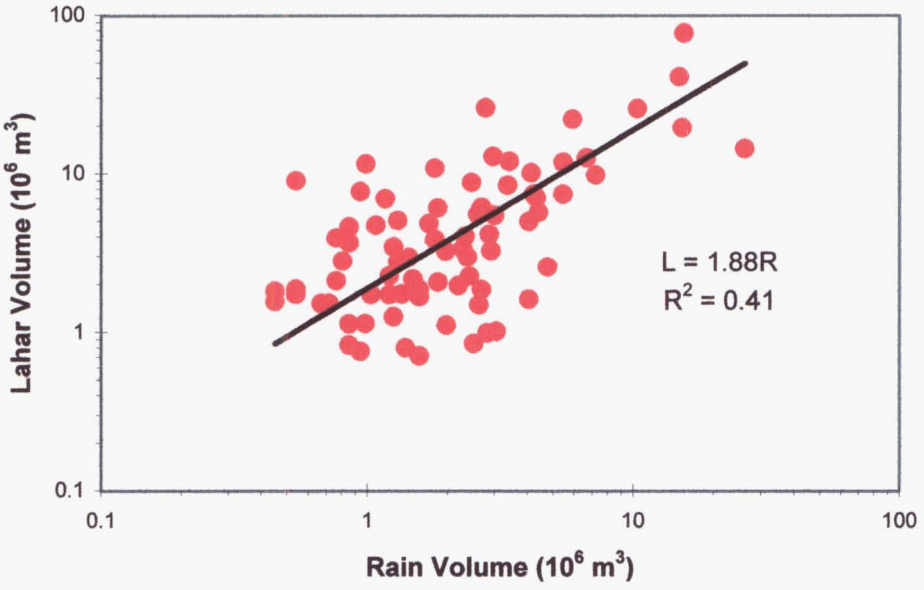

Figure 4.4. Plot of lahar-runoff against rainfall volume (watershed-normalized rainfall) for all coincident lahar and rainstorm events, from 1992 to 1997.

From one individual event to the next, the volumetric ratio of lahar to rainfall varied erratically from 0.34 to 17 (*See rightmost column in* Table 4.5). To be able to see seasonal changes, the yearly totals of coincident lahars and rainstorms were compared, and annual lahar-runoff to rainfall ratios were calculated by dividing the former with the latter (*See rightmost column in the yearly totals in* Table 4.5). A plot of these annual ratios on a yearly time scale is given in Figure 4.5.

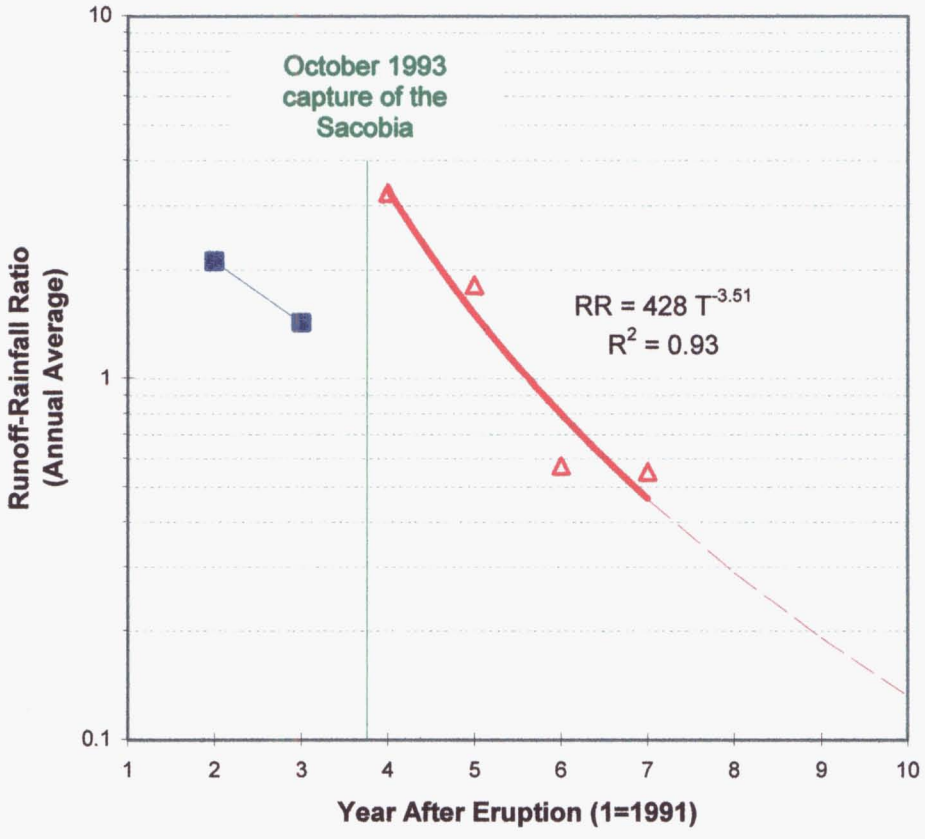

Figure 4.5. Temporal variation of the ratio of annual lahar-runoff to rainfall in the Pasig-Potrero, from 1992 to 1997. Ratios are from the yearly totals given in Table 4.5.

Figure 4.5 shows two declining trends separated in time by the October 1993 capture of the upper Sacobia by the Pasig. While the trend from 1992 to 1993 is inconclusive, the rapid, non-linear decrease in the ratio of lahar-runoff to rainfall, from 3.4 in 1994 to 0.55 in 1997, is quite apparent. The annual decrease during this period may be approximated by a power curve. This curve is extrapolated to predict the amount of rainfall necessary to generate a given volume of lahar, or vice versa. These projections are shown in Table 4.6.

Table 4.6. Projected rainfall requirement (in mm) for different volumes of lahar, calculated from the trendline in Figure 4.5. Rainfall amount is calculated for a catchment size of 45 km^2.

	Lahar volume			
Year	5 x 10^6 m^3	10 x 10^6 m^3	15 x 10^6 m^3	20 x 10^6 m^3
1997	240	480	720	960
1998	380	770	1150	1540
1999	580	1160	1740	2320
2000	840	1680	2520	3360

From experience, disastrous lahars in the Pasig-Potrero had volumes >10 million m^3. Table 4.6 shows that a lahar of such volume would have required 770 mm of rainfall in 1998 and 1160 mm in 1999. Both of these exceed the estimated 100-year probable maximum rainfall for 24 hours, with the latter even exceeding the 100-year 3-day maximum (*See* Figure 2.5, Section 2.3.1).

The last major lahar event coincided with a continuous downpour of 585 mm in a 26-hour period (1570 mm in 5 days), during the peak of Typhoon *Ibiang*, which spawned a total of 15 million m^3 of lahar. This is greater than the rainfall during the passage of Typhoon *Mameng* on 01 October 1995, which generated >20 million m^3 of lahar. It even apparently exceeded rainfall during the calamitous Central Luzon flood of 1972 (JICA, 1978). Isohyetal maps (JICA, 1996c) and limited comparison of upland and lowland rain gauge data around Pinatubo (Newhall, 1994) suggest that rainfall in the upper slopes of the volcano is perhaps 20-25% larger than that in the plains, and the 1972 rains might have been greater in the uplands. Nevertheless, Typhoon *Ibiang* appears to be an unusually large storm event, with an estimated return period of 100 years. The fact that only a moderate-sized lahar was generated by this storm suggests the increased rainfall requirement for generating disastrous lahars.

4.5. Rainfall threshold for lahar generation

The rainfall threshold at which lahars are generated has been studied by Arboleda and Martinez (1996), and Tuñgol and Regalado (1996) for Mount Pinatubo, and by Rodolfo and Arguden (1991) for Mayon Volcano. Caine (1980) has also derived similar trigger thresholds for rain-induced non-volcanic landslides and debris flows worldwide. The threshold is commonly expressed as a power curve in the form $I = cD^n$, where I is rainfall intensity in mm per hour, D is duration in hours, and c and n are empirically derived numbers.

On a log-log plot of intensity against duration, the exponent n controls the slope of the threshold curve, while the coefficient c defines its y-axis position. Ideally, non-lahar rainstorms should plot in a regime below that of lahar-triggering ones, and a threshold curve could then be drawn between the two regimes. This is only partially true for the Pasig-Potrero data, however, as many apparent lahar-triggering rainstorms are less than some non-lahar ones, especially during the 1994 and 1995 seasons. As has been suggested by Newhall (1994), Pierson *et al.* (1996), and Tuñgol and Regalado (1996), rain gauge records can be conservative. Some localized storm cells can generate lahars but their peak intensity may be missed by the rain gauge. This underestimation becomes less likely during regional typhoons, but is nonetheless an inherent limitation of the system. Considering this, a restriction is imposed on the lahar-threshold rainfall: as much as possible, it should plot above the largest rainstorms that did not generate lahars even if some lahar-triggering rain events plot below it.

All lahar-triggering and non-lahar rainstorms from 1992 to 1997 are shown in log-log plots of volumetric intensity against duration in Figure 4.6. Rainfall volume (in m^3) is used instead of the usual rainfall column (in mm), in order to normalize for the change in watershed size resulting from the 1993 Sacobia-Pasig stream piracy. Ideally, the threshold curve may be derived by fitting a curve between the largest non-lahar rainstorm and the lowest lahar-triggering rainstorm that plot above the non-lahar rain events, as was done by Tuñgol and Regalado (1996). Strictly following this procedure however, yielded different n values for the different seasons, making comparative

analysis difficult. To avoid this problem, threshold curves were first derived strictly following the procedure by Tuñgol and Regalado (1996), and then an average n value was chosen from these curves. An n value of -0.6 was thus derived and used for all the data shown in Figure 4.6. For comparison, Caine (1980) used n = -0.39 for shallow landslides and debris flows worldwide; Rodolfo and Arguden (1991) derived n = -0.38 for the debris-flow lahars of Mayon Volcano; while Tuñgol and Regalado derived n = -1.5 for the 1992 lahars in the Sacobia River.

Using one exponent value of -0.6, the coefficient, c, of the threshold curve for each of the rainy seasons was manually adjusted so that it plots above all the non-lahar rainstorms. The only exception here is one non-lahar rainstorm that occurred on 16 August 1994 (Figure 4.6C). A small lahar was in fact observed on that date (Arboleda *et al.*, 1995), but the signal recorded by the AFM did not meet the 200 amplitude units and one-hour duration criteria set in this study. At any rate, the value of c used for 1994 is 1.0; forcing the threshold curve to plot above the 16 August 1994 event would have changed the c value to 1.6. For all practical purposes, the threshold curves in Figure 4.6 show the ultimate limits above which lahars WILL occur, rather than the minimum thresholds above which lahars MAY occur.

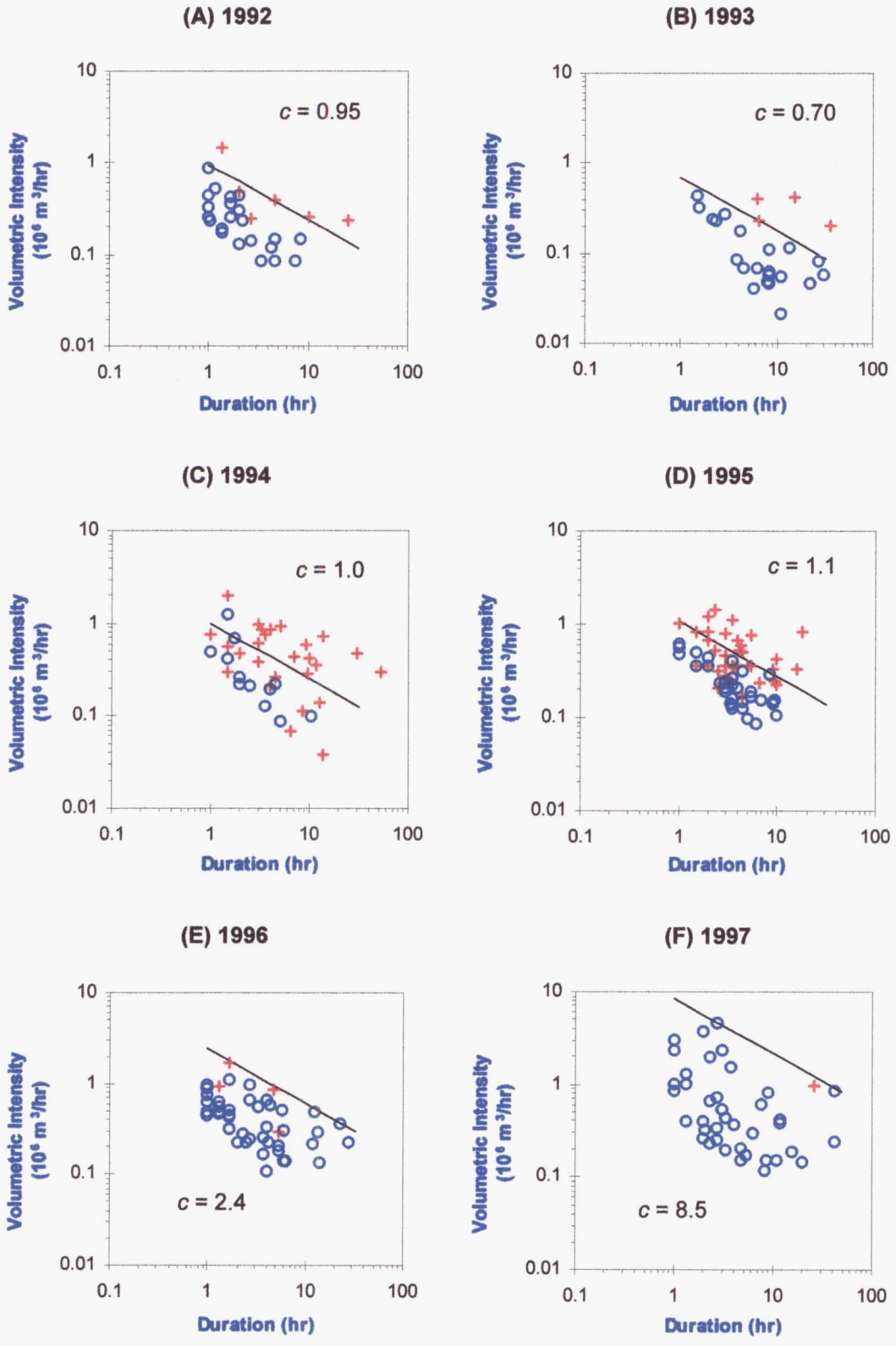

Figure 4.6. Volumetric intensity vs. duration plots of all lahar-triggering (+) and non-lahar rainfall (o) events in the Pasig-Potrero River basin. For each season, a lahar-triggering threshold in the form $I = cD^{-0.4}$ is drawn. The coefficient, c, indicates the threshold intensity at one-hour duration.

A comparison of the yearly thresholds is shown in Figure 4.7. This shows practically identical thresholds from 1992 to 1995, followed by a marked progressive increase until 1997. While the limited number of lahar-generating rainstorms in 1996 and 1997 might raise doubts on sampling bias, the data are judged to realistically reflect the observed decreased lahar activity during the period. The data clearly show the occurrence of many large-magnitude rainstorms that did not generate lahars, confirming that the rainfall threshold for lahar generation had indeed increased during these periods.

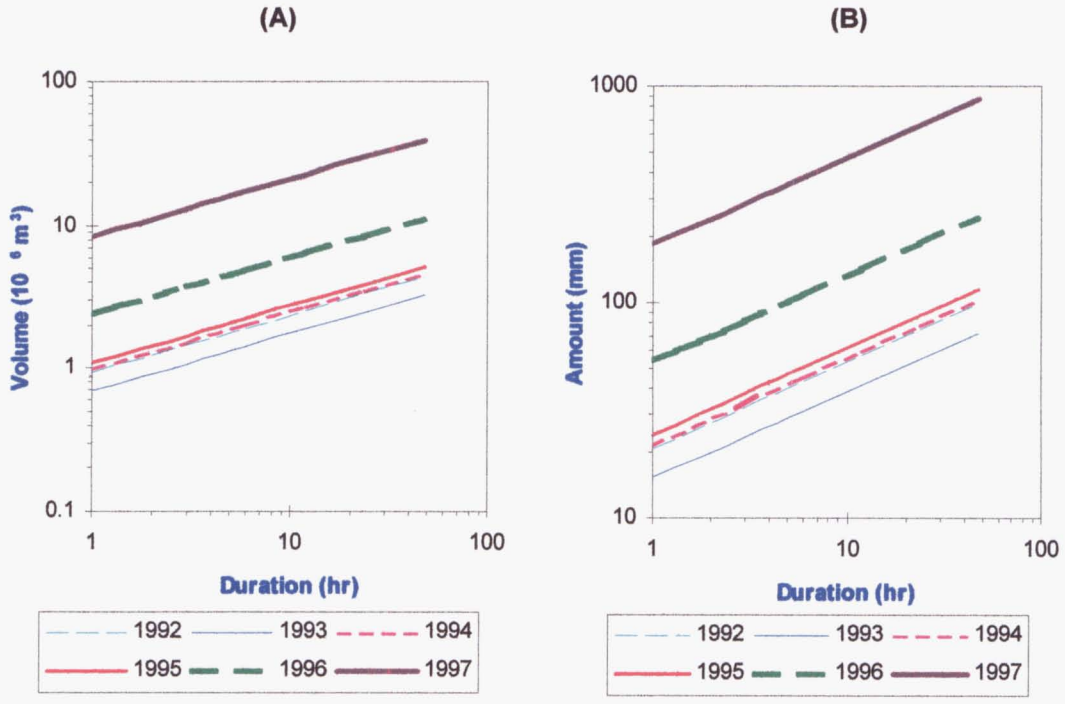

Figure 4.7. Composite plots of annual lahar-triggering rainfall thresholds. The volumetric intensity (m^3/hr) in A is converted to the usual area-normalized intensity unit (mm/hr) using the present Pasig catchment area of 45 km^2 to show the temporal changes for a constant-size watershed in more familiar units.

4.6. Discussions

Two rain-lahar parameters are analyzed in this study: (1) rainfall-normalized sediment yield, as represented by the ratio of lahar-runoff to the amount of coincident rainfall, and (2) the lahar-triggering rainfall threshold. The ratio of lahar-runoff to rainfall peaked twice, in 1992 and 1994, then decreased non-linearly after each peak. The lahar-generating rainfall threshold is found to remain at a low level from 1992 to 1995 before progressively increasing until the last lahar year of 1997. The simplified trends are illustrated in Figure 4.8.

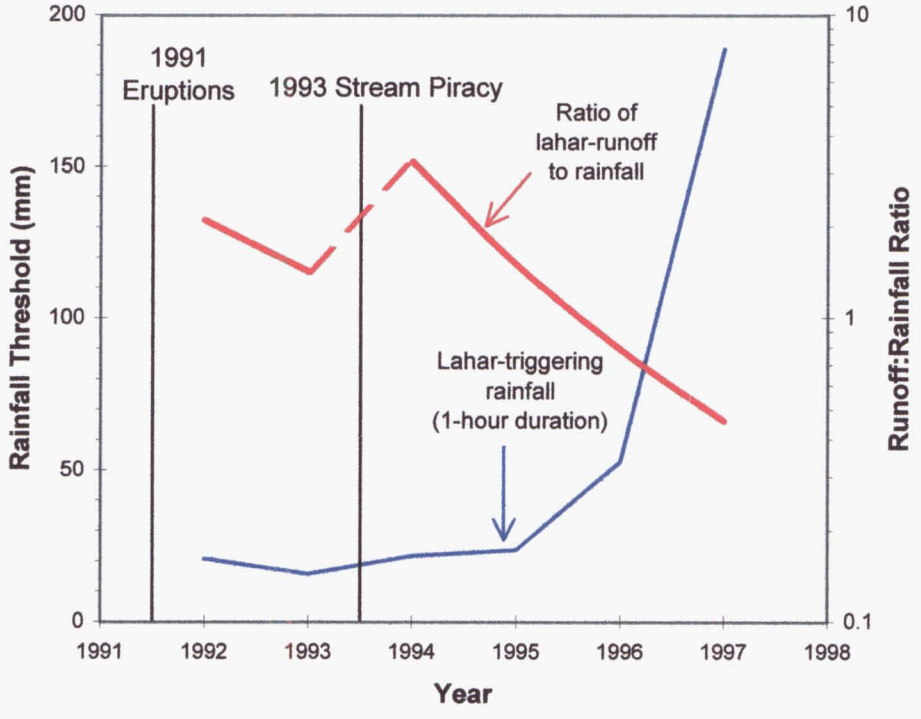

Figure 4.8. Temporal trends in the lahar-generating rainfall threshold (blue line) and the ratio of lahar-runoff to coincident rainfall (red line). The 1991 eruptions and the 1993 stream piracy involving the Pasig and Sacobia Rivers mark instances of severe watershed disturbance. The ratio of lahar-runoff to rainfall peaked after each disturbance then exponentially decreased, while the lahar-threshold remained low until 1994 then increased progressively.

The trends in sediment yield and lahar-triggering rainfall reflect the response of the Pasig-Potrero watershed to massive hydrological disturbances caused by (1) the June 1991 eruptions, and (2) the October 1993 capture of the upper Sacobia catchment by the Pasig River. In the first instance, the disruption came mainly in the form of 0.3 km^3 of loosely emplaced pyroclastic debris which filled the river's head tributaries. In the latter case, it was the product of two related phenomena: the headward extension of the river, which almost doubled its catchment size, and the annexation of a sizeable cache of pyroclastic-flow deposits that were up until then in the Sacobia. The capture brought the total volume of erodible deposits in the Pasig back to 0.3 km^3 at the onset of the 1994 season.

4.6.1. Laharic sediment yield

Sediment yield in watersheds disturbed by major volcanic eruptions has been thought to follow an exponential decrease, based on observations of gross annual sediment yield versus annual rainfall (Pierson *et al.*, 1992; Punongbayan *et al.*, 1994; Janda *et al.*, 1996; Major *et al.*, 2000). Exceptions to the exponential-decay model have been raised by other scientists, however, noting that it cannot be extrapolated to extreme rainfall events and does not account for other lahar-generating mechanisms such as lake-breakouts (Umbal, 1997; Rodolfo, unpublished reports). This study supports a non-linear decay model, although a power-curve rather than an exponential decay seems to be a more appropriate model for the Pasig-Potrero.

In the absence of any direct observations of the physical conditions and processes in the Pasig-Potrero watershed, especially during the period covered by this study, interpreting the trend in laharic sediment yield (Section 4.4) can only be made by logical argumentation. I suggest that the ultimate volume of lahar-runoff during a given rainstorm depends on the amount of erodible materials available to a flow so that the flow can bulk up with sediments as it travels. This is a function of (1) sediment supply, and (2) drainage density and channel width. Without hard data, sensitivity analyses cannot be done to test these factors individually, but sediment supply is believed to be the most significant factor governing sediment yield. The bulk of the sediment supply

comes mostly from the 1991 pyroclastic flow and tephra-fall deposits, but also includes varying amounts of exposed pre-eruption sediments. The volume of pyroclastic deposits in the source area is believed to have progressively decreased in relation to the volume eroded by lahars and streamflows. At Pinatubo however, erosion in the source area – thus the volume of remaining source material – is poorly constrained; GIS-based overlaying techniques have suffered from the lack of a detailed digital elevation model and ground control points (*e.g.*, Daag, 1994; Jones and Newhall, 1996).

Drainage density and channel width controls the amount of erodible material in contact with channelized flow. While lahars at Pinatubo may be initiated by overland flow, the bulk of the flow volume comes from channel bank and bed erosion. Personal observations of active lahars indicate that bank materials account for a large proportion of the sediments that form lahars, an observation shared by Major *et al.* (2000) at Mount St. Helens. As drainages integrate, the drainage density – *i.e.*, stream length per unit area – decreases and channel width increases. These combine to reduce bank areas in contact with the flow. Wider channels also reduce the ability of flows to scour channel beds by spreading them over larger areas. Collins and Dunne (1986) attributed the decline in sediment yield at Mount St. Helens more to the development of a stable rill network than to vegetation recovery. Drainage analysis, perhaps by remote sensing and GIS techniques, need to be done to test the effects of drainage density and channel width to sediment yield. Unfortunately, this was not done during this study because of time and logistical constraints.

4.6.2. Lahar-triggering rainfall

That the rainfall threshold for lahar-generation remained practically the same from 1992 to 1995 even through the dramatic watershed change resulting from the 1993 stream piracy, is contrary to expectations that it would systematically increase with time as the drainage networks integrated and the source-sediments (1991 pyroclastic deposits) got depleted. Experience in other volcanoes, as well as observations at Pinatubo, have shown that drainage integration follows volcanic disturbances immediately (Segerstrom, 1950; Waldron, 1967; Collins *et al.*, 1983; Kadomura *et al.*, 1983; Collins and Dunne,

1986; Leavesley *et al.*, 1989; Pierson *et al.*, 1996; Major *et al.*, 2000). In the Pasig-Potrero watershed, the rapid development of an integrated network of rills and gullies can be inferred from the extensive dissection of the tephra mantle on steep hillslopes by October 1991 (Pierson *et al.*, 1996).

The trend in the lahar-triggering rainfall (Section 4.4) indicates that the lahar-threshold is sensitive to some other factors that override sediment-source volume and drainage development. The lahar-generating rainfall threshold depends mainly on (1) the amount of runoff and (2) the erodibility of the surface material over which runoff flows. Neglecting the contribution of springs, post-eruption runoff may be expressed in terms of the relative proportion of rainwater that does not infiltrate the surface. The amount of runoff therefore is largely controlled by the infiltration capacity of the surface, which is controlled by (1) the nature of the surficial deposit, (2) vegetation and (3) the presence of tephra cover. The same factors also control the erodibility of the surface.

Infiltration capacity and erodibility of the 1991 pyroclastic-flow and tephra-fall deposits

The erodibility of the pumiceous pyroclastic deposits is relatively high in light of their low density, loose emplacement and low clay content. The materials have been observed to be moved by the slightest of water runoff, and pumice clasts have been found to be transported as bedload at water depths half their diameter (Montgomery *et al.*, 1999). Such high erodibility is expected to persist throughout the entire section of the pumiceous pyroclastic-flow deposits, in consonance with their massive, non-welded, poorly sorted stratigraphy (Scott *et al.*, 1996).

The pumiceous pyroclastic-flow deposits may also be expected to be more or less homogenous in terms of infiltration capacity. Daag (ongoing PhD thesis, International Institute for Aerospace Survey and Earth Sciences, the Netherlands) has found little difference in the infiltration capacity of the different deposits of Pinatubo; rather he found that infiltration was chiefly dependent on rainfall intensity. He was not able to sufficiently compare the infiltration capacity of pre-eruption and post-eruption deposits, however. Infiltration is believed to be mainly controlled by the fine tephra – from post-

plinian eruptions and from succeeding secondary explosions – that covered both the valley-fill pyroclastic deposits and the surrounding hillslopes. This tephra cover served to increase runoff volume by providing readily entrainable sediments, and later, by forming a tephra crust that inhibits infiltration.

In general, the 1991 pyroclastic deposits covered roughly the same area from 1992 to 1994 (Daag, 1994). The exhumation of the pre-eruption surface in river channels only began in significant scale during the 1995 season, particularly during the October 1995 Typhoon *Mameng* lahars. During a fieldwork in June 1996, it was observed that almost the entire length of the Pasig River channel was incised into pre-eruption deposits.

Effects of vegetation and tephra cover

In addition to the infiltration capacity and erodibility of the material itself are the contrasting effects of vegetation and tephra cover. Vegetation recovery on the thick valley-fill deposits has been slow, and was probably insignificant during the period covered by this study (1992-1997). However, vegetation has been observed to recover quickly on the tephra-mantled hillslopes because the relatively thin tephra cover was washed away quickly. This should have promoted infiltration and reduced surface erodibility on the hillslopes, which should have raised the lahar-triggering rainfall threshold sooner than it did.

It is postulated that secondary explosions, which commonly occurred during the rainy season, momentarily negate the effects of vegetation on infiltration. The frequency of occurrence of secondary explosions decreased significantly after 1994 (Table 4.7), and large explosions (with >5 km high ash columns), have practically ceased to occur after 1995 (*Please see* Figure 3.7, *Section 3.6*). While the numbers correspond with the trend in the lahar-threshold rainfall data, however, causal relationships cannot be proved by the data alone.

Table 4.7. Number of secondary explosions observed from PVO (PHIVOLCS, unpublished data).

Year	No. of observed secondary explosions
1991 (starting 5 September only)	18
1992	127
1993	90
1994	126
1995	29
1996	16
1997	10
1998	18
1999	19
2000	6

NB:
Secondary explosion is a catch-all term used by PHIVOLCS to denote ash eruptions from the pyroclastic-flow deposits, including true secondary hydroeruptions **(Moyer and Swanson, 1987)** *as well as ash-generating bank collapses and secondary pyroclastic flows and avalanches* **(Torres *et al.*, 1996)**. *The list is by no means complete, as visual observations are sometimes hindered by weather, but nevertheless gives a clear indication of the relative frequency of occurrence of the events.*

Secondary explosions facilitate the erosion of pyroclastic-flow deposits by dilating the deposits, disrupting any previously formed surface crusts and transporting loose debris into active channels (Pierson *et al.*, 1996). Perhaps more significantly, the intermittent explosions covered a large part of the catchment with loose tephra, thus burying vegetation and reverting infiltration capacity and erodibility to a tephra-covered state. As long as secondary explosions occurred frequently enough, this condition became effective during every rainy season, and vegetation recovery only occurred only during the dry season.

The aerial extent of secondary tephra is poorly constrained given the limited coverage of aerial surveys during lahar seasons. A qualitative indication of their extent is the observation that the upper catchment of the Pasig-Potrero was almost always gray during lahar seasons, at least until 1995. Most available aerial photographs and remote sensing data were taken before and after the rainy seasons, and thus do not reflect the conditions during the occurrence of lahars.

The lahar-triggering rainfall threshold is postulated to have varied with the aerial extent of the 1991 pyroclastic-flow and tephra-fall deposits. After 1995, this extent was significantly reduced when the river channel has incised into the pre-eruption bedrock. The effective extent of the tephra-fall deposits during the rainy seasons also decreased after 1995 due to the decrease in secondary explosion activity.

4.7. Conclusions

1. AFM data were calibrated using deposit and flow volumes to represent lahars flowing along the Pasig-Potrero River channel from 1992 to 1997. The calibrated data were used as a proxy for runoff for individual lahar events, taking advantage of the relatively complete AFM records.

2. The AFM-derived lahar-runoff was correlated with coincident rainfall recorded by the telemetered rain gauges to study the relationship of lahars to rainfall on a per-event basis.

3. The ratio of lahar-runoff to coincident rainfall was used to represent rainfall-normalized laharic sediment yield for individual lahar and rainstorm events. The trend in sediment yield was related to two major watershed disturbances: the June 1991 eruptions of Mount Pinatubo and the October 1993 capture of the upper Sacobia catchment by the Pasig River. On a seasonal average, sediment yield peaked immediately after each major watershed disturbance, then decreased non-linearly through time. The declining trend is interpreted to be a function of sediment supply, and drainage density and channel width, which combine to control the amount of erodible material in contact with runoff.

4. The rainfall threshold at which lahars have been generated remained at a uniformly low level from 1992-1995, then increased progressively until the last lahar year of 1997. The lahar-triggering rainfall threshold is inferred to be controlled by the erodibility and infiltration capacity of the surface material. These are in turn controlled by the areal distribution of the pumiceous 1991

pyroclastic-flow and tephra-fall deposits. The tephra-fall deposits from secondary explosions, in particular, served to momentarily negate the effects of vegetation recovery during the rainy season by mantling almost the entire upper catchment with tephra. After 1995, the Pasig River channel has incised down to the pre-eruption surface, while the frequency and magnitude of secondary explosions have diminished considerably. These are believed to have caused the progressive increase in the lahar-triggering rainfall.

Chapter 5

FORMATION AND FAILURE OF TRANSIENT DAMS

CHAPTER 5

Formation and Failure of Transient Dams

While the lahars of Mount Pinatubo are mostly rain-generated, some of the most devastating ones have been triggered by the sudden breakout of transient lakes that were formed by the blockage of tributaries by lahar or pyroclastic-flow deposits. Some of the lakes have shown repeated formation and catastrophic breaching episodes; others still exist several years after their initial formation.

Transient lakes pose a serious hazard at Pinatubo, yet their behavior has not been studied in sufficient detail. In this chapter, the hazards posed by transient lakes at Pinatubo are evaluated by analyzing the mechanical behavior of the blockages that impound them. The classification of volcanic debris dams and their occurrence around Pinatubo are discussed in Section 5.1. Section 5.2 presents the different geomorphic settings in which temporary dams and lakes are formed, and the methods of analysis used to analyze them. The repeated formation and failure of Cutuno Lake, which is considered to be an excellent case study that represents all the aforementioned geomorphic settings at various times, is discussed in detail in Section 5.3. The physical characteristics of the dams relevant to stability analysis are described in Section 5.4. The stability of temporary dams against different modes of failure is analyzed in the succeeding sections: Section 5.5 deals with gravitational failure, Section 5.6 with piping, and Section 5.7 with overtopping. Lahar hazards from the sudden failure of temporary dams are discussed in Section 5.8. Section 5.9 discusses the possible role of secondary explosions in the dam failure process. The chapter is concluded in Section 5.10 with pertinent notes on the hazards that the remaining temporary dams and lakes pose, and some implications on hazard mitigation.

5.1. General discussion of volcanic debris dams

The formation of temporary blockages during and following volcanic eruptions has been a well-documented phenomenon. Impoundments by lava and alluvial deposits were noted by Segerstrom (1950) at Parícutin Volcano in Mexico. Kuenzi *et al.* (1979) described "bordering lakes" along the Samalá River, which they concluded to be the result of rapid aggradation caused by the violent eruption of Santa María Volcano in 1902. As a result of the 1980 eruption of Mount St. Helens, several large impoundments were formed, necessitating serious hazard evaluation (Youd *et al.*, 1981; Meyer *et al.*, 1986). Similar lakes in other volcanic areas around the world have also been studied for the hazards they pose (*e.g.*, Lockwood *et al.*, 1988; Waythomas, 2001).

In the Philippines, dammed lakes around volcanoes undoubtedly abound, but remain largely undocumented. One known example is Lake Buhi, which is dammed by a debris-avalanche deposit from Mount Iriga in Bicol (Aguila *et al.*, 1986). Some lakes around Bulusan Volcano in Sorsogon are also evidently dammed by volcanic deposits (PHIVOLCS, unpublished maps). The crater lakes of Pinatubo and Mount Parker, South Cotabato, although not strictly formed by debris dams, have outlets that are blocked by debris (Catane and Gabinete, 1996; Abigania *et al.*, 2002; PHIVOLCS, unpublished reports). Overall, transient lakes and their hazards have not received much geological attention in the country.

5.1.1. Landslide dams

Volcanic debris dams may be classified as landslide dams, using the definition of *landslide* by Cruden and Varnes (1996). Costa and Schuster (1988) mentioned that volcanic eruptions are one of the leading causes of landslide dams, although their classification did not consider the peculiarities of volcanic landslide dams. They noted that most landslide dams fail shortly after their formation, with about 85% failing within a year. Other papers in the volume edited by Schuster (1986) cited many examples of landslide dams, while a comprehensive list of historical landslide dams around the world was provided by Costa and Schuster (1991).

Volcanic landslide dams are significantly different from the typical landslide dams described and classified by Costa and Schuster (1988). They are formed by mobile flows, rather than slides, along rivers that are often larger than the tributaries they block; while in most landslide dams described by Costa and Schuster (1988), the blocked river channel is typically much larger and less steep than the damming tributary. Pyroclastic flows and lahars are much more mobile than typical landslides and debris avalanches, with runout distances ranging from a few to tens of kilometers. Where unrestricted by valley walls, these flows tend to form relatively smooth, fan-shaped deposits, rather than the hummocky ones characteristic of landslides and avalanches.

5.1.2. Transient dams at Mount Pinatubo

Pinatubo's transient lakes share a similar volcanic setting with those that formed along the flanks of the Samalá River in southwestern Guatemala after the violent eruption of Santa María Volcano in 1902 (Kuenzi *et al.*, 1979), and with those that formed along the North Fork Toutle River during the 1980 eruptions of Mount St. Helens (Meyer *et al.*, 1986; Glicken *et al.*, 1989). The origin of the blockages in the Samalá River is not clear, but is perhaps similar to that of the blockages at Pinatubo – through deposition by pyroclastic flows and lahars. The blockage at Mount St. Helens, in contrast, was formed largely by the 18 May 1980 rockslide-debris avalanche (Glicken *et al.*, 1989).

Since the June 1991 eruptions, many temporary water impoundments have formed in the lahar-affected watersheds around Mount Pinatubo. The impoundments range from small ponds of a few square meters to large lakes of several square kilometers. Prominent among the large lakes are, clockwise from the northern sector of the volcano: Crow Valley Lake in the O'Donnell River basin, Marimla Lake in the Sacobia River, the now drained Cutuno Lake in the Pasig-Potrero River, and Mapanuepe Lake in the Marella - Sto. Tomas River basin (Figure 5.1).

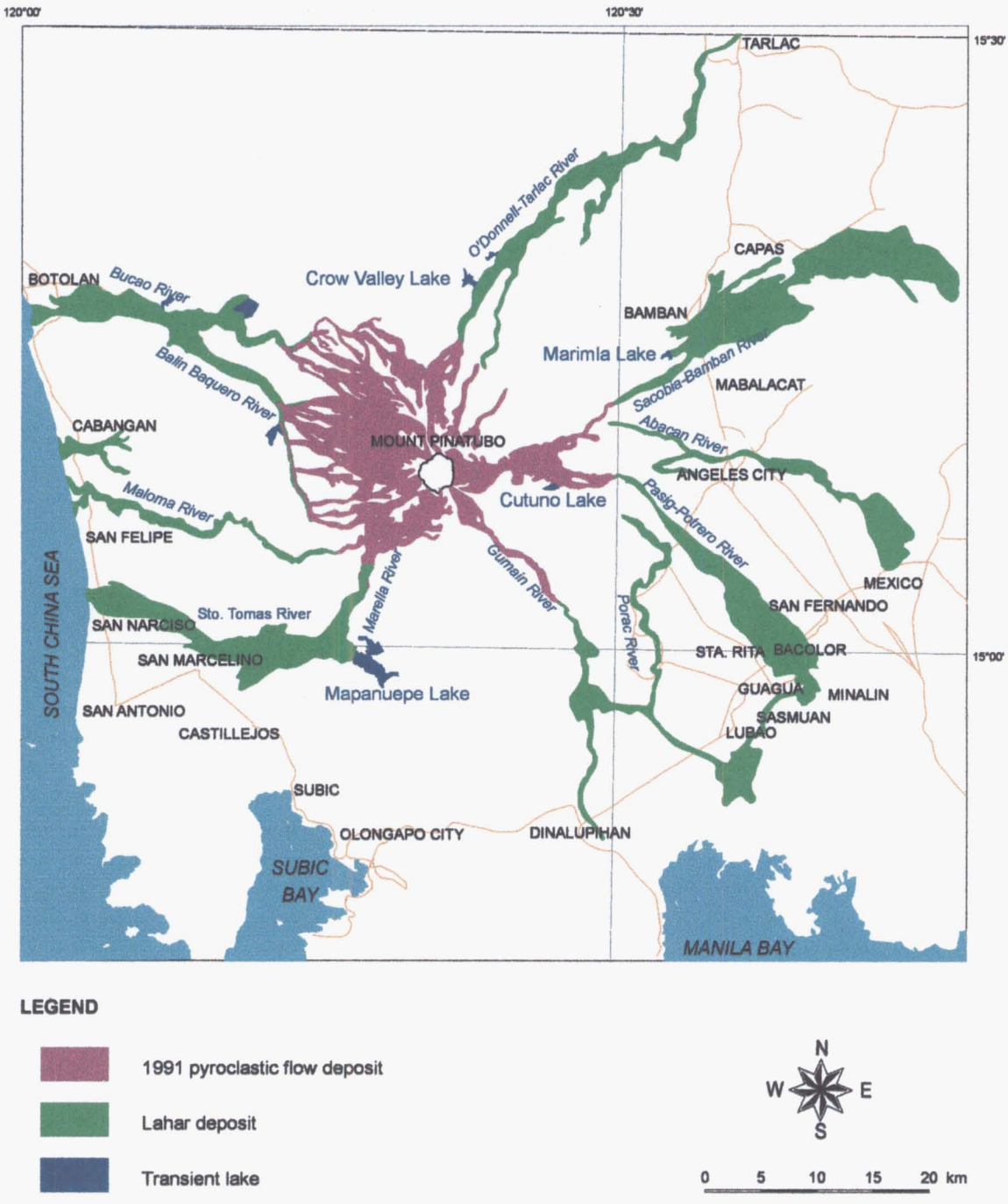

Figure 5.1. Map of temporary lakes that have been formed around Mount Pinatubo after the 1991 eruption.

Classification of transient dams at Pinatubo

The blockages that impound the transient lakes may be classified as *pyroclastic-flow dams* or *lahar dams* according to the dominant process that emplaced them. Many pyroclastic-flow dams formed immediately after Pinatubo's June 1991 eruptions, when pyroclastic flows cascaded down major valleys radiating from the volcano, and blocked tributaries almost instantly with hot deposits as thick as 200 m (W.E. Scott *et al.*, 1996). Such dams were generally confined within about 15 km from the Pinatubo caldera, the runout distance of the 1991 pyroclastic flows. Virtually all of the lakes blocked by primary pyroclastic-flow deposits were short-lived and drained during the 1991 season due to high erosion activity in the upper river catchments where they were formed. Some of them, however, have formed repeatedly, when the primary deposits were remobilized *en masse* as secondary pyroclastic flows (Torres *et al.*, 1996). Dams formed by secondary pyroclastic flows were still confined within a 15-km radius from the summit. They were common until about 1994.

Compared to pyroclastic-flow dams, lahar dams form at much slower aggradation rates, primarily through the cumulative deposition by debris-flow and hyperconcentrated-flow lahars. Generally, they are found in the alluvial fans downstream of the pyroclastic-flow zone. In these areas, the rate of lahar deposition is typically less than 6 m per rainstorm event. All the surviving large lakes in Figure 5.1 were formed by lahar dams.

Historical and geological precedence

No dammed lakes existed in the pre-1991 topography around Pinatubo, indicating that any lakes formed in previous eruptions had eventually drained. From the stratigraphic record, Umbal (1994) inferred repeated damming and breaching episodes of Mapanuepe Lake prior to the 1991 eruption of Pinatubo volcano. The 1991 eruption caused Mapanuepe Lake to form anew, and minor lake-breakouts were observed during the 1991 rainy season (Umbal, 1994; Umbal and Rodolfo, 1996). Other, more devastating, lake-breakout lahars have also been observed in the Sacobia (K.M. Scott *et al.*, 1996) and Pasig-Potrero Rivers (Arboleda and Martinez, 1996).

Surviving dams

In view of the historic and geological precedence, it seems reasonable to expect that in time, most, if not all, of the current dammed lakes around Pinatubo will drain. Yet, several transient lakes still exist around Mount Pinatubo, several years after their initial formation. Of these, Mapanuepe Lake probably poses the greatest threat because of its size (>70 million m^3 of water over a 7 km^2 area), and because it is perched only a few kilometers upstream of population centers (Umbal and Rodolfo, 1996). The lake however, has been made relatively stable by the construction in 1991 of a drain canal through adjacent gabbroic bedrock, which has so far prevented the lake from overtopping the dam. Another lahar-dammed lake, the Marimla Lake on the distal reaches of the Sacobia alluvial fan, has also been engineered to prevent it from breaching. Crow Valley Lake, on the other hand, is located in the remote hinterlands, and has been largely ignored by geologists, engineers and disaster officials. Crow Valley Lake inundates an area of more than 800,000 m^2, along the west flank of the O'Donnell River, about 17 km north of the crater and 6 km upstream of the nearest population center (Figure 5.1).

5.2. Geomorphic settings of Pinatubo transient dams

The stability of transient dams depend on the mode and geomorphic setting of their formation, as well as their physical characteristics. Three different geomorphic settings are considered for transient dams at Pinatubo, based on predominant river processes after the initial formation of the dam (Figure 5.2):

1. The blockage is formed in a predominantly degradational reach of the river, generally within 15 km from the volcano's summit;

2. The blockage is formed in a predominantly depositional environment, as is common for lahar dams that form at the margins of alluvial fans; or

3. The blockage is initially formed under Setting 1 or 2, but lahar activity in the previously blocking channel subsequently becomes greatly reduced, possibly because of stream piracy farther upstream, or simply by gradual reduction in sediment supply.

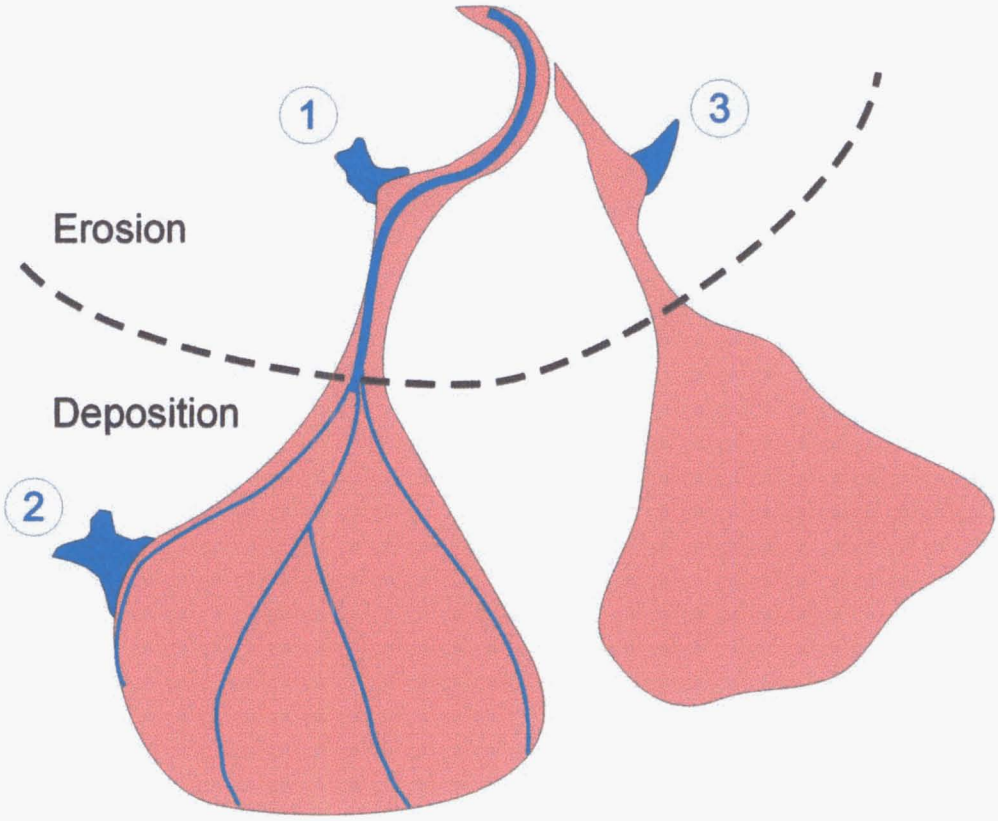

Figure 5.2. Geomorphic settings of transient dams after their initial emplacement: (1) in a degradational environment, (2) in a depositional environment, and (3) in an abandoned channel. The erosional and depositional areas are defined based on the expected evolution of the river basin in which the river reestablishes an equilibrium profile by eroding the deposits in the upper catchment and redistributing them onto the downstream area. In practice, the boundary between these two continually shift.

Setting 1 is commonly the case for pyroclastic-flow dams, which form in the upper reaches of rivers. Lahar processes after formation of the blockage are usually characterized by rapid channel-bed degradation, as the river attempts to reestablish an

efficient concave longitudinal profile in its upper reach. Past observations show that tens of meters of channel-bed erosion in a single rainstorm event were common in this river reach. Most dams that formed in Setting 1 failed shortly – at most, within a few months – after their initial formation.

Dams under Setting 2 include most lahar dams, which are continuously supplied with sediments by lahars and sediment-laden streamflows. The remaining large lakes, Crow Valley, Marimla and Mapanuepe Lakes, exist under such conditions.

Setting 3 may develop from either Setting 1 or Setting 2. A dam in Setting 1 may become insulated from erosive lahar activity if the blocking river channel is cut off from the lahar-sediment source, *e.g.*, by stream piracy upstream of the dam. The 1994 blockage at Cutuno Lake developed in this manner. The main difference between Settings 2 and 3 is the amount of sediments being supplied to the blocking channel. Sediment delivery rates along a blocking lahar channel in Setting 2 are much higher than in a beheaded channel in Setting 3 by virtue of a larger catchment size and larger cache of source sediments. In the long-term, all lahar dams in Setting 2 will effectively evolve into Setting 3 dams, as the influx of sediments into the blocking river channel decreases over time.

Setting 3 permits the analysis of the lake-dam structure as a closed system, free from rapid erosion or deposition along the previously blocking channel. Conceptually, Setting 3 is similar to Setting 1 without the rapid erosion along the blocking river channel, and to Setting 2 without the large amount of sediments supplied by lahars to the dam. The stability of transient dams may thus be analyzed by simply considering Setting 3. The 1994 blockage at Cutuno is the only documented dam that developed under Setting 3.

5.3. Cutuno Lake as case study

Cutuno Lake was a temporary lake that had repeatedly formed by blockage at the foot of Mount Cutuno, about 11 km east of the crater rim of Mount Pinatubo (Figure 5.3; *See*

site marks the confluence of the Yangca and Bucbuc Creeks, which join to form the Papatac River. Morphologically, the wide Bucbuc-Yangca junction is in marked contrast to the Papatac gorge, which is a <100-m wide canyon bounded by near-vertical walls made of indurated pre-1991 volcaniclastic deposits. The Papatac gorge thus acts as a bottleneck, making the Bucbuc-Yangca junction vulnerable to blockages by such large flows as pyroclastic flows and lahars.

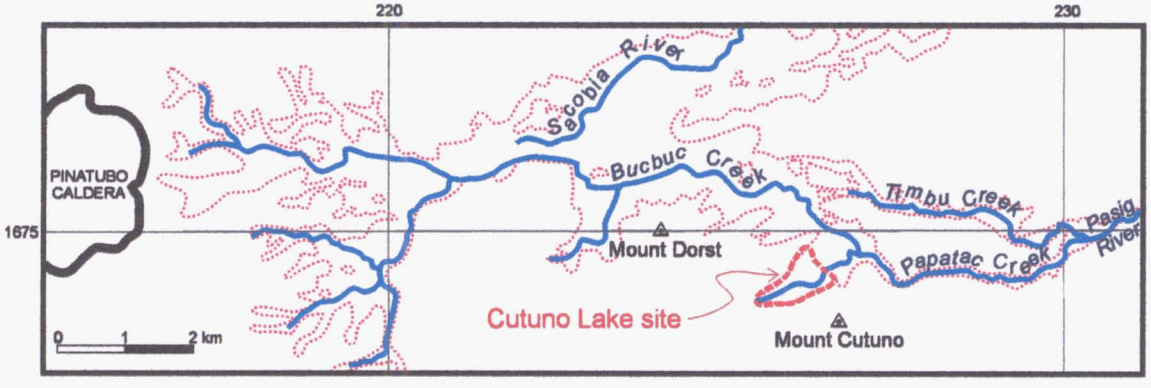

Figure 5.3. Map of the upper Pasig catchment showing the Cutuno Lake site (enclosed by red dashed line), which was formed three times – in 1991, 1992 and 1994. The dotted line marks the extent of the 1991 pyroclastic-flow deposits.

That similar lakes had formed at the Bucbuc-Yangca junction in previous eruptions of Pinatubo is indicated by the presence, before the 1991 eruption, of a dissected terrace of pumiceous deposits that extended more than a kilometer upstream of the Yangca from the junction. This terrace is similar in morphology to the dam and lake deposits that can be seen there now. The longitudinal profile of the Yangca valley also showed a marked flattening of gradient near the junction, characteristic of blocked drainages. After the 1991 eruption of Pinatubo, there have been three known lake formation and breaching episodes at Cutuno, each one generating floods that killed several people in communities near the Pasig-Potrero River. These occurred in 1991, 1992 and 1994.

5.3.1. 1991-1992 evolution

The first lake at Cutuno formed shortly after Pinatubo's climactic eruptions in June 1991 (K.M. Scott *et al.*, 1996). The 1991 pyroclastic flows that cascaded down the upper Sacobia River surmounted the divide that separated the Sacobia from the Pasig catchment. The flows that went down the Pasig deposited a 50-m thick, fan-shaped deposit at the Bucbuc-Yangca junction (W.E. Scott *et al.*, 1996). The sudden massive blockage caused streamflow from the Yangca Creek to pond behind the pyroclastic-flow deposit. The dam was eventually overtopped, and its sudden breaching on 07 September 1991 caused several casualties in the downstream communities of Porac and Bacolor (Arboleda and Martinez, 1996; K.M. Scott *et al.*, 1996).

The second lake to form in the same site was caused by a large secondary pyroclastic flow on 13 July 1992, which emplaced a 5- to 6-km long hot deposit down the Bucbuc and Papatac channels (Arboleda and Martinez, 1996; Torres *et al.*, 1996). The resulting dam not only blocked flows from the Yangca Creek anew, but temporarily impeded flows along the Bucbuc and Papatac Rivers as well. Thus, no lahars were recorded in the Pasig River during several subsequent storm events. The dam eventually breached over a 9-hour period in late August 1992 during heavy typhoon-induced rains. The 1992 dam deposits apparently submerged a pre-eruption bedrock ridge, and the lake drained through a saddle on that ridge. Breach discharge is believed to have been controlled by this bedrock "lip" (Arboleda and Martinez, 1996, p. 1050-1052).

The precise mechanism of breaching of the 1991 and 1992 pyroclastic-flow dams at Cutuno is unknown, and the events themselves were not observed as they occurred in an inaccessible, very hazardous area. The dams undoubtedly developed under Setting 1, since the Cutuno area was then well within the highly erosional lahar-transport reach of the Pasig-Potrero River, with the apex of the depositional fan located 8 km farther downstream. Before it failed, each of the 1991 and 1992 dams had developed a natural spillway along which overtopping lake waters flowed, and dam overtopping may have played a major role in the failure. However, failure may have been greatly aided, if not initiated, by partial erosion of the dam by lahars along the Bucbuc-Papatac channel.

Possible mechanisms of failure of the 1991 and 1992 Cutuno dams are further discussed in Sections 5.5 to 5.7.

5.3.2. 1994 evolution

Initial dam formation

The latest episode of dam formation and breaching at Cutuno occurred in mid-1994. Before the start of the 1994 rainy season, a total of about 60 m of pyroclastic-flow and lahar deposits had accumulated over the pre-eruption surface at the Bucbuc-Yangca confluence (JICA, 1996a). By then, the previous lake had completely drained, and the Yangca Creek was flowing over the deposit near the right (east) side of the Yangca valley, abutting the pre-eruption bedrock, at the downstream edge of the fan-shaped deposit.

At the start of the 1994 rainy season, flows along the Pasig River initially passed through the Bucbuc channel into the Papatac gorge. Video footages of a helicopter survey conducted by PHIVOLCS on 27 June 1994 showed fresh deposits of a secondary pyroclastic flow along the Bucbuc-Papatac valley, which could have occurred during the passage of Typhoon *Gading* on 22-24 June. The emplacement of this secondary pyroclastic-flow deposit had two significant geomorphic effects:

1. It started the formation of a new Cutuno Lake by blocking Yangca Creek again (Figure 5.4); and

2. It leveled the divide between the Timbu and Bucbuc Rivers just upstream of the Cutuno dam site, leading to the eventual capture of the Bucbuc catchment by the Timbu.

Figure 5.4. Incipient formation of Cutuno Lake on 05 July 1994, photo looking southwest, up the Yangca valley. The eventual lake is approximated by the blue outline. The light-colored dam deposit in the Bucbuc-Papatac valley (middle of photo; flow from right to left) was mainly from a secondary pyroclastic flow that occurred in late June. The deposit from this event buried the divide between the Bucbuc and the Timbu (on the other side of the hills in the foreground), just upstream (to the right) of the area shown in the photo. The burial of the divide caused subsequent flows from the upper Bucbuc to be gradually diverted to the Timbu, thus abandoning this dam site. *Photo reprinted with permission from Punongbayan et al. (1996).*

Abandonment of the Cutuno dam site: development into Setting 3

The Cutuno dam site was abandoned by the upper Bucbuc sometime before 10 August 1994 (*Please see Section 2.3.2*). The capture of the upper Bucbuc River by the Timbu severed the Papatac from its main sediment-source (the 1991 pyroclastic-flow deposits), and reduced its drainage area to less than 6 km^2, a large part of which belonged to the Yangca Creek. The pyroclastic-flow/lahar terrace at the piracy site – hereafter referred to as the Papatac Gap – was partly drained by a small ephemeral channel that discharged into Cutuno Lake (Figure 5.5, Figure 5.6). The terrace, which is the upstream extension of the Cutuno dam, provided the only source of pumiceous sediments to the Cutuno blockage after the stream capture.

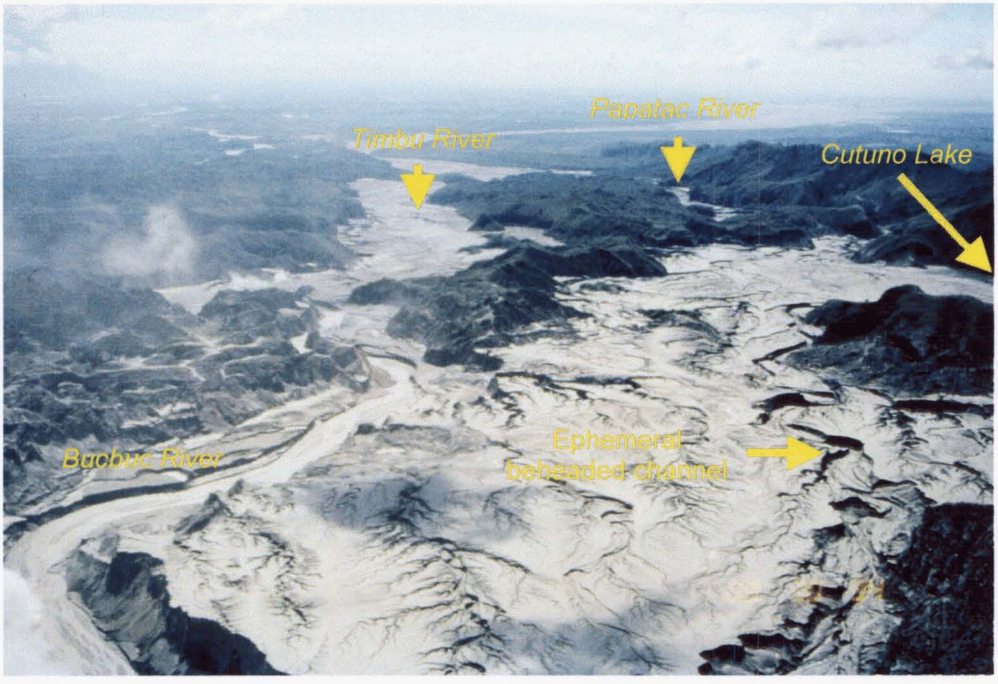

Figure 5.5. The Papatac Gap: drainage divide between the Bucbuc-Papatac (right) and Timbu (left) at the area of stream piracy; photo taken on 30 August 1994 looking downstream (east). The upper Bucbuc (large channel in the left foreground) used to flow into the Papatac; the late-June secondary pyroclastic flow leveled the Papatac Gap, allowing the eventual diversion of the Pasig into the Timbu. A small ephemeral channel partially draining the surface of the secondary-pyroclastic-flow/lahar terrace discharged into Cutuno Lake. *Photo courtesy of C.G. Newhall.*

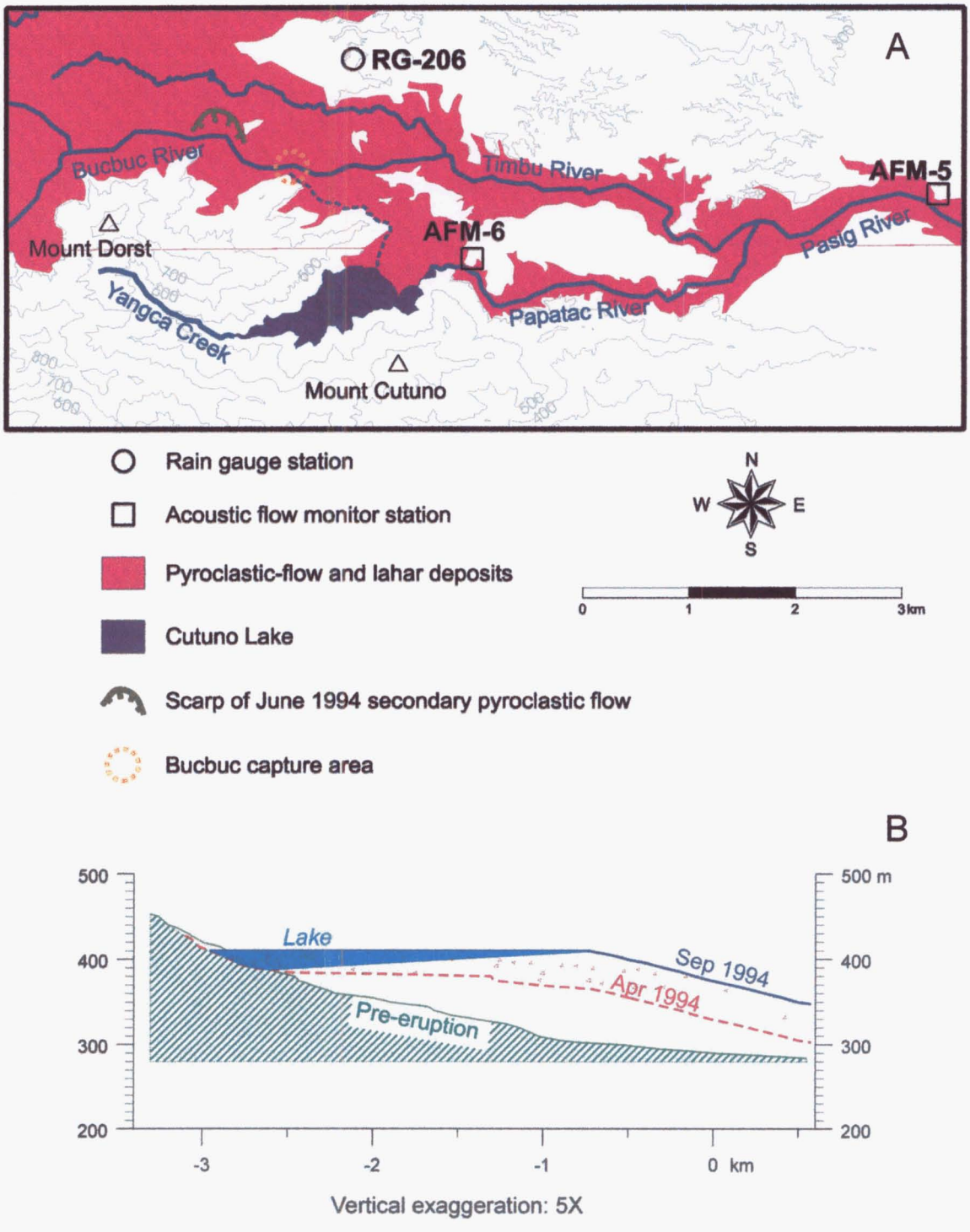

Figure 5.6. Reconstructed map (A) and section (B) of the Cutuno blockage prior to the 22-23 September 1994 breaching. The Bucbuc River had been diverted into the Timbu, which had become the main tributary of the Pasig River. The Papatac River was solely fed by discharge from the lake, which in turn was supplied by springs in the Yangca Creek. The beheaded former Bucbuc channel became an ephemeral channel (dashed blue line), which delivered pumiceous sediments from the Papatac Gap (dotted yellow circle) into the lake during rainstorms.

By 30 August 1994, Cutuno Lake had filled to overtopping levels (Punongbayan *et al.*, 1996), with the water surface estimated to be at around 410 m above sea level, covering an area of about 0.5 km^2 (Figure 5.6A). The depth of the lake was not known, but by extrapolating the general slope of the fan-dam beneath the lake, it is estimated that the lake was probably around 20 m at its deepest part, with an average depth of 10 m (Figure 5.6B). These give an approximate volume of 5 x 10^6 m^3 for the 1994 Cutuno Lake.

The lake was being drained by a natural spillway of unknown dimensions located on the distal end of the fan-shaped blockage, against the bedrock on the east side of the Yangca valley (Figure 5.6A, Figure 5.7A). The ephemeral channel noted in the preceding paragraph and in Figure 5.5, was forming a prograding delta into the lake, continuously supplying the dam with pumiceous sediment, albeit at a greatly reduced rate. These conditions were maintained until the last observation on 16 September, a week before the lake catastrophically drained.

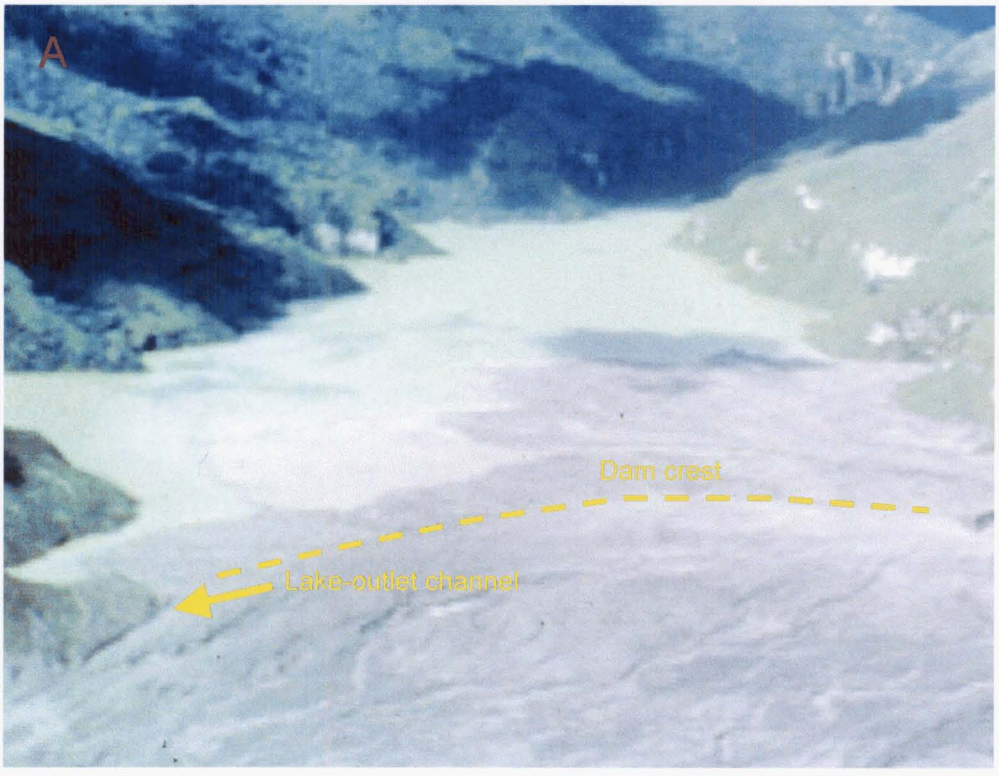

Photo courtesy of R.S. Punongbayan

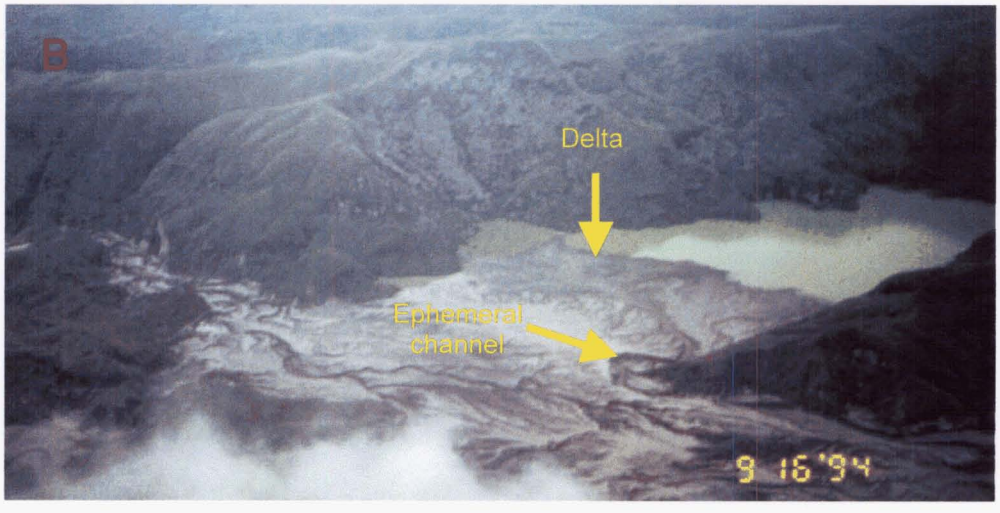

Photo courtesy of PHIVOLCS

Figure 5.7. Cutuno Lake at its full extent on 30 August (A) and 16 September (B) 1994; the crest of the dam is marked by the dashed line in A. A natural spillway had formed at the distal end of the blockage (lower left in A). The ephemeral channel (lower right in B) partially draining the Papatac Gap formed a fan-shaped delta prograding into the lake.

5.4. Physical characteristics of transient dams

5.4.1. Dam morphology

Morphologically, pyroclastic-flow and lahar dams are typical fan deposits. In cross-section, looking along the blocking channel, they are lens-shaped, thickest along the valley axis and gradually thinning out laterally. Longitudinally, they are wedge-shaped, with the surface gradient dependent on the mobility of the flows that emplaced them. Top surfaces of pyroclastic-flow deposits at Pinatubo generally have longitudinal slopes of about 5% (2.8°), while those of lahar deposits are usually less than 2.5% (1.4°). An idealized section of a pyroclastic-flow dam, as exemplified by the Cutuno dam, is illustrated in Figure 5.6B. Generalizing this section, several critical morphological features of Pinatubo transient dams that must be considered in their analysis are identified:

1) A relatively gentle downstream face, with a gradient assumed to be similar to the longitudinal slope of the dam deposit (approximately 5% and 2.5% for pyroclastic-flow and lahar dams, respectively);

2) An equally gentle slope going into the reservoir;

3) A long downstream face, depending on the mobility of the flow that emplaced the dam deposit; and

4) A dam toe that is much lower than the lakebed, which is a function of the length of the downstream face.

The downstream length of the dam may be hundreds of meters to a few kilometers for pyroclastic-flow dams, and as much as tens of kilometers for lahar dams. In practice, the length of the downstream face is almost arbitrarily chosen given that its slope is not much greater than the channel on which the flow deposit is emplaced. Other parameters that may be important in dam modeling include the width of the dam, which is usually topographically controlled, and the presence of a spillway.

5.4.2. Distinction between pyroclastic-flow and lahar dams

Methods of distinguishing between pyroclastic-flow and lahar deposits have been well established among volcanologists. At Pinatubo, this is made easy by the freshness of the deposits. Primary pyroclastic-flow deposits still bear signs of hot emplacement, such as hot water seepages, pinkish or white coloration, dry interior and gas escape pipes.

Secondary pyroclastic-flow deposits are harder to recognize. In fact, if some of these flows were not directly observed, their deposits could have been easily missed. For the purpose of this study, the difference between primary and secondary pyroclastic-flow deposits is not critical. The distinction between secondary pyroclastic-flow deposits and lahar deposits, however, merits attention. Secondary pyroclastic-flow and lahar deposits are both characteristically massive and poorly sorted, with similar grain-size distribution. Thermoremanent magnetization (TRM), often used to distinguish primary pyroclastic-flow from lahar deposits, is not particularly effective for secondary pyroclastic-flow deposits. Titanomagnetite and hemo-ilmenite, the main magnetic components of Pinatubo pumice, have Curie temperatures of ~480°C and ~250°C, respectively (Bina *et al.*, 1999). In comparison, the emplacement temperature of secondary pyroclastic-flow deposits is typically 250-300°C (Torres *et al.*, 1996). Their TRM polarity thus tends to be more randomly distributed compared to primary pyroclastic-flow deposits, and may be indistinguishable from lahar deposits (Torres *et al.*, 1996).

Nevertheless, there are some distinctive features identifiable in the field that indicate pyroclastic-flow origin, including: (1) a whitish or pinkish coloration previously observed on known hot pyroclastic-flow deposits of Pinatubo, (2) relative abundance of fines-depleted pipes that were formed by escaping steam during and after deposition, and (3) the presence of hot water seepages through the deposit. These are shown in Figure 5.8. A thin mud-crust often coats the deposits, presumably from finer-grained material being washed onto the surface by sheetwash and rainsplash. The fine-grained material may come from the deposits themselves, the elutriation ash from pyroclastic flows, or from ash columns from secondary hydroeruptions.


A

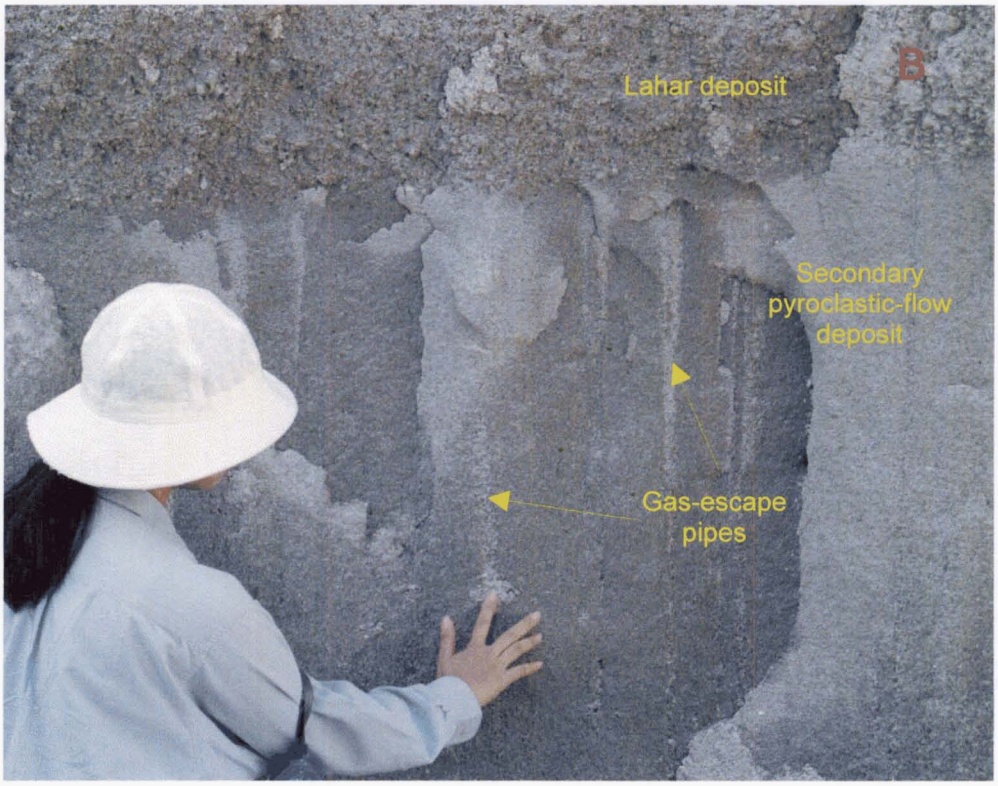
B
Lahar deposit
Secondary pyroclastic-flow deposit
Gas-escape pipes

Figure 5.8. Sections of the secondary pyroclastic-flow deposit which dammed Cutuno Lake. The deposit has a characteristic pinkish coloration (A) and, in portions, features abundant gas-escape structures (B). Exposed sections are up to 40 m thick, are massive, and often have steep faces (C). Hot water was seeping out at the base of the deposit when this photo was taken in November 1999.

5.4.3. Mass properties of dam deposits

The material properties of transient dams at Pinatubo are somewhat peculiar, being composed mostly of low-density, sandy, pumiceous material. Manville *et al.* (1998) have concluded from laboratory experiments that the low density and pore structure of pumice govern its saturation behavior, which strongly influence its geotechnical and hydraulic characteristics. Pyroclastic-flow and lahar deposits of Mount Pinatubo normally consist of poorly sorted gravelly sand, with a median grain size between 0.2

mm and 1 mm, and with about 15% silt and clay-sized particles (Figure 5.9; *See also* JICA, 1996b, Torres *et al.*, 1996, Pierson *et al.*, 1996, W.E. Scott *et al.*, 1996 and H. Shields, 1998). The clay fraction is typically less than 3%, and the material is invariably non-plastic.

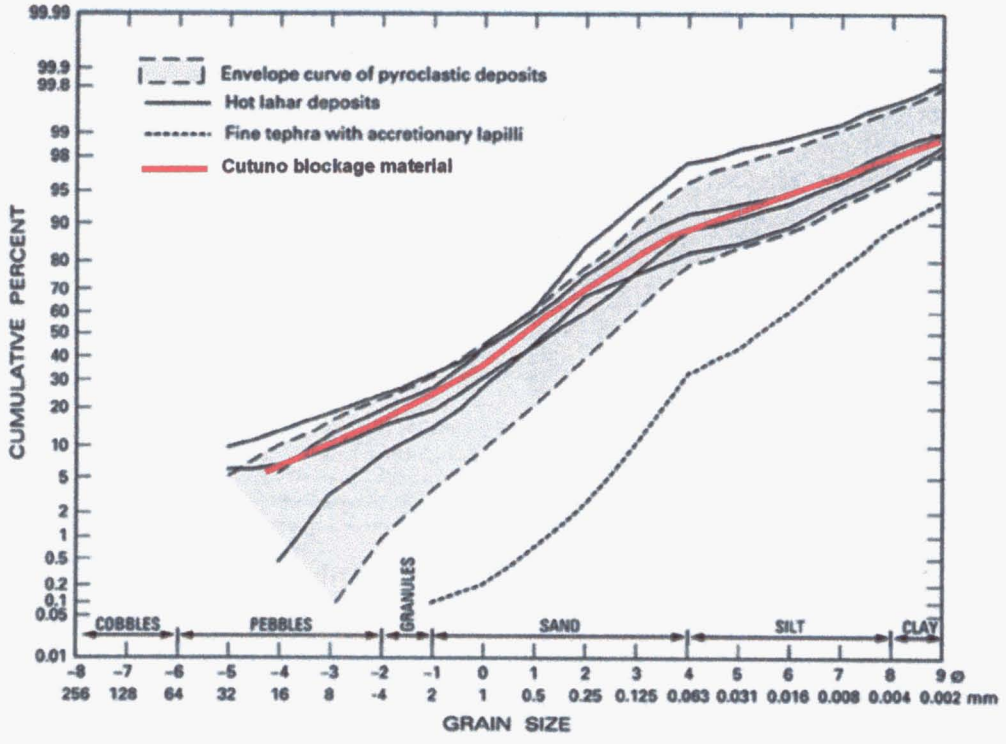

Figure 5.9. Average grain-size distribution of dam deposit at Cutuno. Other data from W.E. Scott *et al.* (1996) and Pierson *et al.* (1996).

Although dominantly composed of sand-sized particles, dam deposits appear to possess some strength that enables them to maintain near-vertical slopes of several meters. Five-meter high vertical lahar banks are very common at Pinatubo, while faces of pyroclastic-flow deposits often sustain heights of several tens of meters at very steep slope angles (Figure 5.10; *See also Section 3.5.2*). This apparent cohesion may be due in part to the extreme angularity of the grains, which are mostly broken mineral fragments

and vesiculated volcanic glass (Figure 5.11). Mud-crusts on pyroclastic-flow and debris-flow lahar deposits may also contribute to the overall strength of the deposits.

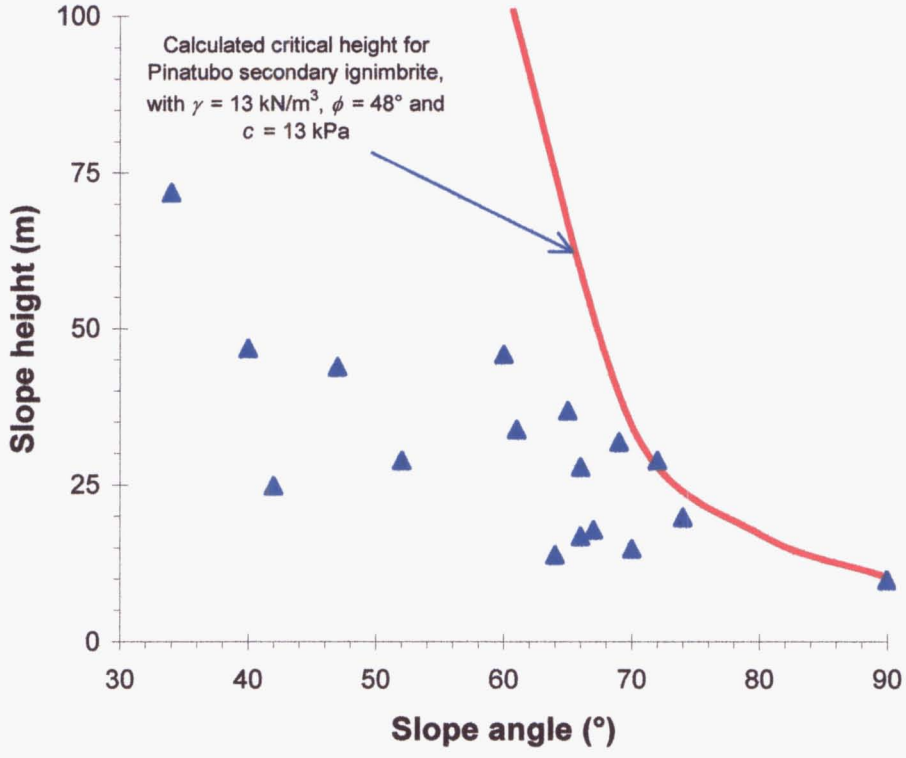

Figure 5.10. Height vs. angle of bank slopes at the Cutuno dam. The measurements were made in 1999 using a hand-held clinometer and a laser rangefinder. The data are for natural escarpments on pumiceous deposits, and excludes talus cones. A critical-height curve that passes through the maxima is calculated by the Culmann method of slope stability analysis (Lohnes and Handy, 1968; Matsukura, 1987).

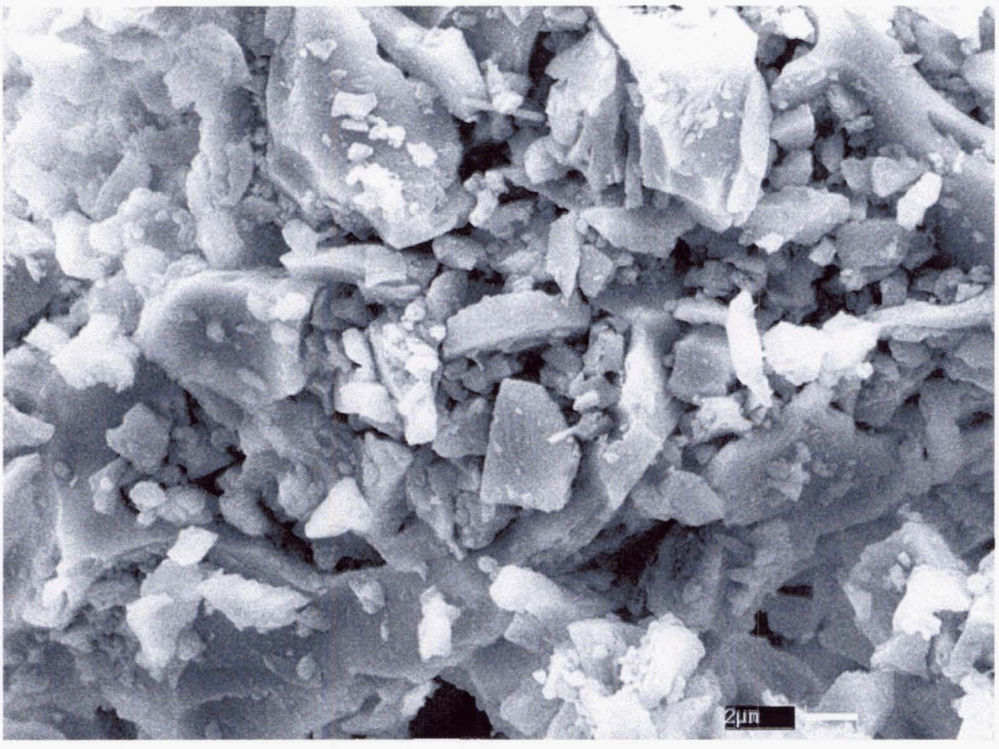

Figure 5.11. Scanning electron microscope photograph of loose grains of secondary pyroclastic-flow deposits, showing very angular fragments.

In addition to their geotechnical properties, primary pyroclastic-flow deposits possess one other unique, critical characteristic: high emplacement temperature, which is generally greater than 450°C for primary deposits (Bina *et al.*, 1999), and >250°C for secondary deposits (Torres *et al.*, 1996). This makes the deposits susceptible to secondary explosions, which have played a major role in the formation and failure of transient dams at Pinatubo.

A summary of pertinent material properties of pyroclastic-flow and lahar dams is summarized in Table 5.1.

Table 5.1. Summary of mass properties of pyroclastic-flow and lahar deposits.

	Pyroclastic-flow deposit	Lahar deposit
Dry unit weight, γ_d (kN/m^3)	13	17
Specific gravity of solids, G_s	2.5	2.5
Saturated unit weight, γ_s (kN/m^3)	17.6	20
Porosity, n (%)	47	31
Median grain size, D_{50} (mm)	0.2 - 1.0	0.2 – 1.0
Friction angle, ϕ (°)	48	45
Cohesion, c (kPa)	13	15

5.5. Stability of transient dams against slope failure

Transient dams may fail by any of the following mechanisms: (1) gravitational slope movement, (2) piping, or (3) overtopping. All these mechanisms may operate under any of the geomorphic settings given in Section 5.2.

The stability of transient dams against gravitational slope failure, including liquefied flow, may quickly be assessed by an infinite-slope analysis. The factor of safety of an infinite slope derived from the Mohr-Coulomb criterion (*e.g.*, Craig, 1992, p. 376-377) is:

$$F = \frac{c' + (\sigma - u)\tan\phi'}{\tau} \qquad \text{Equation 5.1.}$$

where c' is effective cohesion of the material;

σ is total normal stress;

u is pore water pressure;

ϕ' is effective friction angle; and

τ is shear stress.

The expressions for the stress parameters are:

$$\sigma = [(1-m)\gamma + m\gamma_{sat}]z\cos^2\beta$$

$$\tau = [(1-m)\gamma + m\gamma_{sat}]z\sin\beta\cos\beta$$

$$u = mz\gamma_w\cos^2\beta$$

where m is the ratio of the height of the water table above the failure plane to the depth of the failure plane, z;

γ and γ_{sat} are the dry and saturated unit weight of the material;

γ_w is the unit weight of water; and

β is the slope of the failure plane.

To illustrate how stable the dams are, the following worst-case conditions are assumed: (1) the dam material has no cohesion ($c = 0$), and (2) the water table is assumed to be at the surface ($m = 1$). Equation 5.1 then reduces to:

$$F = \frac{(\gamma_{sat} - \gamma_w)\tan\phi'}{\gamma_{sat}\tan\beta} \qquad \text{Equation 5.2}$$

The least stable dam in terms of the slope of the downstream face is a pyroclastic-flow dam, which typically has a slope of 5%. Assuming worst-case values of γ_{sat} = 15 kN/m^3, ϕ = 32°, and substituting γ_w = 9.8 kN/m^3 in Equation 5.2, yields a factor of safety of 4.3 which is a "reasonably safe" value. This probably underestimates the actual stability of

Pinatubo transient dams. Still assuming zero cohesion, but using more realistic values of γ_{sat} = 17 kN/m^3 and ϕ = 48° (JICA, 1996b; *See also Section 5.4.3*), yields a factor of safety of 9.4. Adding cohesion to the dam material raises the factor of safety even further.

The dam may conceivably be destabilized by the development of excess pore pressure. For the transient dams of Pinatubo, however, this is considered unlikely because the deposits are unconfined. The exit gradient of groundwater is not likely to exceed the surface slope of the deposits.

Considering the above, transient dams are judged to be stable against gravitational failure. This agrees with the absence of observation of gravitational mass failure of pyroclastic-flow or lahar deposits other than those from very steep banks. Youd *et al.* (1981), using the same method of analysis, arrived at a similar conclusion for the North Fork Toutle River blockage at Mount St. Helens. A possible exception to this is a dam under Setting 1, where subsequent flows from the erstwhile blocking channel may erode the dam. Such erosion may lead to mass failure by creating a steep downstream face and reducing the effective width of the dam.

5.6. Stability of transient dams against piping

For piping to occur, the exit gradient of groundwater must exceed the critical hydraulic gradient of the deposit. The groundwater exit gradient for Pinatubo transient dams is assumed to be equal to the surface slope of the deposit, which ranges from 2.5% to 5%. Since the deposits are unconfined, steeper hydraulic gradients are considered unlikely. The critical hydraulic gradient of the deposit is given by the equation (*e.g.*, Bell, 1983):

$$i_c = \frac{G_s - 1}{1 + e} \qquad \text{Equation 5.3.}$$

where G_s is the specific gravity of the solid particles; and

e is the void ratio.

Following ASTM standards (American Society for Testing and Materials, 1995), the specific gravity of solid particles (grains passing the 4.75-mm sieve) of Pinatubo deposits was measured to be around 2.5. The void ratio of pumiceous deposits is typically 0.9. These yield a critical hydraulic gradient of around 0.8, which is an order of magnitude larger than the expected exit gradient of groundwater (<0.05). Transient dams are therefore considered safe from piping failure, which is supported by the lack of observation thereof. Youd *et al.* (1981) had a similar conclusion for the North Fork Toutle River.

5.7. Stability of transient dams against overtopping

Landslide dams most commonly fail through breach erosion by overtopping lake water (Costa and Schuster, 1988). The complicated topic of physical modeling of breach erosion has been the subject of many laboratory and field experiments, notably by Fread (1988), Singh *et al.* (1988), Singh (1996), Andrews (1998), Fread and Lewis (1998), Schilling (1998), Visser (1998), and Coleman and Andrews (2000). These models apply to man-made embankments or laboratory scale models, however, and do not account for the many complexities of natural dams. In this section, basic elements of breach erosion mechanics are used in conjunction with sediment mass balance analysis to assess the vulnerability of Pinatubo transient dams to failure by breach erosion.

5.7.1. Susceptibility of transient dams to breach erosion

Each of the dammed lakes around Mount Pinatubo has eventually developed a natural spillway channel, usually located at the downstream edge of the fan-dam and abutting against pre-eruption bedrock. Sediment transport along the spillway is critical in analyzing the potential of the blockage for overtopping failure. Assuming outflow from the lake is clean water, sediment transport along the spillway is chiefly by bedload. Bedload transport can be considered to occur when the shear stress exerted by the

column of water above the bed exceeds a critical shear stress, τ_c. The general expression for basal shear stress is

$$\tau_c = \gamma_w h_c \sin\beta \qquad \text{Equation 5.4}$$

where γ_w is fluid density, assumed to be 9.8 kN/m^3;

h_c is the critical depth at which bedload transport starts; and

β is the gradient of the flow surface

Montgomery *et al.* (1999), using Shields' (1936) equation for threshold bed movement, found that for low-flow conditions in the post-eruption Pasig-Potrero River, bedload transport is highly selective with respect to grain size. Furthermore, for any grain size, D, greater than the median grain size of the bed deposit, they found that bedload transport begins when h_c/D = 0.5. Using this relation for D = 1 mm, and substituting values of γ_w = 9.8 kN/m^3 and β = 1.4° to 2.8° (*See Section 5.4*) in Equation 5.4 yields τ_c = 0.12 to 0.24 Pa. This is an order of magnitude lower compared to critical shear stress measured by Reid (1989) for unvegetated cohesionless soils. This very low threshold of bedload transport at Pinatubo supports common field observations of rolling and sliding gravel-sized clasts that protrude above the flow.

If one considers such high bed mobility in a dam spillway, it becomes apparent that the spillway channel is highly susceptible to vertical incision, which can be expected to lead to breach-erosion failure. The question thus arises on how some dams have survived for years.

5.7.2. Sediment mass balance analysis

The stability of transient dams against catastrophic breaching through the spillway may be analyzed by considering the balance of sediment that controls the level of the spillway bed relative to the lake level at the lake boundary (Figure 5.12).

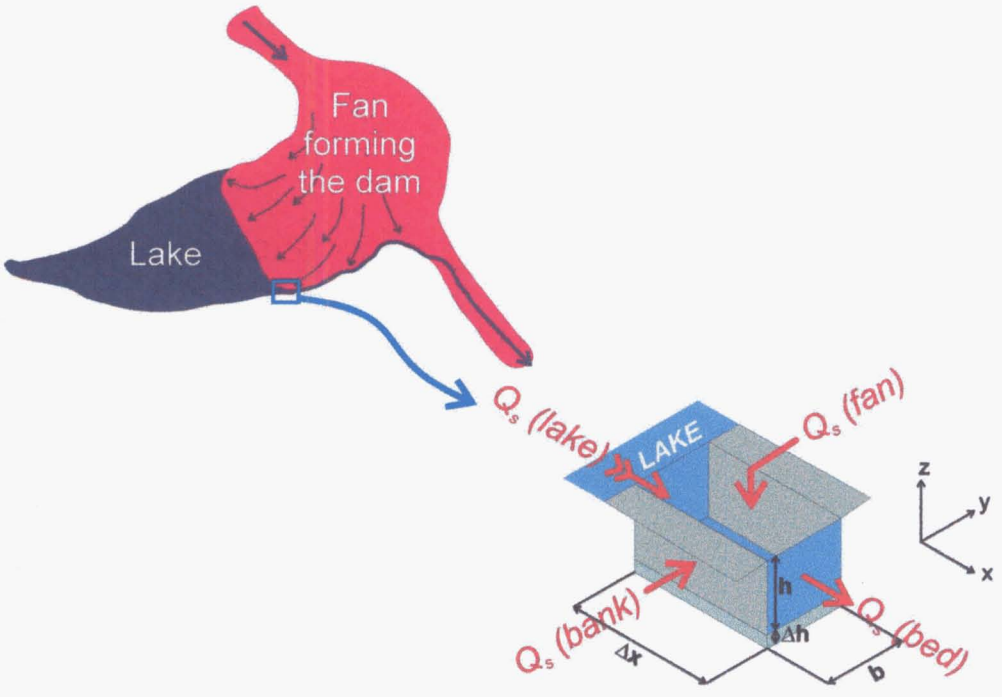

Figure 5.12. Diagram showing sediment mass balance in the dam spillway.

The sediment balance can be regarded as the change in storage volume, S, per unit time, t, on the bed of the spillway, which is the sum of sediment fluxes brought into and taken out of the bed:

$$\frac{\Delta S}{\Delta t} = Q_{s(lake)} + Q_{s(bank)} + Q_{s(fan)} - Q_{s(bed)} \qquad \text{Equation 5.5}$$

where $Q_{s(lake)}$ is the sediment flux from the reservoir;

$Q_{s(bank)}$ is the flux of material that collapses from the channel banks;

$Q_{s(fan)}$ is the sediment flux from runoff on the fan-dam surface; and

$Q_{s(bed)}$ is the rate of bedload transport along the channel

This equates to zero at the limiting condition where the bed is neither aggrading nor scouring. Furthermore, at the lake-spillway boundary, $Q_{s(lake)}$ may be assumed to be zero since flow velocity in the lake is very low. Thus, Equation 5.5 reduces to:

$$Q_{s(bed)} = Q_{s(bank)} + Q_{s(fan)} \qquad \text{Equation 5.6}$$

That is, for the lake not to drain catastrophically, material scoured from the bed of the spillway must be replenished at an equal or greater rate by bank collapse and surface transport across the dam.

5.7.3. Rate of bedload transport along spillway channel

Using sediment transport formulae

Bedload transport may be expressed in terms of basal shear stresses using the generalized Du Boys formula (Graf, 1971):

$$Q_{s(bed)} = k(\tau - \tau_c)^n \qquad \text{Equation 5.7}$$

where τ is the effective basal shear stress at flow depth h;

τ_c is the critical shear stress required to initiate bedload transport

k is an empirically derived coefficient largely dependent on grain size; and

n is an empirical exponent usually equal to 1.5 (Meyer-Peter and Müller, 1948)

In Section 5.7.1, it is clear that $\tau >> \tau_c$. The shear stress expression (Equation 5.4) shows that at h = 0.01 m, τ is still an order of magnitude larger than τ_c. According to Singh (1996), for flows with high Froude numbers, in SI units,

$$k = \frac{0.7923}{\rho - \rho_w} \qquad \text{Equation 5.8}$$

where ρ and ρ_w are the densities of the sediment and water, respectively. Equation 5.7 may thus be approximated by

$$Q_{s(bed)} = \frac{0.7923}{\rho - \rho_w}(\gamma_w h \sin\beta)^{1.5} \qquad \text{Equation 5.9}$$

Substituting different values in Equation 5.9 yields the following estimates for $Q_{s(bed)}$, in m^3/s per meter of channel width,

Flow depth, h (m)	Lahar dam (β = 1.4°)	Pyroclastic-flow dam (β = 2.8°)
0.01	0.01	0.03
0.1	0.3	5
0.5	3	180
1	10	850

5.7.4. Bank collapse

The sediment contribution of bank collapses along the outlet channel may be evaluated by the Cullman method of slope-stability analysis, as illustrated in Figure 5.13.

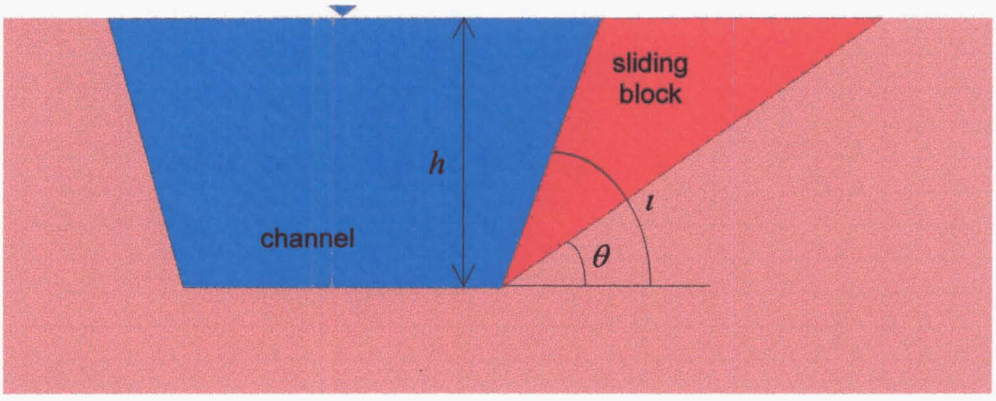

Figure 5.13. Diagram showing idealized geometry of a sliding block of bank material. The angle ι represents the slope of the bank, while θ represents the angle of the potential failure plane.

In this diagram, the angle that the failure plane makes with the horizontal, θ, depends on the slope angle, ι, and the angle of internal friction of the material, ϕ, as $\theta = \frac{1}{2}(\iota + \phi)$ (Lohnes and Handy, 1968). The size of the block is largest when $\iota = 90°$, assuming the slope does not overhang. Thus, considering $\phi = 48°$, θ is calculated to be equal to 69°. The maximum cross-sectional area of the sliding block may be calculated from the geometry of the block:

$$A = \tfrac{1}{2} h^2 \tan\theta \qquad \text{Equation 5.10}$$

The volume per meter of channel length may be calculated from Equation 5.10:

Flow depth, h (m)	Volume of sliding block (m^3/m channel length)
0.1	0.01
0.5	0.3
1	1.3

Bank failure is considered only for one side of the channel inasmuch as the spillway of most transient dams are located on the downstream end of the fan-dam, and is thus bounded on one side by pre-eruption bedrock. The calculated volumes are an order of

magnitude lower than the volumetric rate of bedload transport in the spillway channel shown in Section 5.7.3. In addition, these volumes are for each discrete event. Actual bank collapse rates are probably much lower because collapses do not occur continuously. This analysis and the observation that spillway channels of surviving dams have not widened indefinitely support the conclusion that bank failure alone does not contribute enough sediment to offset bed erosion along the spillway channel.

5.7.5. Flow on the dam surface

Under Settings 2 and 3, transient dams are continuously fed by sediments by the blocking channel through lahars or through sediment-laden flows along many small fan distributaries. Figure 5.14, for example, shows how flow along the O'Donnell River has delivered sediments to the Crow Valley Lake blockage, in effect continuously building up the dam. The flow rate along the O'Donnell varies from ~10 m^3/s distributed among small fan-distributaries, to several hundred m^3/s transported by floods or lahars during rainstorms. At Cutuno, sediment is delivered to the outlet channel largely by rills that have formed on the blockage surface (*Please see* Figure 5.7, *Section 5.3.2*). The ephemeral channel that discharges mostly into the lake may also have occasionally delivered sediment into the outlet channel.

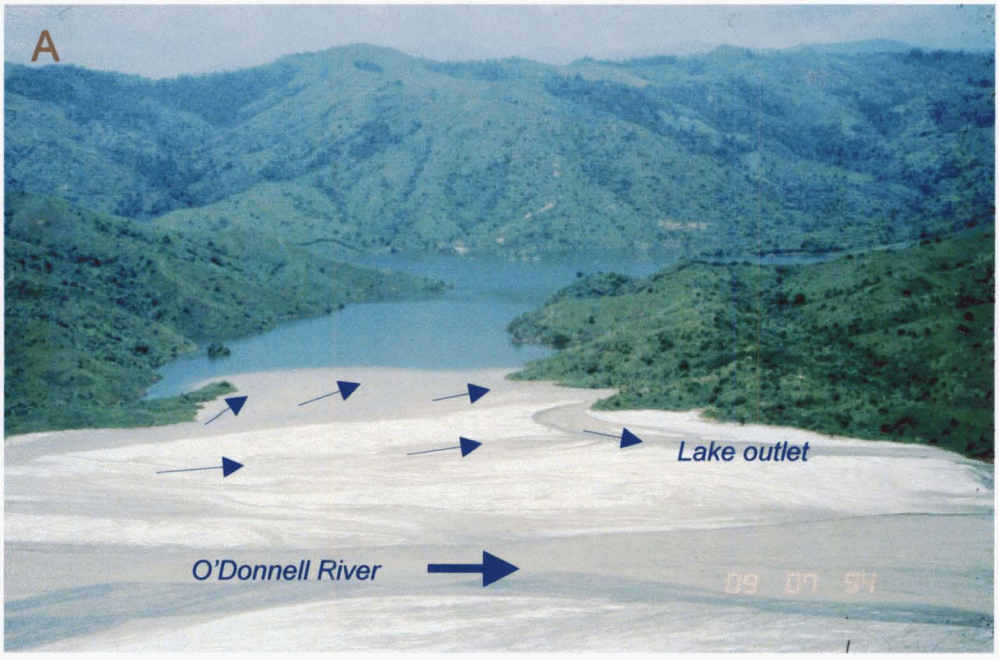

Crow Valley Lake, September 1994 (*Photo courtesy of C.G. Newhall*)

Crow Valley Lake, July 1999 (*Photo courtesy of PHIVOLCS*)

Figure 5.14. West-looking photos of the Crow Valley Lake, which was formed by rapidly aggrading lahar deposits from the O'Donnell River (flow direction indicated by thick arrow in A) that have fanned out into the drowned valley. The photos show net aggradation between 1994 and 1999, indicating continuous supply of sediments to the dam by sediment-laden streamflows (small arrows). A small debris fan had formed where a small tributary joins the outlet channel on the downstream (north) side of the dam. The outlet channel has more or less maintained its width and depth from 1994 to 1999.

Sediment transport by flows on the fan-dam may be estimated using the low-flow sediment-rating curves determined specifically for the Pasig-Potrero River during the 1997 and 1998 rainy seasons (Hayes, 1999). These are given by the equations

$$G_{s(bed)} = 9.5Q^{0.87} \qquad \text{Equation 5.11}$$

and

$$G_{s(sus)} = 9.5Q^{1.76} \qquad \text{Equation 5.12}$$

where $G_{s(bed)}$ is the bedload transport in kg/s;

$G_{s(sus)}$ is suspended load transport in kg/s; and

Q is the volumetric flow discharge in m^3/s

The total sediment load can be calculated by adding bedload and suspended load. The sediment rating curves depend on bed-material properties and channel-bed conditions, which are believed to be similar for all channels around Pinatubo that are underlain by pumiceous sediments. Thus, Equations 5.11 and 5.12 can be used to estimate sediment transport rates from the flow discharge along a channel. Most main lahar channels around Pinatubo have discharges that vary from <10 m^3/s to about 100 m^3/s during low-flow, non-lahar conditions. These translate to total (suspended and bedload) sediment transport rates ranging from 0.5 m^3/s to about 25 m^3/s using sediment density of 1300 kg/m^3. These figures are considered sufficient to possibly offset bed erosion along the transient dam spillway, even if only a fraction of the fan-flows regularly end up in the spillway channel. Sediment transport rates across the fan-dam increase even more during rainstorms, when both flow discharge and sediment concentration increase considerably. Net aggradation of the Crow Valley Lake blockage from 1994 to 1999

(Figure 5.14) suggests that fan-flow sedimentation may more than compensate for erosion along the dam spillway.

5.7.6. Sediment supply is key to stability of transient dams

The foregoing sediment mass balance calculations show that in a non-eroding or aggradational environment such as under Setting 2 or 3, transient dams may remain stable for as long as enough sediment is supplied to the dam spillway to compensate for bed erosion along that channel. The 1994 Cutuno dam had such abundant supply until about a month after it was formed. The eventual capture of the upper Bucbuc River by the Timbu deprived the dam – and the dam spillway – of this resource. After the capture, the pumice-source area for the dam was reduced to less than 1 km^2, partly drained by an ephemeral stream that discharged into the lake (*See* Figures 5.6 *and* 5.7). While other rills on the blockage and some bank collapses may have transported sediments into the spillway, the sedimentation rate had undoubtedly been considerably reduced. Assuming intermittent discharge from these ephemeral channels averaged, say, 5 m^3/s, Hayes' (1999) sediment rating curves indicate that a maximum of 0.2 m^3/s could have been transported into the spillway. This was barely sufficient to offset bedload transport along the spillway.

During rainfall events, discharge along a channel increases in proportion to its catchment size. For dams under Setting 2, where the blocking channel's catchment is much larger than that of the dammed tributary, rainstorms result in more sediments delivered to the dam spillway. But for dams under Setting 3, where the lake's catchment area is larger, the opposite happens: spillway erosion increase in larger proportion than sedimentation rate along the beheaded blocking channel. The ultimate cause of the failure of the 1994 Cutuno dam is hypothesized to have been caused by such sediment mass imbalance. The capture of the upper Bucbuc River by the Timbu drastically reduced the catchment size of the Bucbuc-Papatac channel to about 1 km^2, as well as cut it off from the pyroclastic deposits, thus dramatically reducing the amount of sediments delivered to the spillway across the fan-dam. This could have resulted in net erosion along the spillway channel. The capture also made the blocked Yangca Creek larger

than the blocking channel. During rainfall events, the increase in discharge along the spillway would have been greater than that along the blocking channel, thereby magnifying net erosion along the spillway.

5.8. Lahar hazards from dam breaching

5.8.1. Time of breaching of Cutuno dam

Cutuno Lake is believed to have drained catastrophically on the night of 22 September until the early morning of 23 September 1994 (Punongbayan *et al.*, 1996). The last visual observation of the 1994 Cutuno Lake was during a helicopter survey by PHIVOLCS on 16 September. The next aerial survey on 23 September showed a fully drained lake.

AFM record

Many lahars actually occurred between 16 and 23 September (Figure 5.15). A large event observed in the field and detected by the AFM on 18 September is suspicious because it was apparently accompanied by very little rainfall. PHIVOLCS' field personnel, however, did not report any indication that the flows they observed at Delta 5 at that time were from the Papatac channel.

Three large lahars occurred in the Pasig River from 21 to 23 September 1994, each of the first two marked by a sharp increase in rainfall intensity (Figure 5.15). The third, which was recorded by the acoustic flow monitor AFM-5 from 22:17 of 22 September to 3:17 the next day, was preceded by significantly less intense rainfall, and is believed to correspond to the lake-breakout event. The acoustic flux from this supposed lake-breakout signal translates to a total lahar volume of 5 x 10^6 m^3, with an average discharge of 260 m^3/s (*Please see Chapter 4 for discussions on the methods of calibrating instrument data to predict flow volumes*). This AFM signal, however, was probably attenuated, considering that the lake-breakout lahars created a new channel through a sugarcane field several hundred meters away from Delta 5. PHIVOLCS

mapped 3 x 10^7 m^3 of fresh lahar deposits over a 16-km^2 area based on aerial surveys conducted on 23 and 24 September 1994 (Arboleda *et al.*, 1995). Assuming this volume was emplaced solely by the 5-hour lake-breakout event yields, an average discharge of 1700 m^3/s is estimated for the event.

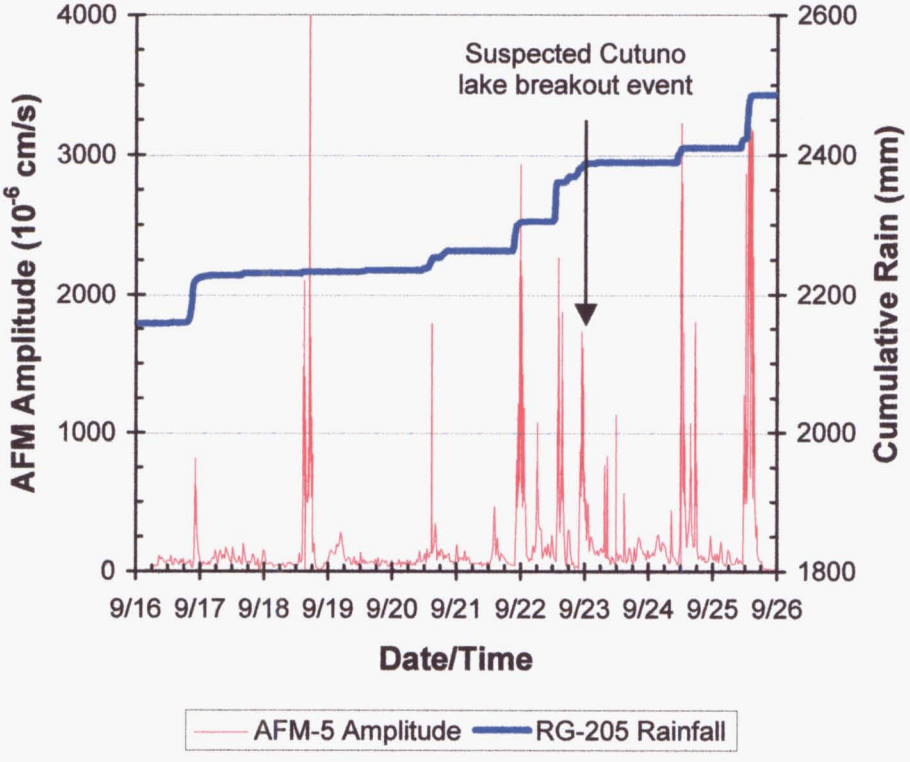

Figure 5.15. Acoustic flow monitor proxy-hydrograph and rain gauge records for 16-25 September 1994, showing the many lahars before, during and after the 22-23 September 1994 breakout of Cutuno Lake.

Photographic record

That the lake-breakout occurred on 22-23 September 1994 is supported by photographs taken during the aerial survey conducted by PHIVOLCS in the morning of 23 September. These show numerous fresh secondary pyroclastic slide scarps along the left bank of the breach channel, and fresh ash covering the surrounding ground surfaces (Figure 5.16).

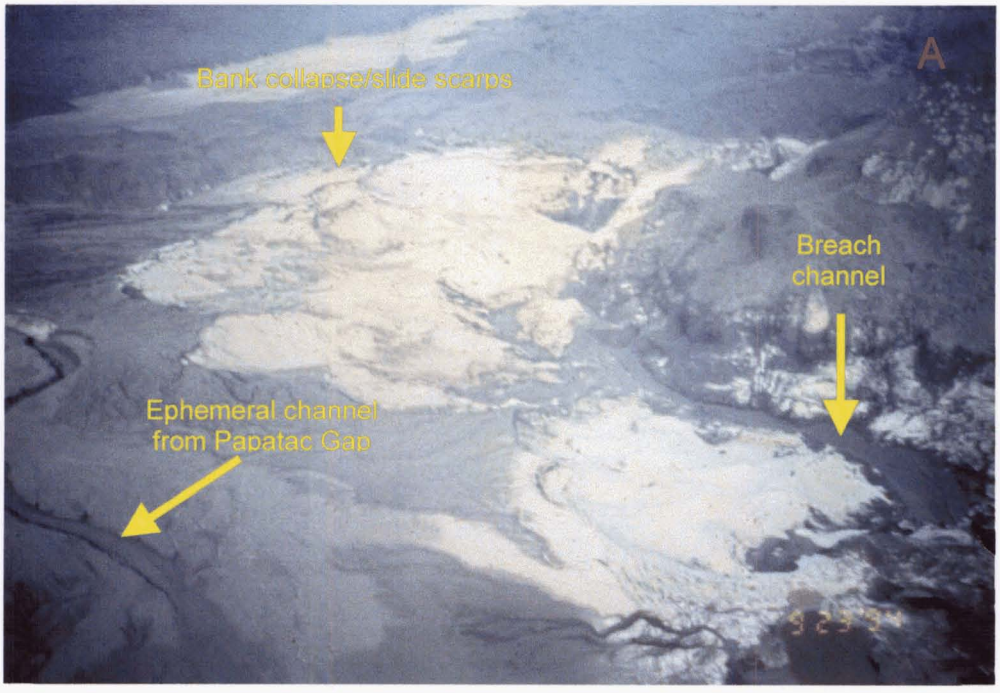

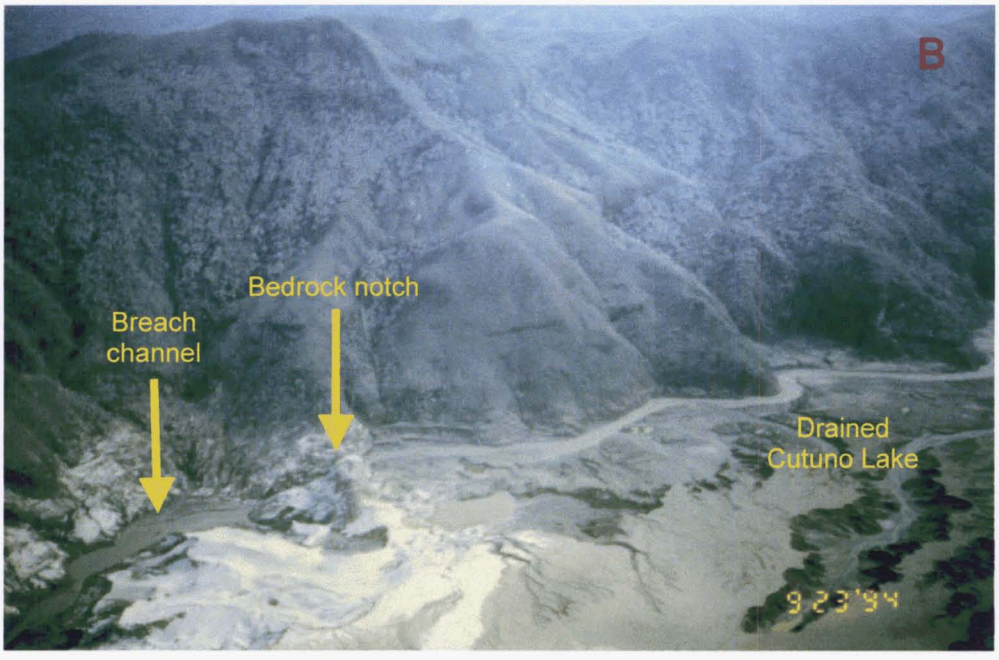

Figure 5.16. Newly drained Cutuno Lake, 23 September 1994. The lake breakout was accompanied by numerous secondary pyroclastic slides along the banks of the breach channel (A). The freshness of the slide scarps and ash-covered surfaces indicates that the breakout happened shortly before the photograph was taken. Just like in 1992, the lake drained through a notch in a bedrock ridge (B). (*Photo courtesy of PHIVOLCS*)

Further evidence that suggests that the lake-breakout indeed occurred on 22-23 September was the observation that the breach channel had apparently not yet reached a stable level when it was observed on 23 September. As shown in Figure 5.17A (also in Figure 5.16B), the breach channel (the Yangca Creek) initially passed through a notch in a bedrock ridge, which was at an elevation 380-390 m asl on 23 September. This was the same bedrock notch through which Cutuno Lake drained in 1992 (Arboleda and Martinez, 1996, p. 1051-1052). Subsequent aerial observations on 30 September showed a further lowering and lateral shifting of the breach channel (Figure 5.17B and 5.17C). Instead of passing through the bedrock notch, the breach channel was now going around the ridge, at an estimated elevation of 360 m asl, 20-30 m lower than on 23 September (Figure 5.17C). The Yangca channel has maintained this alignment and elevation until 1999 (Figure 5.17D).

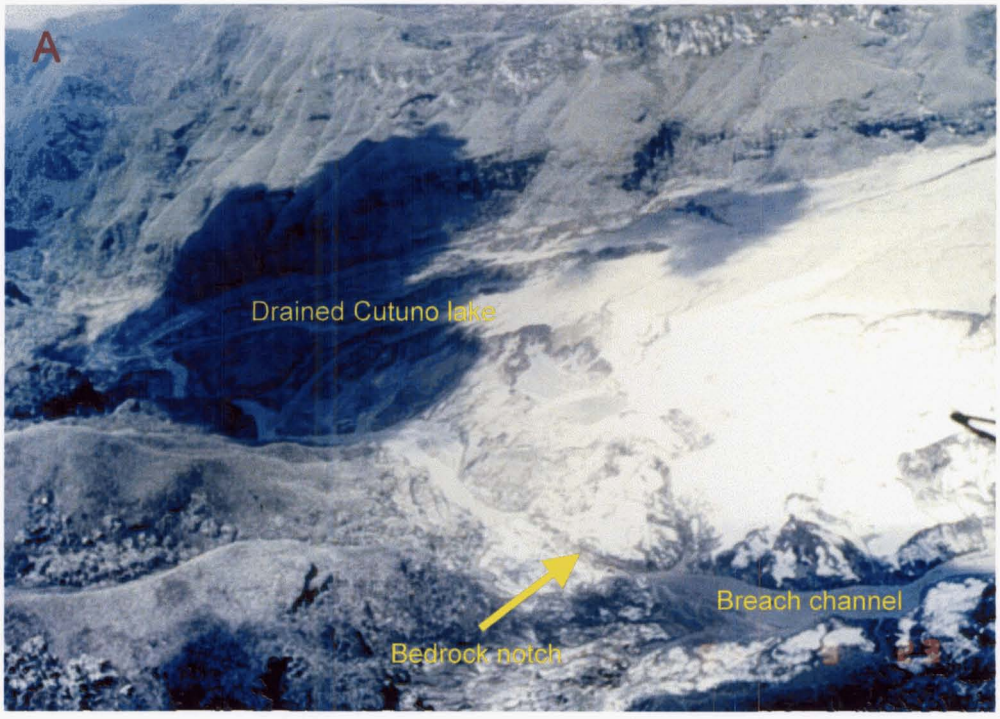

Drained Cutuno Lake, 23 September 1994, looking obliquely across the Yangca (west). The Yangca Creek flows towards the bottom right of the photo. (*Photo courtesy of R.S. Punongbayan*)

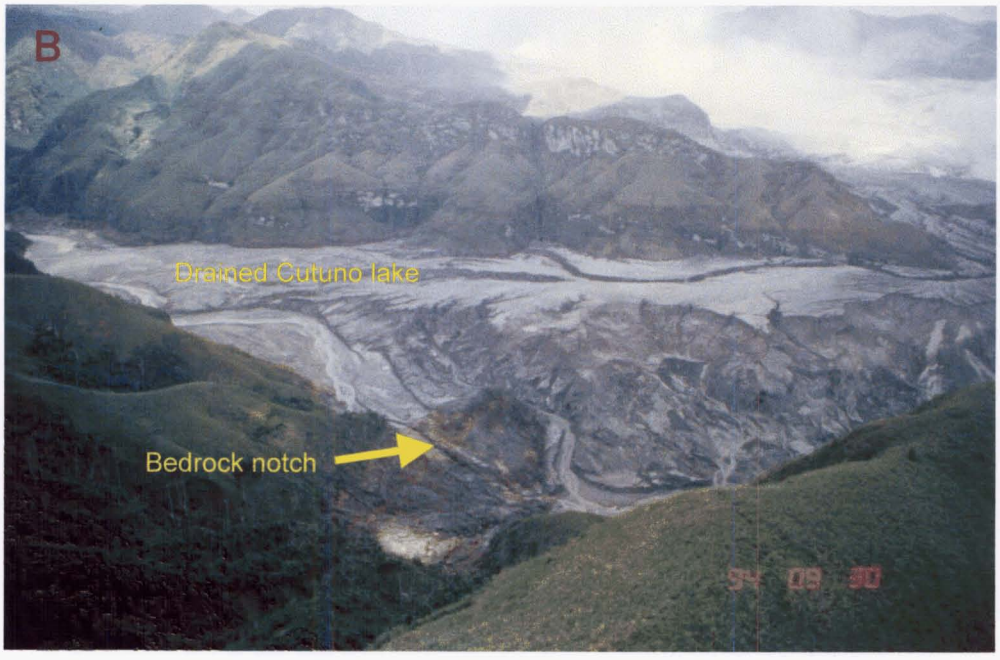

Drained Cutuno Lake, 30 September 1994, look similar to A (northwest). The Yangca Creek flows towards the right of the photo. (*Photo courtesy of C.G. Newhall*)

Drained Cutuno Lake, 01 October 1994, looking up the Yangca Creek (southwest). (*Photo courtesy of R.S. Punongbayan*)

Former Cutuno Lake, November 1999, similar view direction as in C.

Figure 5.17. Evolution of the dam breach channel after the 22-23 September 1994 Cutuno lake breakout; both photos looking up the Yangca. The breach channel that initially passed through a notch in a bedrock ridge (A) had shifted around the ridge by 30 September (B and C), where the channel has remained until 1999 (D). The channel further incised by 20 - 30 m, which suggests it was still in the process of adjusting when it was observed on 23 September. This indicates that the lake-breakout probably occurred shortly before that observation.

Downstream of the former lake site, massive incision occurred along the Yangca-Papatac channel between 23 and 30 September 1994 (Figure 5.18). The lahars detected by AFM-5 on 24 and 25 September (*See* Figure 5.15) were probably from this rapid erosion along the Yangca-Papatac channel. The incision occurred even as the Papatac remained severed from the upper Bucbuc and Cutuno Lake had completely drained.

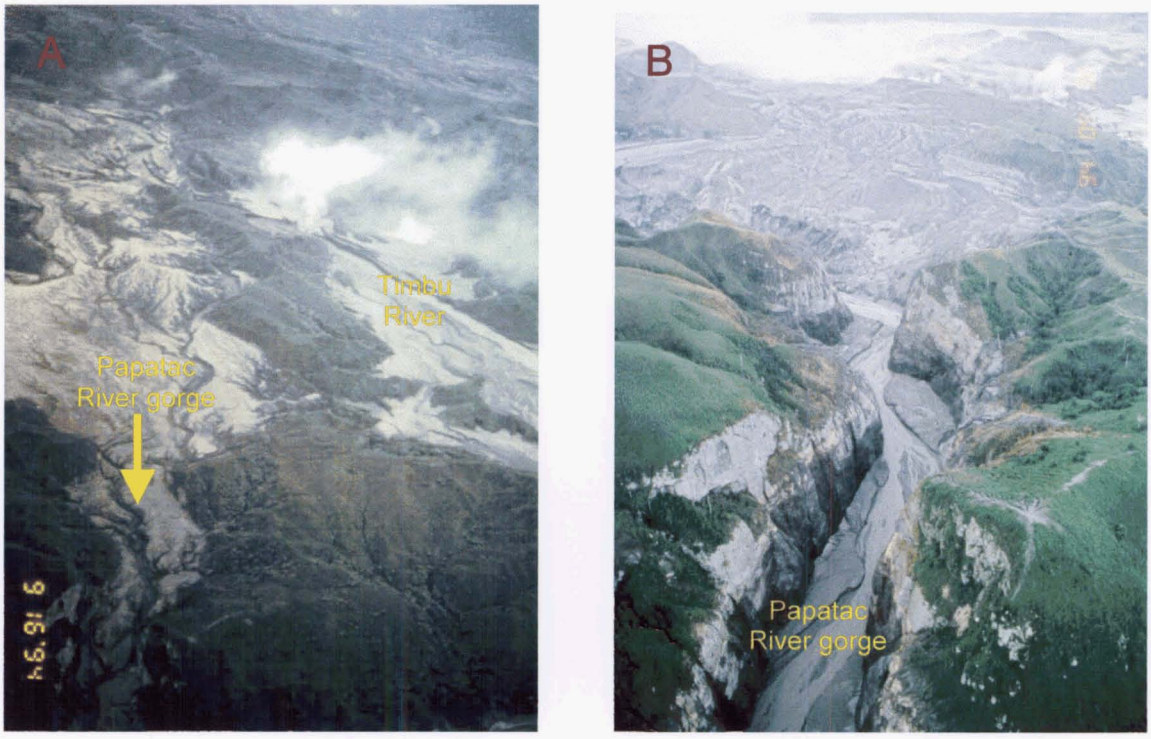

Figure 5.18. Channel incision along the Papatac River channel in the aftermath of the Cutuno lake-breakout. Before the breakout (A), the Papatac was filled with pyroclastic-flow and lahar deposits. Lahars during and following the lake-breakout, from 23 to 25 September 1994, lowered the Papatac channel bed by about 50 m (B). (*Photo A courtesy of PHIVOLCS; Photo B courtesy of C.G. Newhall*)

The rapid incision between 23 and 30 September is interpreted to be the immediate channel response of the Yangca Creek to the lake breakout. The 23 September photo must have been taken during a transition period right after the full drainage of the lake, but before the Yangca channel was able to completely stabilize its gradient. The

mechanics of how the Yangca managed to lower its bed and go around the bedrock ridge it was previously flowing through is poorly understood, especially considering the small size of the Yangca watershed. Several possibilities may be considered:

1. Flood discharge from the Yangca was not accommodated by the narrow bedrock notch, with the bedrock ridge effectively damming the flow. The flood-flows eventually avulsed around the ridge, then onto the steep bank of the breach channel The steep nickpoint rapidly migrated upstream until a stable river profile was attained. Or,

2. The sediments previously submerged by the lake remained fully saturated and flowed as a liquefied mass. The steep banks along the breach channel may have provided the free face for such liquefied flow to occur. Or,

3. A secondary explosion occurred near the bedrock ridge, causing en masse remobilization of some of the remaining dam deposit, followed by a series of lahars.

5.8.2. Geomorphic impacts of the 1994 Cutuno Lake breakout

The 22-23 September lahars re-exhumed the Pasig channel downstream of Delta 5 and dumped the remobilized deposits in the lower alluvial fan, burying several barangays of Porac and Bacolor, and killing more than 20 people. These lahars initially deposited thick deposits near Delta 5 that almost buried the pre-eruption terraces in the area (Figure 5.19A). Succeeding lahars on the 24-25 September, however, caused great channel erosion from the Papatac gorge down past Delta 5 (Figure 5.19B; *See also* Figure 5.18B), and remobilized the deposits farther downstream.

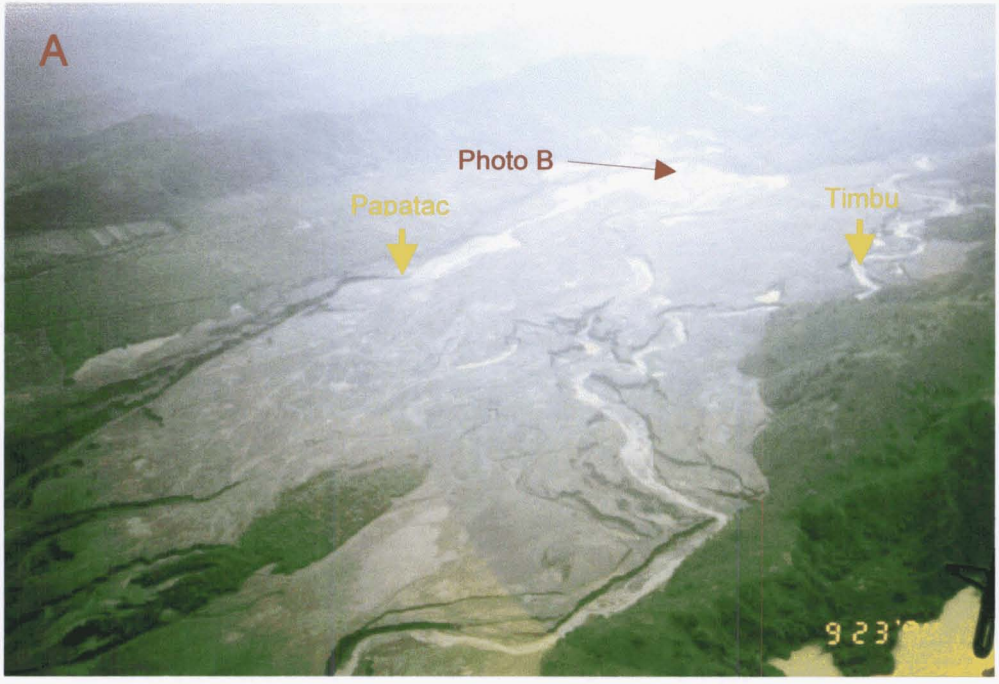

Photo taken on 23 September 1994, courtesy of PHIVOLCS

Photo taken on 30 September 1994, courtesy of C.G. Newhall

Figure 5.19. Impacts of the 1994 Cutuno lake-breakout lahars on the Pasig-Potrero alluvial fan. The 22-23 September lahars deposited thick, bouldery sediments up to the level of the pre-eruption terraces just upstream of Delta 5, before incising a new Papatac channel through the right-bank terrace (A). Photo B shows the lithic-rich bouldery deposits in section. The lake-breakout lahars probably combined with simultaneous lahars along the Timbu channel to carve a deep canyon near Delta 5, which funneled the flows to the lower alluvial fan (C). The area covered by A is approximated by the dotted rectangle in C.

5.8.3. Dam-break prediction using analytical models

Predicting flood hydrographs from dam breaching has been modeled by many engineers and scientists. The methods of analysis can be grouped into three: (1) empirical dimensional analysis, (2) empirical dimensionless analysis, and (3) physically-based mathematical models (Singh, 1996). The methods presented by Walder and O'Connor (1997) for predicting peak discharge from dam-breaching are examples of dimensional and dimensionless analyses. Mathematical models are more varied, but perhaps the most widely used are BREACH and FLDWAV, which are available from the U.S. National Weather Service website (*e.g.*, Fread, 1988; Fread and Lewis, 1998). In addition, Visser (1998) has modeled breach development in sand dikes in the Netherlands. The Civil Engineering Department of the University of Auckland, New Zealand, has also modeled the development of breach channels in noncohesive embankments in a laboratory scale model (Andrews, 1998; Coleman and Andrews, 2000).

For the purpose of showing the applicability of dam-break models to the transient dams of Pinatubo, the relatively simple method by Walder and O'Connor (1997) and Fread's (1988) BREACH model are considered.

Walder and O'Connor's (1997) method

Walder and O'Connor (1997) used scaled (dimensionless) geometric parameters to predict dam-breach peak discharge from a lake of known dimensions. Their method relates peak discharge Q_p to the volume of water released, V_0, net drop in lake level, d, and an assumed constant rate of erosion, k. The parameters V_0, d and k are encapsulated by the dimensionless parameter, η, by the equation

$$\eta = \frac{kV_0}{g^{1/2} d^{1/2}} \qquad \text{Equation 5.13}$$

From η, a dimensionless peak discharge, Q_p*, can be determined graphically using one of several graphs, and Q_p calculated using the scaling relation

$$Q_p = g^{1/2} d^{5/2} Q_p^* \qquad \text{Equation 5.14}$$

For most cases, Q_p can also be calculated from "benchmark" relations (Walder and O'Connor, 1997, p. 2344)

$$Q_p = 1.51 (g^{1/2} d^{5/2})^{0.06} \left(\frac{kV_0}{d} \right)^{0.94} \qquad \text{for } \eta < \sim 0.6 \qquad \text{Equation 5.15}$$

$$Q_p = 1.94 g^{1/2} d^{5/2} \left(\frac{D_c}{d} \right)^{3/4} \qquad \text{for } \eta >> 1 \qquad \text{Equation 5.16}$$

where D_c is the total depth of the lake, which is equal to d for a totally drained lake. Applying Walder and O'Connor's method to the 1994 Cutuno dam situation yields the following:

V_0 (10^6 m^3)	d (m)	k (m/hr)	η	$Q_p{}^*$	Q_p (m^3/s)
5	10	0.1	0.01	0.03	27
5	10	0.5	0.07	0.12	123
5	10	1	0.14	0.24	236
5	10	2	0.28	0.46	453
5	10	5	0.70	1.08	1071
5	10	10	1.40	1.50	1485
5	10	20	2.81	1.80	1782
5	10	50	7.01	1.94	1921
5	10	100	14.03	1.94	1921

At Cutuno, the lake drained completely in 5 hours, indicating an average erosion rate of 2 m/hr. Walder and O'Connor's (1997) method predicts a peak discharge of about 450 m^3/s for such situation. This refers to water discharge along the breach channel at the lake margin, however, and does not account for bulking farther downstream. Lahars are believed to bulk up by about three times (Pierson, 1998), which suggests a peak discharge of 1400 m^3/s. This is slightly lower than the 1700 m^3/s average – not peak – discharge obtained by dividing the 3 x 10^7 m^3 of deposits by the 5-hour duration of the lake-breakout event.

For prediction purposes, one obvious limitation of Walder and O'Connor's (1997) method is in determining the erosion rate before the event, the values for which span several orders of magnitude. They suggested using analogs from other dam scenarios to estimate the breach erosion rate, but the criteria for choosing this were not specified, and are believed to be prone to subjective bias, considering that conditions vary greatly from site to site. The question of the validity of assuming a constant erosion rate also arises because erosion rate is a function of flow depth, and flow depth varies substantially in the course of breaching.

BREACH

The BREACH program is a relatively simple physically based mathematical model from the U.S. National Weather Service to predict breach characteristics and discharge hydrographs from a breached earthen dam (Fread, 1988). The required input includes both the geometry of the dam and lake, as well as some hydraulic and geotechnical parameters, as fully described in the program manual.

In applying BREACH to the 1994 Cutuno dam, it was found that the model needed a large reservoir inflow (about 20 m^3/s or 700 ft^3/s) and a dam material density not greater than 1300 kg/m^3 (81 lbs/ft^3) to initiate breaching. The low gradient of the dam probably precluded failure for stronger material or lower inflow discharges. Nevertheless, once the conditions for breaching were satisfied, the predicted hydrograph was found to be relatively insensitive to any of the geotechnical or hydraulic parameters. Figure 5.20 is an output from BREACH using parameters that were deemed reasonable for Cutuno. This shows that BREACH has grossly underestimated the peak discharge if compared to the AFM-derived hydrograph, and its prediction of a 35-hr breach duration is seven times longer than the actual event. A probable explanation for this discrepancy is that although it incorporates a routine for bank collapse, BREACH could not have possibly predicted the occurrence of secondary pyroclastic slides, which undoubtedly accelerated the actual breaching process. By manually compressing the predicted flood hydrograph from BREACH into a 5-hour duration (by dividing duration, and multiplying discharge, by 7), the peak discharge becomes 470 m^3/s, which is similar to the prediction based on Walder and O'Connor's (1997) method. As in other dam-break models, this figure applies to discharge along the breach channel, and does not incorporate possible bulking up farther downstream.

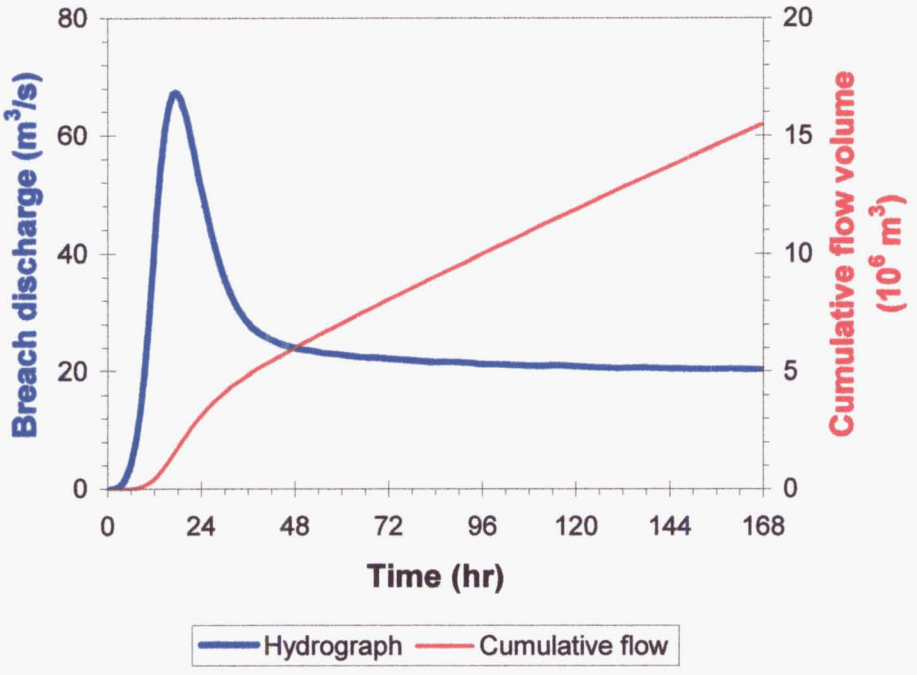

Figure 5.20. Predicted breach hydrograph for the 1994 Cutuno dam using the BREACH model (Fread, 1988). Note that the 20 m^3/s discharge at the falling limb of the hydrograph is largely due to the input lake inflow parameter.

5.9. The role of secondary explosions in the breaching process

Arboleda *et al.* (1995) has suggested the possible triggering effect of secondary hydroeruptions on dam breaching. In this mechanism, the secondary hydroeruption occurs once the confining pressure exerted by the overlying layer of deposit and column of water is overcome by the vapor pressure within the hot interior of the pyroclastic-flow deposit. This may happen gradually, and the timing of explosion is simply fortuitous. Alternatively, the hydroeruption may occur after part of the overburden is removed by surface erosion. There is no direct evidence to either confirm or reject the hypothesis that this is how the breaching of Cutuno dam was initiated. Nevertheless, this study proves that secondary hydroeruptions are not required to initiate breakouts of transient lakes.

The morphology and distribution of the scarps along the breach channel, as observed on 23 September 1994, suggest that these were most probably from secondary pyroclastic slides, which began when the outlet channel had incised its bed such that a progressively taller bank was created, and the hot sections of the pyroclastic-flow dam were exposed. The secondary pyroclastic slides are believed to have accelerated the breaching process.

The evolution of the breach channel at Cutuno may also have been influenced by secondary explosions. An explosion is a possible mechanism by which the Yangca channel was able to shift around the bedrock ridge after the lake had completely drained. No available information can confirm this possibility, however.

Naturally, secondary pyroclastic avalanches and hydroeruptions occur only in hot pyroclastic deposits. Thus, these phenomena are important factors in the dam-breaching process only where the dam is of pyroclastic-flow origin.

5.10. Summary of Chapter 5

Transient dams at Pinatubo are found to be stable against mass failure, either by gravitational collapse, or by piping, owing largely to their very gentle slopes. This holds true except under Setting 1, where subsequent flows along the previously blocking lahar channel may erode the dam, thus creating a steep slope on the downstream face of the dam and reducing the dam's effective width.

Transient dams are however naturally susceptible to failure by breach erosion from overtopping water. Pumiceous deposits of Mount Pinatubo are extremely erodible; thus, channel beds of such material are very prone to bed scour. However, sediment mass balance analyses show that transient dams can remain stable for as long as enough sediment is brought onto the dam and into the spillway at a rate at least equal to the rate of bed scour. Bank collapse contributes a small fraction of the sediments that are transported by bedload along the spillway. Sediments therefore need to be delivered by flows across the dam. This is normally achieved by lahars, or non-lahar but sediment-

laden streamflow, along the blocking channel. If the rate of sediment delivery across the fan-dam is about equal to or greater than the erosion rate along the spillway channel, the dam may survive. If, however, the sediment delivery slows down, erosion along the spillway may proceed unabated leading to breach-erosion failure. The failure of the 1994 Cutuno dam may be attributed to a drastic reduction of sediment supply brought about by the capture of the Bucbuc River by the Timbu.

The foregoing analyses further imply that all transient dams around Pinatubo, barring engineering intervention, will eventually fail. This can occur when sediment transport onto the dam has been sufficiently reduced to allow bed scour in the dam spillway. Ironically, efforts to stabilize the pyroclastic-flow deposits, say by reforestation, may contribute to the failure of transient dams by reducing sediment supply to the dams. Erosion along the blocking river can also lead to dam failure by creating steep slopes on the downstream face of the blockage, reducing the dam's effective width, and cutting off sediment supply to the dam spillway.

Secondary hydroeruptions and secondary pyroclastic slides may also play major roles in the breaching process of pyroclastic-flow dams at Pinatubo. The possibility that these have actually triggered lake-breakouts cannot be totally discounted, although there is no direct proof to support it either. More likely, secondary hydroeruptions and pyroclastic slides can be by-products of lake-breakouts, produced when confining pressures are relieved sufficiently to be overcome by steam pressure within the pyroclastic-flow deposit. Certainly, the analyses show that they are not absolutely required for transient dams to fail. Once breaching commences in a pyroclastic-flow dam, however, secondary hydroeruptions and pyroclastic slides may accelerate breaching beyond what any dam-breaching model can predict.

The conclusion that all transient dams will eventually fail requires that studies be made on the surviving dams around Pinatubo. These may be in the form of more detailed sedimentation and erosion studies, or hydraulic and geotechnical analyses. The hazards that transient dams pose make such studies imperative.

Chapter 6

SUMMARY AND CONCLUSIONS

CHAPTER 6

Summary and Conclusions

6.1. Lahar initiation processes

Lahar initiation processes were analyzed by considering rapid erosion and mass wasting processes in different parts of a river basin disturbed by a large-magnitude volcanic eruption. These involve several intimately interacting processes: (1) rill erosion, both on tephra-covered hillslopes and on the valley-filling pyroclastic-flow deposits; (2) main channel erosion; (3) mass failure of banks made of loose pyroclastic deposits; and (4) secondary explosions, which often result when mass failures suddenly release steam pressure in the hot pyroclastic deposits. Erosion by rills is enhanced by the blanket of tephra on hillslopes, which temporarily reduces infiltration and provides large amounts of sediments. Because of their ability to quickly incise through the loose tephra, rills may form lahars by themselves. Rill erosion processes interact dynamically with rapid fluctuations in the main rivers to which they connect. Processes in the main river channel involve large-scale collapse of hot bank material, which sometimes lead to secondary pyroclastic flows. High sediment flux from tributary rills combines with bank failures in the main channel to quickly form lahars. Lahars bulk up in the main channel by further entraining bank materials and by scouring the channel bed. The latter is made possible by the high shear stress that the dense and deep flow exerts on the channel bed.

Erosion processes slow down as the channel and rill network attempts to attain dynamic equilibrium. This equilibration, however, is complicated by secondary explosions, which influence sediment movement by mass remobilization of pyroclastic debris and by repeatedly generating fine ash that retard hillslope recovery. As the pyroclastic deposits are depleted, the frequency of secondary explosions decreases, rill erosion slows down, and the main channel regains a more stable longitudinal profile that is in synchrony with its tributary rills, leading to the cessation of lahar activity.

In the Pasig-Potrero, the first signs of river channel stability were manifested in 1996, when the river channel became incised into pre-eruption deposits through much of its length. Since the calamitous Typhoon *Mameng* lahar on 01 October 1995, the only other major lahar event occurred in August 1997 during an unusually heavy rainstorm. After this, flows along the Pasig have been dominated by muddy streamflow, at worst bordering on hyperconcentrated flow. By 1999, the upper Pasig River had developed an apparently stable drainage network characterized by a wide channel incised through pre-eruption material, and rills that have largely equilibrated with the base level provided by the main channel. The hillslopes have regained their lush vegetation, and the surface of the now depleted pyroclastic-flow deposits have been partly revegetated.

6.2. Laharic sediment yield and triggering rainfall

Temporal variations in rainfall-normalized sediment yield and lahar-triggering rainfall in the Pasig-Potrero River were analyzed using AFM and rain gauge data, with AFM data as proxy for lahar hydrographs. Data for coincident lahars and rainstorms show the river's response to two major watershed disturbances: the emplacement of 300 million m^3 of pumiceous pyroclastic debris during the 1991 eruption, and the capture of the upper Sacobia catchment in October 1993. Sediment yield peaked immediately after each of these major watershed disturbances, followed by a non-linear decrease through time. The progressive decline in sediment yield, even when the channels were still in very erodible pyroclastic deposits, indicates that the decline was not only a function of the erodibility of the surface per se, but more a function of sediment supply and the development of the drainage network, particularly the overall decrease in drainage density and increase in channel width. These parameters influence the volume of pumiceous sediments in contact with runoff. The decline in sediment yield reflects both the depletion of the source sediments – the 1991 pyroclastic-flow deposits – and the recovery of the catchment.

The rainfall threshold at which lahars are generated was found to remain at about the same low level until 1995, after which it increased progressively until 1997. No major

lahar has been observed or detected by the AFM since then. The increase in triggering rainfall coincides with (1) the incision of the Pasig River channel into the pre-eruption surface, and (2) a significant decrease in the frequency and magnitude of secondary explosions. The triggering rainfall is postulated to be a function of the erodibility and infiltration capacity of the surface, which together control the amount of runoff and entrainable sediments. These factors in turn are largely controlled by the areal distribution of pumiceous 1991 pyroclastic deposits including the intermittent ash generated by secondary explosions.

The temporal variations in sediment yield and lahar-triggering threshold demonstrate the increasing amount of rainfall needed to generate a lahar of a given magnitude. By 1999, a rainstorm with a return period of more than 100 years was needed to generate a lahar with a volume of at least 10 million m^3, which by experience has been the minimum volume of "disastrous" lahars.

6.3. Initiation mechanisms of lake-breakout lahars

Four conceivable mechanisms for the failure of pyroclastic dams were analyzed in this study: (1) erosion of the dam by flows along the lahar channel; (2) gravitational collapse and/or piping; (3) lake overtopping; and (4) secondary explosions. When the formation of the dam is followed by erosion along the blocking channel, dam failure is inevitable and usually occurs quickly. Most dams in such eroding environments have been short-lived.

For dams in non-eroding settings, analyses show that the blockages are naturally stable against gravitational collapse and piping. They are, however, susceptible to overtopping failure through breach erosion. The survival of some dams may be explained by sediment mass balance analysis, which shows that material lost to bed erosion along the breach-channel may be initially compensated for by sediments delivered onto the dam by lahars along the blocking channel, and by local runoff. Once sediment supply to the

dam is cut off, *e.g.*, due to the depletion of source sediments, by revegetation, or by stream beheading, the dam is predicted to fail by breach erosion.

6.4. Conclusions

The trends in laharic sediment yield and lahar-triggering rainfall together demonstrate the progressively increasing rainfall requirement for lahar generation through time. Cautious extrapolation of the data suggests that to trigger and sustain a modest lahar (<10 million m^3) in the Pasig-Potrero River now requires a rainstorm with a return period exceeding 100 years. This shows that hazards from rain-triggered lahars have been considerably reduced. However, hazards from excessive sedimentation by sediment-rich flows remain. With the reduction in lahar activity, the river has gradually become more stable, although further adjustments in the river's longitudinal profile are expected. Future activity will probably be dominated by remobilization of sediments farther downstream. Mitigation strategies should now aim to mitigate this eventuality.

Remaining lahar hazards are posed by surviving lakes that have been formed by the blockage of tributaries by lahar or pyroclastic-flow deposits. Three such lakes of considerable size remain around Pinatubo: the Mapanuepe in the Marella-Sto. Tomas basin, Marimla in the Sacobia basin, and Crow Valley in the O'Donnell. A similar dam, the Cutuno blockage, has, in the past, repeatedly formed and breached, each time resulting in catastrophic lahars. Barring engineering intervention, this study suggests that all pyroclastic-flow or lahar dams around Mount Pinatubo will eventually fail. This is also suggested by their absence before the 1991 eruptions. However, it is beyond this study to predict the actual timing of dam breaching for any of the remaining blockages.

6.5. Possible topics for future research

The study of lahar initiation is a complex field, and this study could only cover a fraction of it. In some cases, direct observations of active processes during and immediately following an eruption are invaluable.

Specific topics that may be explored further include:

1) Mechanics of erosion on tephra-covered hillslopes – this may include the formation and effects of tephra crusts, and the development of rills;

2) Dynamic interaction between river channels and their tributary rills in a rapidly fluctuating system;

3) Source of cohesion of granular pyroclastic deposits;

4) Mechanics of secondary explosions and their effects on erosion; and

5) Prediction and evaluation of breach-failure hazards from the remaining lahar dams.

REFERENCES

References

Abigania, M.I.T., Alanis, P.K.B., and Javier, D.V., 2002, Report on the January 18, 2002 Investigation of Lake Maughan and the 1995 Ga-ao Creek Landslide Dam, South Cotabato Province, Mindanao Island: Quezon City, Philippine Institute of Volcanology and Seismology, 18 p.

Aguila, L.G., Newhall, C.G., Miller, C.D., and Listanco, E.L., 1986, Reconnaissance geology of a large debris avalanche from Iriga Volcano, Philippines: Philippine Journal of Volcanology, v. 3, no. 1, p. 54-72.

American Society for Testing and Materials (ASTM), 1995, Annual Book of ASTM Standards: Philadelphia, Pa., American Society for Testing and Materials, v. 04.08: Soils and Rock.

Andrews, D.P., 1998, Embankment Failure Due to Overtopping Flow: Auckland, New Zealand, University of Auckland, Master of Engineering thesis, 350 p.

Arante, R., Arboleda, R.A., Delos Reyes, P.J., Javier, D., Panol, M., and Tubianosa, B.S., 1997, Hydrologic Events in the Pasig-Potrero River System During the Passage of Typhoon Ibiang: Report of investigation for the fieldwork conducted on 21-29 August 1997 (unpublished): Quezon City, Philippine Institute of Volcanology and Seismology, 9 p.

Arboleda, R.A., Catane, S.G., Delos Reyes, P.J., Martinez, M.M.L., Mirabueno, M.H.T., Regalado, M.T.M., Tubianosa, B.S., Tuñgol, N.M., Umbal, J.V., Punongbayan, R.S., Newhall, C.G., and Alonso, R.A., 1995, Chronology of the 1994 Lahars at Pinatubo Volcano and Consequent Hazards and Risks [unpub. report]: Quezon City, Philippine Institute of Volcanology and Seismology, 37 p.

Arboleda, R.A., Catane, S.G., Delos Reyes, P.J., Mirabueno, M.H.T., Regalado, M.T.M., Torres, R.C., and Umbal, J.V., 1994, Lake breakout lahars: a case study of the 22-23 September 1994 lahar events along the Pasig-Potrero River [abs.], *in* Geology in Construction and Tourism, Geological Society of the Philippines, 7th Annual Geological Convention, Program and Abstracts.

Arboleda, R.A., and Martinez, M.M.L., 1996, 1992 lahars in the Pasig-Potrero River system, *in* Newhall, C.G., and Punongbayan, R.S., eds., Fire and Mud: Eruptions and Lahars of Mount Pinatubo, Philippines: Quezon City / Seattle, Philippine Institute of Volcanology and Seismology / University of Washington Press, p. 1045-1052.

Barberi, F., Martini, M., and Rosi, M., 1990, Nevado del Ruiz Volcano (Colombia): pre-eruption observations and the November 13, 1985 catastrophic event, *in* Williams, S.N., ed., Nevado del Ruiz Volcano, Colombia, II: Journal of Volcanology and Geothermal Research, v. 42, no. 1-2, p. 1-12.

Bautista, C.B., 1996, The Mount Pinatubo disaster and the people of central Luzon, *in* Newhall, C.G., and Punongbayan, R.S., eds., Fire and Mud: Eruptions and Lahars of Mount Pinatubo, Philippines: Quezon City / Seattle, Philippine Institute of Volcanology and Seismology / University of Washington Press, p. 151-163.

Bell, F.G., 1983, Engineering Properties of Soils and Rocks (2nd ed.): London, Butterworths, 149 p.

Bina, M.M., Tanguy, J.C., Hoffmann, V.H., Prevot, M., Listanco, E.L., Keller, R., Fehr, K.T., Goguitchaichvili, A.T., and Punongbayan, R.S., 1999, A detailed magnetic and mineralogical study of self-reversed dacitic pumices from the 1991 Pinatubo eruption (Philippines): Geophysical Journal International, v. 138, no. 1, p. 159-178.

Bornas, M.A.V., Suto, S., Martinez-Villegas, M.M.L., Listanco, E.L., Umbal, J.V., Tuñgol, N.M., Torres, R.C., Yamamoto, T., Takarada, S., and Itoh, J., 2000, 1995-1999 temperature vs. depth measurement of the 1991 Pinatubo pyroclastic flow deposits: an evaluation of the Pinatubo thermal surveys project, *in* Geological Survey of Japan, ed., Research on Volcanic Hazard Assessment in Asia: Report of International Research and Development Cooperation ITIT Projects: Tokyo, Japan, Agency of Industrial Science and Technology, Ministry of International Trade and Industry, p. 22-34.

Bryan, R.B., 2000, Soil erodibility and processes of water erosion on hillslope: Geomorphology, v. 32, no. 3-4, p. 385-415.

Caine, N., 1980, The rainfall intensity-duration control of shallow landslides and debris flows: Geografiska Annaler: Series A, Physical Geography, v. 62, no. 1-2, p. 23-27.

Catane, S.G., and Gabinete, E.R., 1996, A Report Into the Investigation of the Landslide Debris Blockage Aong the Ga-ao Creek, Lake Maughan, Parker Volcano, South Cotabato: Philippine Institute of Volcanology and Seismology.

Coleman, S.E., and Andrews, D.P., 2000, Overtopping Breaching of Noncohesive Homogeneous Embankments: School of Engineering Report No. 589: Auckland, New Zealand, University of Auckland, Department of Civil and Resource Engineering, 339 p.

Collins, B.D., and Dunne, T., 1986, Erosion of tephra from the 1980 eruption of Mount St. Helens: Geological Society of America Bulletin, v. 97, no. 7, p. 896-905.

Collins, B.D., Dunne, T., and Lehre, A.K., 1983, Erosion of tephra-covered hillslopes north of Mount St. Helens, Washington: May 1980-May 1981, *in* Okuda, S., Netto, A., and Slaymaker, O., eds., Extreme Land Forming Events: Zeitschrift für Geomorphologie, Supplementband 46, p. 103-121.

Costa, J.E., and Schuster, R.L., 1988, The formation and failure of natural dams: Geological Society of America Bulletin, v. 100, no. 7, p. 1054-1068.

Costa, J.E., and Schuster, R.L., 1991, Documented Historical Landslide Dams From Around the World: U. S. Geological Survey Open-File Report 91-239: Vancouver, Wash., U.S. Geological Survey, 486 p.

Craig, R.F., 1992, Soil Mechanics (5th ed.): London/New York, Chapman & Hall, 427 p.

Cruden, D.M., and Varnes, D.J., 1996, Landslide types and processes, *in* Turner, A.K., and Schuster, R.L., eds., Landslides: Investigation and Mitigation: National Research Council (U.S.), Transportation Research Board, Special Report 247: Washington, D.C., National Academy Press, p. 36-75.

Daag, A.S., 1994, Geomorphic Development and Erosion of the Mount Pinatubo 1991 Pyroclastic Flows in the Sacobia Watershed - A Study Using Remote Sensing and Geographic Information System (GIS): Enschede, The Netherlands, International Institute for Aerospace Survey and Earth Sciences (ITC), Master of Science in Applied Geomorphology and Engineering Geology thesis (unpublished), 106 p.

Defant, M.J., Jacques, D., Maury, R.C., de Boer, J.Z., and Joron, J.L., 1989, Geochemistry and tectonic setting of the Luzon arc, Philippines: Geological Society of America Bulletin, v. 101, no. 5, p. 663-672.

Delfin, F.G., Jr., 1984, Geology and Geothermal Potential of Mt. Pinatubo: Philippine National Oil Company-Energy Development Corporation (PNOC-EDC) internal report, 36 p.

Delfin, F.G., Jr., Villarosa, H.G., Layugan, D.B., Clemente, V.C., Candelaria, M.R., and Ruaya, J.R., 1996, Geothermal exploration of the pre-1991 Mount Pinatubo hydrothermal system, *in* Newhall, C.G., and Punongbayan, R.S., eds., Fire and Mud: Eruptions and Lahars of Mount Pinatubo, Philippines: Quezon City / Seattle, Philippine Institute of Volcanology and Seismology / University of Washington Press, p. 197-212.

Fread, D.L., 1988, BREACH: An Erosion Model for Earthen Dam Failures: Computer program, source code and documentation: Silver Spring, Md., National Oceanic and Atmospheric Administration (NOAA), National Weather Service (NWS), Hydrologic Research Laboratory, 35 p.

Fread, D.L., and Lewis, J.M., 1998, NWS FLDWAV Model: Computer program, source code and documentation: Silver Spring, Md., National Oceanic and Atmospheric Administration (NOAA), National Weather Service (NWS), Hydrologic Research Laboratory, 335 p.

Glicken, H.X., Meyer, W., and Sabol, M.A., 1989, Geology and Ground-Water Hydrology of Spirit Lake Blockage, Mount St. Helens, Washington, With Implications for Lake Retention: U. S. Geological Survey Bulletin 1789, 33 p.

Graf, W.H., 1971, Hydraulics of Sediment Transport: McGraw-Hill Series in Water Resources and Environmental Engineering: New York, McGraw-Hill, 513 p.

Hadley, K.C., and LaHusen, R.G., 1995, Technical Manual for the Experimental Acoustic Flow Monitor: U. S. Geological Survey Open-File Report 95-0114, 24 p.

Hawkins, J.W., and Evans, C.A., 1983, Geology of the Zambales Range, Luzon, Philippine Islands: ophiolite derived from an island arc-back arc basin pair, *in* Hayes, D.E., ed., The Tectonic and Geologic Evolution of Southeast Asian Seas and Islands, Part 2: Geophysical Monograph 27: Washington, D.C., United States, American Geophysical Union, p. 95-123.

Hayes, S.K., 1999, Low-flow Sediment Transport on the Pasig-Potrero Alluvial Fan, Mount Pinatubo, Philippines: Seattle, University of Washington, Master of Science thesis (unpublished), 73 p.

Hayes, S.K., Montgomery, D.R., and Newhall, C.G., 2002, Fluvial sediment transport and deposition following the 1991 eruption of Mount Pinatubo: Geomorphology, v. 45, no. 3-4, p. 211-224.

Hodgson, K.A., and Manville, V.R., 1999, Sedimentology and flow behavior of a rain-triggered lahar, Mangatoetoenui Stream, Ruapehu Volcano, New Zealand: Geological Society of America Bulletin, v. 111, no. 5, p. 743-754.

Horton, R.E., 1945, Erosional development of streams and their drainage basins: hydrophysical approach to quantitative morphology: Bulletin of the Geological Society of America, v. 56, no. 3, p. 275-370.

Iverson, R.M., 1997, The physics of debris flows: Reviews of Geophysics, v. 35, no. 3, p. 245-296.

Janda, R.J., Daag, A.S., Delos Reyes, P.J., Newhall, C.G., Pierson, T.C., Punongbayan, R.S., Rodolfo, K.S., Solidum, R.U., Jr., and Umbal, J.V., 1996, Assessment and response to lahar hazard around Mount Pinatubo, 1991 to 1993, *in* Newhall, C.G., and Punongbayan, R.S., eds., Fire and Mud: Eruptions and Lahars of Mount Pinatubo, Philippines: Quezon City / Seattle, Philippine Institute of Volcanology and Seismology / University of Washington Press, p. 107-139.

Japan International Cooperation Agency (JICA), 1978, Planning Report on the Pasig-Potrero River Control and Sabo Project: Main Report, 133 p.

Japan International Cooperation Agency (JICA), 1996a, Digital topographic data for the eastern flank of Mount Pinatubo for 1991, 1992 and 1994.

Japan International Cooperation Agency (JICA), 1996b, The Study on Flood and Mudflow Control for Sacobia-Bamban/Abacan River Draining Mt. Pinatubo: Databook DB-3, Geotechnical Data.

Japan International Cooperation Agency (JICA), 1996c, The Study on Flood and Mudflow Control for Sacobia-Bamban/Abacan River Draining Mt. Pinatubo: Main Report, 354 p.

Jones, J.W., and Newhall, C.G., 1996, Preeruption and posteruption digital-terrain models of Mount Pinatubo, *in* Newhall, C.G., and Punongbayan, R.S., eds., Fire and Mud: Eruptions and Lahars of Mount Pinatubo, Philippines: Quezon City / Seattle, Philippine Institute of Volcanology and Seismology / University of Washington Press, p. 571-582.

Kadomura, H., Imagawa, T., and Yamamoto, H., 1983, Eruption-induced rapid erosion and mass movements on Usu Volcano, Hokkaido, *in* Okuda, S., Netto, A., and Slaymaker, O., eds., Extreme Land Forming Events: Zeitschrift für Geomorphologie, Supplementband 46, p. 123-142.

Kinnell, P.I.A., 1990, The mechanics of raindrop-induced flow transport: Australian Journal of Soil Research, v. 28, no. 4, p. 497-516.

Kuenzi, W.D., Horst, O.H., and McGehee, R.V., 1979, Effect of volcanic activity on fluvial-deltaic sedimentation in a modern arc-trench gap, southwestern Guatemala: Geological Society of America Bulletin, v. 90, no. 9, p. I 827-I 838.

Kusakabe, M., 1996, Hazardous crater lakes, *in* Scarpa, R., and Tilling, R.I., eds., Monitoring and Mitigation of Volcano Hazards: Berlin, Springer-Verlag, p. 573-598.

LaHusen, R.G., 1996, Detecting Debris Flows Using Ground Vibrations: U. S. Geological Survey Fact Sheet 236-96, 2 p.

Lavigne, F., Thouret, J.C., Voight, B., Suwa, H., and Sumaryono, A., 2000, Lahars at Merapi Volcano, Central Java: An Overview, *in* Voight, B., Sukhyar, R., and Wirakusumah, A.D., eds., Merapi Volcano: Journal of Volcanology and Geothermal Research, v. 100, no. 1-4, p. 423–456.

Leavesley, G.H., Lusby, G.C., and Lichty, R.W., 1989, Infiltration and erosion characteristics of selected tephra deposits from the 1980 eruption of Mount St. Helens, Washington, USA: Hydrological Sciences Journal (Journal des Sciences Hydrologiques), v. 34, no. 3, p. 339-353.

Lockwood, J.P., Costa, J.E., Tuttle, M.L., Nni, J., and Tebor, S.G., 1988, The potential for catastrophic dam failure at Lake Nyos maar, Cameroon: Bulletin of Volcanology, v. 50, no. 5, p. 340-349.

Lohnes, R.A., and Handy, R.L., 1968, Slope angles in friable loess: Journal of Geology, v. 76, no. 3, p. 247-258.

Major, J.J., Janda, R.J., and Daag, A.S., 1996, Watershed disturbance and lahars on the east side of Mount Pinatubo during the mid-June 1991 eruptions, *in* Newhall, C.G., and Punongbayan, R.S., eds., Fire and Mud: Eruptions and Lahars of Mount Pinatubo, Philippines: Quezon City / Seattle, Philippine Institute of Volcanology and Seismology / University of Washington Press, p. 895-919.

Major, J.J., and Newhall, C.G., 1989, Snow and ice perturbation during historical volcanic eruptions and the formation of lahars and floods: a global review: Bulletin of Volcanology, v. 52, no. 1, p. 1-27.

Major, J.J., Pierson, T.C., Dinehart, R.L., and Costa, J.E., 2000, Sediment yield following severe volcanic disturbance: a two-decade perspective from Mount St. Helens: Geology, v. 28, no. 9, p. 819-822.

Malihan, T.D., 1987, The gold-rich Dizon porphyry copper mine in the western central Luzon Island, Philippines: its geology and tectonic setting, *in* Pacific Rim Congress 87: An International Congress on the Geology, Structure, Mineralisation and Economics of the Pacific Rim, 26-29 August 1987, Gold Coast, Queensland, Australia: Parkville, Victoria, Australia, Australasian Institute of Mining and Metallurgy, p. 303-307.

Manville, V.R., Hodgson, K.A., Houghton, B.F., Keys, J.R.H., and White, J.D.L., 2000, Tephra, snow and water: complex sedimentary responses at an active snow-capped stratovolcano, Ruapehu, New Zealand: Bulletin of Volcanology, v. 62, no. 4-5, p. 278-293.

Manville, V.R., White, J.D.L., Houghton, B.F., and Wilson, C.J.N., 1998, The saturation behaviour of pumice and some sedimentological implications: Sedimentary Geology, v. 119, no. 1-2, p. 5-16.

Manville, V.R., White, J.D.L., Houghton, B.F., and Wilson, C.J.N., 1999, Paleohydrology and sedimentology of a post-1.8 ka breakout flood from intracaldera Lake Taupo, North Island, New Zealand: Geological Society of America Bulletin, v. 111, no. 10, p. 1435-1447.

Marcial, S., Melosantos, A.A., Hadley, K.C., LaHusen, R.G., and Marso, J.N., 1996, Instrumental lahar monitoring at Mount Pinatubo, *in* Newhall, C.G., and Punongbayan, R.S., eds., Fire and Mud: Eruptions and Lahars of Mount Pinatubo, Philippines: Quezon City / Seattle, Philippine Institute of Volcanology and Seismology / University of Washington Press, p. 1015-1022.

Martinez, M.M.L., Arboleda, R.A., Delos Reyes, P.J., Gabinete, E., and Dolan, M.T., 1996, Observations of 1992 lahars along the Sacobia-Bamban river system, *in* Newhall, C.G., and Punongbayan, R.S., eds., Fire and Mud: Eruptions and Lahars of Mount Pinatubo, Philippines: Quezon City / Seattle, Philippine Institute of Volcanology and Seismology / University of Washington Press, p. 1033-1043.

Mastin, L.G., and Witter, J.B., 2000, The hazards of eruptions through lakes and seawater, *in* Varekamp, J.C., and Rowe, G.L., Jr., eds., Crater Lakes: Journal of Volcanology and Geothermal Research, v. 97, no. 1-4, p. 195-214.

Matsukura, Y., 1987, Critical height of cliff made of loosely consolidated materials: Annual Report of the Institute of Geoscience, University of Tsukuba, v. 13, p. 68-70.

McGimsey, R.G., Waythomas, C.F., and Neal, C.A., 1994, High stand and catastrophic draining of intracaldera Surprise Lake, Aniakchak Volcano, Alaska, *in* Till, A.B., and Moore, T.E., eds., Geologic Studies in Alaska by the U.S. Geological Survey, 1993: U. S. Geological Survey Bulletin 2107, p. 59-71.

Mercado, R.A., Lacsamana, J.B.T., and Pineda, G.L., 1996, Socioeconomic impacts of the Mount Pinatubo eruption, *in* Newhall, C.G., and Punongbayan, R.S., eds., Fire and Mud: Eruptions and Lahars of Mount Pinatubo, Philippines: Quezon City / Seattle, Philippine Institute of Volcanology and Seismology / University of Washington Press, p. 1063-1069.

Meyer, D.F., and Martinson, H.A., 1989, Rates and processes of channel development and recovery following the 1980 eruption of Mount St. Helens, Washington: Hydrological Sciences Journal (Journal des Sciences Hydrologiques), v. 34, no. 2, p. 115-127.

Meyer, W., Sabol, M.A., Glicken, H.X., and Voight, B., 1985, The Effects of Ground Water, Slope Stability, and Seismic Hazards on the Stability of the South Fork Castle Creek Blockage in the Mount St. Helens Area, Washington: U. S. Geological Survey Professional Paper 1345, 42 p.

Meyer, W., Sabol, M.A., and Schuster, R.L., 1986, Landslide-dammed lakes at Mount St. Helens, Washington, *in* Schuster, R.L., ed., Proceedings: Landslide Dams: Processes, Risk, and Mitigation: Geotechnical Special Publication No. 3: New York, American Society of Civil Engineers, p. 21-41.

Meyer-Peter, E., and Müller, R., 1948, Formula for bed-load transport, *in* International Association for Hydraulic Structures Research, Report on the Second Meeting, Stockholm, Sweden: Delft.

Mitchell, J.K., 1993, Fundamentals of Soil Behavior (2nd ed.): New York, John Wiley and Sons, 437 p.

Mizuyama, T., and Kobashi, S., 1996, Sediment yield and topographic change after major volcanic activity, *in* Walling, D.E., and Webb, B.W., eds., Erosion and Sediment Yield: Global and Regional Perspectives - Proceedings of an International Symposium: IAHS-AISH Publication No. 236: Louvain, International Association of Hydrological Sciences, p. 295-301.

Montgomery, D.R., Panfil, M.S., and Hayes, S.K., 1999, Channel-bed mobility response to extreme sediment loading at Mount Pinatubo: Geology, v. 27, no. 3, p. 271-274.

Moyer, T.C., and Swanson, D.A., 1987, Secondary hydroeruptions in pyroclastic-flow deposits: examples from Mount St. Helens: Journal of Volcanology and Geothermal Research, v. 32, no. 4, p. 299-319.

National Hydraulic Research Center (NHRC), 1998, Hydraulic Simulation of the Pasig-Potrero River System: University of the Philippines Engineering Research and Development Foundation, Inc. Report No. 112.A, 44 p.

Newhall, C.G., 1994, Serious But Rapidly Diminishing Hazards at Mount Pinatubo: Progress report of joint PHIVOLCS-USGS collaboration, 1992 through mid-1994 (unpublished), 59 p.

Newhall, C.G., Daag, A.S., Delfin, F.G., Jr., Hoblitt, R.P., McGeehin, J.P., Pallister, J.S., Regalado, M.T.M., Rubin, M., Tubianosa, B.S., Tamayo, R.A., Jr., and Umbal, J.V., 1996, Eruptive history of Mount Pinatubo, *in* Newhall, C.G., and Punongbayan, R.S., eds., Fire and Mud: Eruptions and Lahars of Mount Pinatubo, Philippines: Quezon City / Seattle, Philippine Institute of Volcanology and Seismology / University of Washington Press, p. 165-195.

Newhall, C.G., and Punongbayan, R.S., eds., 1996a, Fire and Mud: Eruptions and Lahars of Mount Pinatubo, Philippines: Quezon City / Seattle, Philippine Institute of Volcanology and Seismology / University of Washington Press, 1126 p.

Newhall, C.G., and Punongbayan, R.S., 1996b, The narrow margin of successful volcanic-risk mitigation, *in* Scarpa, R., and Tilling, R.I., eds., Monitoring and Mitigation of Volcano Hazards: Berlin, Springer-Verlag, p. 807-838.

Paladio-Melosantos, M.L.O., Solidum, R.U., Jr., Scott, W.E., Quiambao, R.B., Umbal, J.V., Rodolfo, K.S., Tubianosa, B.S., Delos Reyes, P.J., Alonso, R.A., and Ruelo, H.B., 1996, Tephra falls of the 1991 eruptions of Mount Pinatubo, *in* Newhall, C.G., and Punongbayan, R.S., eds., Fire and Mud: Eruptions and Lahars of Mount Pinatubo, Philippines: Quezon City / Seattle, Philippine Institute of Volcanology and Seismology / University of Washington Press, p. 513-535.

Pallister, J.S., Meeker, G.P., Newhall, C.G., Hoblitt, R.P., and Martinez, M.M.L., 1993, 30,000 years of the "same old stuff" at Pinatubo [abs.], *in* AGU 1993 Fall Meeting: Eos, Transactions, American Geophysical Union, v. 74, no. 43, Suppl., p. 667-668.

Philippine Institute of Volcanology and Seismology (PHIVOLCS), 1994, Pinatubo Lahar Studies 1993: Final report on the UNESCO-funded lahar studies program: Quezon City, PHIVOLCS Press.

Pierson, T.C., 1995, Flow characteristics of large eruption-triggered debris flows at snow-clad volcanoes: constraints for debris-flow models, *in* Ida, Y., and Voight, B., eds., Models of Magmatic Processes and Volcanic Eruptions: Journal of Volcanology and Geothermal Research, v. 66, no. 1-4, p. 283-294.

Pierson, T.C., 1998, An empirical method for estimating travel times for wet volcanic mass flows: Bulletin of Volcanology, v. 60, no. 2, p. 98-109.

Pierson, T.C., ed., 1999a, Hydrologic Consequences of Hot-Rock/Snowpack Interactions at Mount St. Helens Volcano, Washington: U. S. Geological Survey Professional Paper 1586: Reston, Va., U. S. Geological Survey, 117 p.

Pierson, T.C., 1999b, Transformation of water flood to debris flow following the eruption-triggered transient-lake breakout from the crater on March 19, 1982, *in* Pierson, T.C., ed., Hydrologic Consequences of Hot-Rock/Snowpack Interactions at Mount St. Helens Volcano, Washington: U. S. Geological Survey, Professional Paper 1586, p. 19-36.

Pierson, T.C., and Costa, J.E., 1987, A rheologic classification of subaerial sediment-water flows, *in* Costa, J.E., and Wieczorek, G.F., eds., Debris Flows/Avalanches: Processes, Recognition and Mitigation: Reviews in Engineering Geology, v. 7, p. 93-105.

Pierson, T.C., Daag, A.S., Delos Reyes, P.J., Regalado, M.T.M., Solidum, R.U., Jr., and Tubianosa, B.S., 1996, Flow and deposition of posteruption hot lahars on the east side of Mount Pinatubo, July-October 1991, *in* Newhall, C.G., and Punongbayan, R.S., eds., Fire and Mud: Eruptions and Lahars of Mount Pinatubo, Philippines: Quezon City / Seattle, Philippine Institute of Volcanology and Seismology / University of Washington Press, p. 921-950.

Pierson, T.C., and Janda, R.J., 1994, Volcanic mixed avalanches: a distinct eruption-triggered mass-flow process at snow-clad volcanoes: Geological Society of America Bulletin, v. 106, no. 10, p. 1351-1358.

Pierson, T.C., Janda, R.J., Thouret, J.C., and Borrero, C.A., 1990, Perturbation and melting of snow and ice by the 13 November 1985 eruption of Nevado del Ruiz, Colombia, and consequent mobilization, flow and deposition of lahars: Journal of Volcanology and Geothermal Research, v. 41, p. 17-66.

Pierson, T.C., Janda, R.J., Umbal, J.V., and Daag, A.S., 1992, Immediate and Long-Term Hazards from Lahars and Excess Sedimentation in Rivers Draining Mount Pinatubo, Philippines: U. S. Geological Survey Water-Resources Investigations Report 92-4039, 37 p.

Punongbayan, R.S., Newhall, C.G., and Hoblitt, R.P., 1996, Photographic record of rapid geomorphic change at Mount Pinatubo, 1991-94, *in* Newhall, C.G., and Punongbayan, R.S., eds., Fire and Mud: Eruptions and Lahars of Mount Pinatubo, Philippines: Quezon City / Seattle, Philippine Institute of Volcanology and Seismology / University of Washington Press, p. 21-66.

Punongbayan, R.S., Tuñgol, N.M., Arboleda, R.A., Delos Reyes, P.J., Isada, M., Martinez, M.M.L., Melosantos, M.L.P., Puertollano, J.R., Regalado, M.T.M., Solidum, R.U., Jr., Tubianosa, B.S., Umbal, J.V., Alonso, R.A., and Remotigue, C.T., 1994, Impacts of the 1993 lahars, and long-term lahar hazards and risks around Pinatubo Volcano, PHIVOLCS, Pinatubo Lahar Studies 1993: Final report on the UNESCO-funded lahar studies program: Quezon City, PHIVOLCS Press, p. 1-40.

Reid, L.M., 1989, Channel Incision by Surface Runoff in Grassland Catchments: Seattle, University of Washington, Doctor of Philosophy thesis (unpublished), 135 p.

Rodolfo, K.S., and Arguden, A.T., 1989, Intensity and duration of lahar-generating rainfall on Mayon Volcano, Philippines [abs.], *in* Dymek, R.F., and Shelton, K.L., eds., 1989 Annual Meeting: Geological Society of America, Abstracts with Programs, v. 21, no. 6, p. A61.

Rodolfo, K.S., and Arguden, A.T., 1991, Rain-lahar generation and sediment-delivery systems at Mayon Volcano, Philippines, *in* Fisher, R.V., and Smith, G.A., eds., Sedimentation in Volcanic Settings: SEPM Special Publication No. 45: Tulsa, Okla., SEPM (Society for Sedimentary Geology), p. 71-87.

Rodolfo, K.S., Umbal, J.V., Alonso, R.A., Remotigue, C.T., Paladio-Melosantos, M.L.O., Salvador, J.H.G., Evangelista, D., and Miller, Y., 1996, Two years of lahars on the western flank of Mount Pinatubo: initiation, flow processes, deposits, and attendant geomorphic and hydraulic changes, *in* Newhall, C.G., and Punongbayan, R.S., eds., Fire and Mud: Eruptions and Lahars of Mount Pinatubo, Philippines: Quezon City / Seattle, Philippine Institute of Volcanology and Seismology / University of Washington Press, p. 989-1013.

Rossman, D.L., Castanada, G.C., and Bacuta, G.J.C., Jr., 1989, Geology of the Zambales Ophiolite, Luzon, Philippines, *in* Flower, M.F.J., and Hawkins, J.W., eds., Ophiolites and crustal genesis in the Philippines.: Tectonophysics, v. 168, no. 1-3, p. 1-22.

Schilling, S.P., 1998, LAHARZ: GIS Programs for Automated Mapping of Lahar-Inundation Hazard Zones: U. S. Geological Survey Open-File Report 98-0638, 80 p.

Schuster, R.L., 1986, Proceedings: Landslide dams: Processes, Risk, and Mitigation: Geotechnical Special Publication No.3: New York, American Society of Civil Engineers, 162 p.

Scott, K.M., Janda, R.J., de la Cruz, E.G., Gabinete, E., Eto, I., Isada, M., Sexon, M., and Hadley, K.C., 1996, Channel and sedimentation responses to large volumes of 1991 volcanic deposits on the east flank of Mount Pinatubo, *in* Newhall, C.G., and Punongbayan, R.S., eds., Fire and Mud: Eruptions and Lahars of Mount Pinatubo, Philippines: Quezon City / Seattle, Philippine Institute of Volcanology and Seismology / University of Washington Press, p. 971-988.

Scott, W.E., Hoblitt, R.P., Torres, R.C., Self, S., Martinez, M.M.L., and Nillos, T., Jr., 1996, Pyroclastic flows of the June 15, 1991, climactic eruption of Mount Pinatubo, *in* Newhall, C.G., and Punongbayan, R.S., eds., Fire and Mud: Eruptions and Lahars of Mount Pinatubo, Philippines: Quezon City / Seattle, Philippine Institute of Volcanology and Seismology / University of Washington Press, p. 545-570.

Segerstrom, K., 1950, Erosion studies at Paricutin volcano, state of Michoacan, Mexico: U. S. Geological Survey Bulletin 0965-A, p. 1-164.

Segerstrom, K., 1960, Erosion and related phenomena at Paricutin (Mexico) in 1957: U. S. Geological Survey Bulletin 1104-A, p. 1-18.

Segerstrom, K., 1966, Paricutin, 1965 - aftermath of eruption, *in* Geological Survey Research 1966: U. S. Geological Survey Professional Paper 0550-C, p. C93-C101.

Self, S., and Torres, R.C., 2001, Vent-derived and deposit-derived pyroclastic flow generation and emplacement of the 1991 Pinatubo ignimbrite sheet [abs.], *in* AGU 2001 Fall Meeting: Eos, Transactions, American Geophysical Union, v. 82, no 47, Suppl.

Shields, A., 1936, Anwendung der Ähnlichkeitsmechanik und der Turbulenzforschung auf die Geschiebebewegung (Application of similitude and turbulence research to bed-load movement): Mitteilungen der Preussischen Versuchsanstalt für Wasserbau und Schiffbau Nr. 26: Berlin.

Shields, H., 1998, Engineering Geology of the Megadyke Lahar Protection Measures in the Pasig-Potrero River System, Mount Pinatubo, Philippines: Christchurch, New Zealand, University of Canterbury, Master of Science in Engineering Geology thesis (unpublished), 292 p.

Shimokawa, E., and Jitousono, T., 1987, Rate of erosion on tephra-covered slopes of volcanoes, *in* Takeshita, K., ed., Influence of Large-Scale Tephra Cover on Mass Movements: Chikei (Transactions), Japanese Geomorphological Union, v. 8, no. 4, p. 269-286.

Shimokawa, E., and Taniguchi, Y., unknown date, Sediment yield from hillside slope of active volcanoes: Unidentified publication, p. 155-181.

Singh, V.P., 1996, Dam Breach Modeling Technology: Water Science and Technology Library, v. 17: Dordrecht/Boston/London, Kluwer Academic Publishers, 242 p.

Singh, V.P., Scarlatos, P.D., Collins, J.G., and Jourdan, M.R., 1988, Breach erosion of earthfill dams (BEED) model: Natural Hazards, v. 1, no. 2, p. 161-180.

Smith, G.A., and Lowe, D.R., 1991, Lahars: volcano-hydrologic events and deposition in the debris flow-hyperconcentrated flow continuum, *in* Fisher, R.V., and Smith, G.A., eds., Sedimentation in Volcanic Settings: SEPM Special Publication No. 45: Tulsa, Okla., Society for Sedimentary Geology, p. 59-70.

Smith, R.C.M., 1991, Landscape response to a major ignimbrite eruption, Taupo volcanic center, New Zealand, *in* Fisher, R.V., and Smith, G.A., eds., Sedimentation in Volcanic Settings: SEPM Special Publication No. 45: Tulsa, Okla., SEPM (Society for Sedimentary Geology), p. 123-137.

Tognacca, C., and Bezzola, G.R., 1997, Debris flow initiation by channel-bed failure, *in* Chen, C.L., ed., First International Conference on Debris-Flow Hazards Mitigation: Mechanics, Prediction and Assessment: New York, American Society of Civil Engineers, p. 44-53.

Torres, R.C., Self, S., and Martinez, M.M.L., 1996, Secondary pyroclastic flows from the June 15, 1991 ignimbrite of Mount Pinatubo, *in* Newhall, C.G., and Punongbayan, R.S., eds., Fire and Mud: Eruptions and Lahars of Mount Pinatubo, Philippines: Quezon City / Seattle, Philippine Institute of Volcanology and Seismology / University of Washington Press, p. 665-678.

Tuñgol, N.M., and Regalado, M.T.M., 1996, Rainfall, acoustic flow monitor records, and observed lahars of the Sacobia River in 1992, *in* Newhall, C.G., and Punongbayan, R.S., eds., Fire and Mud: Eruptions and Lahars of Mount Pinatubo, Philippines: Quezon City / Seattle, Philippine Institute of Volcanology and Seismology / University of Washington Press, p. 1023-1032.

Umbal, J.V., 1994, Lahar-Dammed Mapanuepe Lake: Two-Year Evolution After the 1991 Eruption of Mount Pinatubo, Philippines, University of Illinois at Chicago, Master of Science thesis (unpublished), 141 p.

Umbal, J.V., 1997, Five years of lahars at Pinatubo volcano: declining but still potentially lethal hazards: Journal of the Geological Society of the Philippines, v. 52, p. 1-19.

Umbal, J.V., and Rodolfo, K.S., 1996, The 1991 lahars of southwestern Mount Pinatubo and evolution of the lahar-dammed Mapanuepe Lake, *in* Newhall, C.G., and Punongbayan, R.S., eds., Fire and Mud: Eruptions and Lahars of Mount Pinatubo, Philippines: Quezon City / Seattle, Philippine Institute of Volcanology and Seismology / University of Washington Press, p. 951-970.

United States Army Corps of Engineers (USACE), 1994, Mount Pinatubo Recovery Action Plan: Long Term Report: Portland, Oregon, 3 vols. + 5 appendices.

Visser, P.J., 1998, Breach Growth in Sand-Dikes: Communications on Hydraulic and Geotechnical Engineering No. 98-1: Delft, The Netherlands, Delft University of Technology, 172 p.

Voight, B., 1996, The management of volcano emergencies: Nevado del Ruiz, *in* Scarpa, R., and Tilling, R.I., eds., Monitoring and Mitigation of Volcano Hazards: Berlin, Springer-Verlag, p. 719-769.

Walder, J.S., and O'Connor, J.E., 1997, Methods for predicting peak discharge of floods caused by failure of natural and constructed earthen dams: Water Resources Research, v. 33, no. 10, p. 2337-2348.

Waldron, H.H., 1967, Debris flow and erosion control problems caused by the ash eruptions of Irazu Volcano, Costa Rica: U. S. Geological Survey Bulletin 1241-I, p. I1-I37.

Waythomas, C.F., 2001, Formation and failure of volcanic debris dams in the Chakachatna River valley associated with eruptions of the Spurr volcanic complex, Alaska: Geomorphology, v. 39, no. 3-4, p. 111-129.

Waythomas, C.F., Walder, J.S., McGimsey, R.G., and Neal, C.A., 1996, A catastrophic flood caused by drainage of a caldera lake at Aniakchak Volcano, Alaska, and implications for volcanic hazards assessment: Geological Society of America Bulletin, v. 108, no. 7, p. 861-871.

Wolfe, E.W., and Hoblitt, R.P., 1996, Overview of the eruptions, *in* Newhall, C.G., and Punongbayan, R.S., eds., Fire and Mud: Eruptions and Lahars of Mount Pinatubo, Philippines: Quezon City / Seattle, Philippine Institute of Volcanology and Seismology / University of Washington Press, p. 3-20.

Wolfe, J.A., and Self, S., 1983, Structural lineaments and Neogene volcanism in southwestern Luzon, *in* Hayes, D.E., ed., The Tectonic and Geologic Evolution of Southeast Asian Seas and Islands, Part 2: Geophysical Monograph 27: Washington, D.C., United States, American Geophysical Union, p. 157-172.

Youd, T.L., Wilson, R.C., and Schuster, R.L., 1981, Stability of blockage in North Fork Toutle River, *in* Lipman, P.W., and Mullineaux, D.R., eds., The 1980 Eruptions of Mount St. Helens, Washington: U. S. Geological Survey Professional Paper 1250, p. 821-828.

Yumul, G.P., Jr., 1994, A Cretaceous to Paleocene-Eocene South China Sea basin origin for the Zambales ophiolite complex, Luzon, Philippines?: The Island Arc, v. 3, no. 1, p. 35-47.